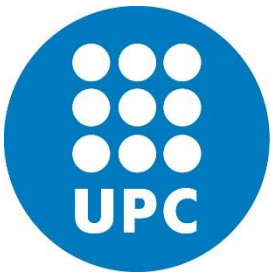

UNIVERSITAT POLITÈCNICA DE CATALUNYA
BARCELONATECH

Degree Thesis of
Georgios Bantemits
Undergraduate student

TITLE:

MODELING OF CROWD BEHAVIOR DURING INDOOR/OUTDOOR EVACUATION

Guided by
prof. Antonio Rubio
prof. Georgios Ch. Sirakoulis

Table of Contents

Abstract

In pedestrian dynamics, there are forces that usually define the trajectories between the moving individuals. These can be more easily understood in corresponding video scenes where the crowd movement results also from the application of such forces like Newton laws as friction and action-reaction. Nevertheless, the complexity of the individuals' movement insinuates that, between them, there are also more complex or "invisible" unknown forces as the ones described by psychological terms that apply and dictate the crowd movement. In this thesis, we want to indicate the existence of those forces by modeling the movement of a human as an oscillation described by rhythms and/or frequencies perceived from its environment. Moreover, we intend to describe with the help of appropriate computational tools and detection and tracking software, the movement of a crowd as a network of rhythms and show that the correlation among the individuals' rhythm can lead to phenomena of synchronization and self-organization of the moving crowd.

Prologue

The support of the human body is achieved by the mutual imbalance of the two lower limbs. This directly affects the way people move. More specifically, in the case of walking that it will concern us most in this thesis and in the forward movement that occurs in most of the cases, human moves in two dimensions. The first dimension is bounded by the direction of the shortest route to its destination. The second dimension is a movement perpendicular to the first, where the human's center of gravity is shifted successively from one limb to the other in order to achieve balance. The perpendicular movement is symmetrical due to the symmetry of the human body and periodic due to the reciprocal alternation of the two lower limbs. As a result, human walking presents great similarities with the oscillation example. The above description refers to the movement of a person who is free from the influence of external forces. However, if we extend the level of our confrontation to include more people and make it more realistic then complexity grows up. First of all, among the people that are in contact, there are forces which are described by Newton's laws. Apart from these, it has been observed that additional forces are developed, which are based on social and psychological factors that do not need direct contact and their influence must be taken into account in the formation of the final human motion [1]. In addition, when many people are getting in the same place, it is created what we call human crowd. It has been observed that human crowds exhibit some collective behaviors that have the ability to solve problems of cooperation and efficient organization, but without people who constitute the crowd being aware that they are involved in such a collective process [2].

In the context of this thesis, we have examined scenes of videos that depict the movement of people and we have approached their movement with the theory of oscillations. We focused more on the dimension of frequency and less on the width and phase and we described pedestrian movement as the superposition of more oscillations and frequencies. Some of the oscillations have their origin in the way we approach human movement and in the physiology of her walk, while others come from the interactions that are developed between pedestrians. To support our reasoning, we analyzed with signal processing functions the frequencies spectrum of real pedestrian motion data. In addition, we searched and discovered analytical equations that describe pedestrian movement with the help of a genetic algorithm using the data mentioned before. Finally, we compared in two fields the results with the real data, in the time domain and in the frequency domain. These comparisons help us to draw our conclusions. It became apparent that the proposed methodology could help the development of new models that simulate crowd movement, as well as enhancement of building to avoid congestion and efficient use, as well as safe

evacuation of the area in case of emergency. It can also contribute to the realistic representation of crowd movement in the case of computer graphics and the design of motion and obstacles avoidance for robots.

The thesis has a structure of six chapters. The first chapter presents some introductory details that help the reader to understand key factors associated with the under study problem.

In the second chapter, the experimental analysis takes place. We analyze the choices made about the experiment, namely the way we approach human movement, the basic assumptions about the experiment, and the division of the study in two levels: microscopic and macroscopic.

The third chapter describes the process of searching for equations using Genetic Algorithms and symbolic regression. Firstly, introductory and historical data on genetic algorithms are presented. Next, it is presented the three search cases that explain in detail how the search for equations took place. Finally, details are provided on the operation of the specific genetic algorithm that was used.

In the fourth chapter, we present the signal processing process. With the help of the cross-correlation and autocorrelation signal processing functions, the spectrum of frequencies that make up the data from real video recordings is examined.

In the fifth chapter, the results of the search for equations are presented and a comparison is made in the field of time with the real data. The results for each of the three search cases and all the video scenes that were examined, are presented in details.

Finally, the sixth chapter summarizes the results obtained from the search for equations and the resulting conclusions. Also, a comparison is made in the frequency domain with the real data and we come to some conclusions.

1. Introduction

1.1 Some historical details of pedestrian modeling

The study of pedestrian behavior and pedestrian modeling has attracted over the years a large number of scientists and researchers. Pedestrians have been a subject of such studies for more than five decades. The first approaches were empirical studies focused on the pedestrian flow analysis. The purpose of those works for many years, owing to the growing construction of large facilities intended for pedestrians, was the design and development of functional and safe pedestrian facilities. One of the first approaches that tried to describe and quantify the comfort and safety of pedestrian facilities was the level-of-service concept, which was a study of Fruin (1971) [3]. This concept is a qualitative measure that was first used in order to analyze the quality of traffic service in highways. The traffic flow is categorized in different levels and a quality level is assigned in each flow based on performance metrics like speed and density. The same concept is used to analyze the level of service in facilities that should accommodate a large number of people. Also, it examines the necessary space for walking pedestrians as well it correlates quantitatively the speed and density of pedestrian flow with the feeling of convenience.

The same period, Henderson [4] studied pedestrian behavior in a way that could be described as an early form of pedestrian modeling. In his study, he suggested that movement of pedestrian within a crowd exhibits a similar behavior to that of a collection of gas molecules. In particular, he suggested that Maxwell-Boltzmann's classical theory of molecular systems can also successfully describe the distribution of human speeds during their movement. This means that pedestrian movement can be described by the same statistical equations that successfully describe systems made up of separate molecules. These conclusions, of course, presupposed that the density of individuals would be small enough so that the crowd could be approached by the behavior of gases, and that the movement of people at these low flow densities is the result of social interactions.

Furthermore, these initial empirical studies concerned with design solutions for faster and safer evacuation of facilities by humans in normal and high crowd density conditions, such as the Pauls study [5]. Pauls examined the improvement in performance of the evacuation time using different output geometries. It has been found that by widening the shape and width of stairs as well as by improving the visibility of pedestrians in low visibility areas, it is possible to increase the feeling of comfort and safety of pedestrians under normal conditions. Also, with the same practices it is

possible to reduce the risk that people is facing in cases of large crowd density due to emergencies.

A few years later, Helbing [6] working in the same direction with the parallel use of pedestrian movement simulations, experimented with different pedestrian environments. Such environments were corridors, congestion areas and intersections. These experiments have shown that the geometry of the boundaries of the environment influences significantly the capacity of pedestrian facilities and is also responsible for creating phenomena of self-organization among pedestrians. The term "self-organization" means co-operation among the moving persons without, however, any external control or pre-planned schedule. In addition, it can be seen that the self-organizing phenomena created can be used in the process of design elements for pedestrian facilities in order to optimize the evacuation process. It is reported that the installation of some "obstacles" in the installation environment or the specific design of peripheral boundaries such as zigzag geometries can increase the efficiency and safety of public buildings, railway stations, terminals and stages in cases Emergency evacuation.

1.2 Basic methods

There are several modeling approaches that try to represent the movement behavior of pedestrian. These modes examine the pedestrian's motion from two different disciplines, i.e. microscopic and macroscopic level.

1. Microscopic models treat the pedestrian as individual elements with enhanced attributes. The variety of interactions in different conditions is considered in detail and the movement of each pedestrian is the result of the effect of those interactions within its environment.

2. Macroscopic models treat the pedestrian movement more abstractly modeling the pedestrian flow as a whole. The interactions among the individuals are not taken into account directly and the crowd is represented as a continuous flow with a certain density and velocity.

There is also a third level, the mesoscopic [7] that is located between the microscopic and the macroscopic level. The basic idea behind the mesoscopic models is that the structural element of the model is the group of people. Unlike the microscopic models that the structural element is represented by an exact person and the macroscopic models that model the movement of a large number of people scattered in a space. In this category of models, there are two types of groups,

the physical groups that correspond to individuals in a particular space, and virtual groups whose members are individuals who have similar behavior because they have the same objective. The members of a virtual group are usually divided into individual physical groups. Thus, at each distinct time step the model calculates the movement of the two different group categories. Changing the position of pedestrians results in a modification in the formation of old teams and the creation of new teams.

The main difference between models belonging to different levels is the degree of analysis or discretization that is applied between individuals. The microscopic level has the advantage of high resolution because individuals are considered as discrete entities and interactions are counted separately. This means that microscopic approaches can follow and simulate more complex phenomena that have been observed in human movement. However, the main drawback of detailed simulation is the excessive cost of computing such an analytical approach. On the other hand, macroscopic approaches require less numerical and computational effort, but in the same time, they can only be used in areas of less interest or as an initial approach to find locations of big congestion.

Macroscopic models treat crowd movement as a continuous flow and do not distinguish individual interactions of individuals. For this reason, they are used more to calculate the level of comfort felt by pedestrians, but also to assess the signs of congestion. The most common macroscopic approaches are gas propulsion models, dynamic fluid models, regression models, path selection models, and queuing models [8], [9], [10].

Gas and dynamic fluid models use an analogy with the movement of liquids or gases to describe the changes in the density and velocity of the crowd movement. In these models it is essentially assumed that the movement of the crowd is characterized by natural laws similar to those applicable to the dynamics of liquids and gases and therefore pedestrian movement is described by some differential equations. Helbing presented a collective pedestrian traffic model, based on gas movement approaches as described by Boltzmann.

Microscopic models can be divided into more subcategories, such as physical models, cellular automata (C.A.), rules-based models, and multi-agent models. Physical models have as a basic element the individual pedestrian that interacts with the surrounding people and with his environment. These models have been used to simulate human behavior in emergency situations and panic. The model of social forces is an example of such a physical model. The C.A. models also known as matrix-based models, i.e. divide the space of the under study building into grids or

cells. Each person occupies one or more cells and moves in the direction that empty cells are available. In the case of collisions where two individuals compete for the same cell, a conflict resolution condition shares the priorities. Rule-based models have been widely used in computer graphics to model animal groups and virtual crowds. An example of this model is the model of Reynolds [11] which models bird herds and is based on three local rules. Multi-agent models use autonomous agents that interact with their environment. These models are commonly used to approximate the movement of individuals in large-scale and high complexity simulations.

In the microscopic level among the existing models we have distinguish the Newtonian force model, the social distance model and a model based on simple rules from the approach of behavioral heuristics.

- **Social force model**

The social force model or Newtonian force model is a microscopic model that approaches the movement of individuals taking into account the Newtonian nature of the pedestrian interactions. This means that among the individuals, attractive, repulsive interactions and friction forces as it results from the solution of the equations of Newton laws for the movement of pedestrians are apparent. The motion of each pedestrian is the result of the superposition of several forces.

The social force model provides a realistic representation of the interactions among the pedestrians. In order to have a realistic model that simulates the real pedestrian behavior, the procedure of force modeling that take into account the forces among the pedestrians is very important. The social force model constructs the behavior of the human crowd by assuming a mixture of socio-psychological and physical factors that affect the pedestrians.

For any given time the model calculates for each pedestrian the coordinates, the velocity and the interactions with the environment. In the social force model, each pedestrian is represented by a circle and is given to him a specified mass value. Moreover, each pedestrian likes to move with a certain desired speed in a certain direction and therefore tends to adapt his actual velocity within a certain characteristic time [12]. Furthermore, he tries to keep an interpersonal distance from other pedestrians and walls, due to developed interactions. The tendency of pedestrians to avoid collisions between them is modeled with the use of repulsive forces. Individuals are getting into contact only if the distance between them is less than the sum of their radius. In this situation, the contribution of two more additional forces are used, which are necessary to understand the

particular reactions in the panic crowds: a "physical force" that reacts against the body's compression and a "sliding force" that prevents relative tangent movement, when two people come close to each other. Interaction with the walls and boundaries are treated accordingly.

Some advantages of the social force model, are that due to its microscopic approach it can model several properties from crowd dynamics such as observed self-organization phenomena. One example of these phenomena is the formation of different walking direction lanes when bidirectional flows of movement exist.

The most basic disadvantage is the unrealistic behavior of simulated pedestrian especially in the presence of high crowd densities. The problem is Newton's third law application in pedestrian dynamics. According to Newton's third law if two objects are interacting they apply each other forces that have equal magnitude and opposite directions. Although, in pedestrian dynamics, this law is unrealistic in many situations, since the force that a pedestrian applies to another that is behind him, does not have equal magnitude with the reaction of the back pedestrians to him. The result of this situation is that pedestrians in simulation with high crowd densities present an unrealistic motion because they are trembling due to the huge in amount and magnitude counteractions of the nearby pedestrians.

- **Social distances model**

The social distances model is a CA model of pedestrian dynamics that is rely on the sociological theory of *Social Distances* [13]. The *Social Distances* theory is a theory that deals the issues of the space requirements of people and the optimal distance between them. There are different distance zones around the human being and the presence of another human in each of them triggers

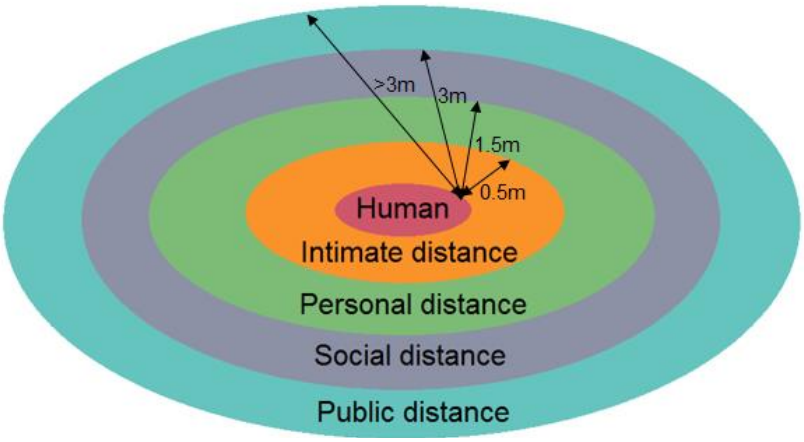

Figure 1.1 Approximate distances around humans according to Social Distances Theory

different situations and behaviors. Approximately, there are four sorts of distances that result in ascending order as the distance from a human is getting bigger: the intimate distance, the personal distance, the social distance and the public distance. These distances may vary according to cultural background, personality and environmental factors. It is clear that the interactions developed among the pedestrian according to this model have a non-Newtonian nature. Those interactions have a psychological nature and are the result of biological boundaries, cultural and social rules..

CA are models of physical systems in which space and time are discrete. Each cell is characterized by an internal state. The internal state represents physical quantities that can obtain values from a finite set of values. In our situation, the possible values are two '0' and '1' for the absence and the presence of a human in the cell respectively. There is also a set of cells called 'neighborhood' and is defined in accordance to the specified cell. At an initial state (time *t = 0*) every cell is assigned to a specified state. A new generation is created in the next point in time (time *t = 1*) according to some fixed rule that determines the new state of each cell in terms of the current state of the cell and the states of the cells in its neighborhood. The fixed rule in our situation is the way that humans are moving around the space namely the algorithm of the described model. The interactions between the observer and a person that intrude inside the social area of the observer are described by a "social distance force". The value of this force depends only on the distance between the observer and the intruder. There are different models for the social distance force. Thus, the total force that affects the observer is a superposition of the forces for each person that is in the social area of the observer (Figure 1.2).

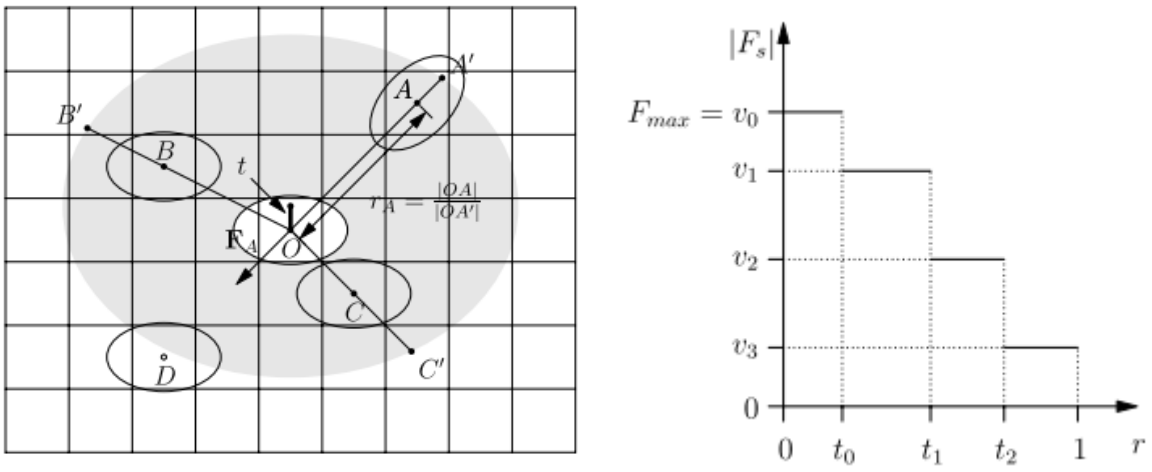

Figure 1.2 The social distances model
(a): The social area represented by an ellipse for the individual O. We also see how the interactions are calculated for different cases.
(b): The calculation of the social distance force. Force is described by a step function corresponding to the four categories of social zones.

- **Model based on behavioral heuristics**

This model is a microscopic approach to the pedestrian movement that is constructed by two simple cognitive procedures which are based on behavioral heuristics. These two simple heuristics are guided by visual information and can adequately describe the movement of pedestrians. Additionally, they can predict many observed phenomena at the level of the crowd [14].

The term "heuristic" is of Greek origin, it is adjective of the ancient Greek verb εὕρηκα and its meaning is "serving to find out or discover"[15]. From its introduction into English "heuristic" referred to useful, cognitive processes for solving problems that cannot be handled by logic and probability theory. Nowadays, in computer science and artificial intelligence, a heuristic is a technique designed for solving a problem when there is a lack of time and the classic methodologies are extremely slow or even in order to find an approximate solution when the classic methodologies fail to find any exact solution. Heuristic approaches are considered many times as incomplete due to the incomplete available knowledge and thus unavoidably false, but which is very useful nonetheless for guiding the future effort and thinking in appropriate directions.

The model constructs a representation of the visual information by assigning at each pedestrian his current position and velocity. Moreover, for each pedestrian, there is a comfortable walking speed and a destination point, namely the place that he finally wants to reach. Another assumption is that pedestrians are continuously adapting their walking behavior in order to match with their desired behavior within a relaxation time.

The first movement heuristic concerns the desired walking direction and is the following “A pedestrian chooses the direction that allows the most direct path to the destination point, taking into account the presence of obstacles.”

The second heuristic determines the desired walking speed. In order to avoid the collision with an obstacle in an emergent situation, due to the delay that introduces the relaxation time between the actual and desired speed, the pedestrian should keep a safe distance. Thus the second heuristic is:

“A pedestrian maintains a distance from the first obstacle in the chosen walking direction that ensures a time to collision of at least one relaxation time.”

There is also in the model a discrimination for the situation of great crowd density between the intentional movement behavior due to the external visual information and the unintentional motion caused by collision with other pedestrians and walls. In these cases, it is considered the contribution of another term that describes these repulsive forces and is zero when there is no physical contact. All the above are analytically depicted in Figure 1.3.

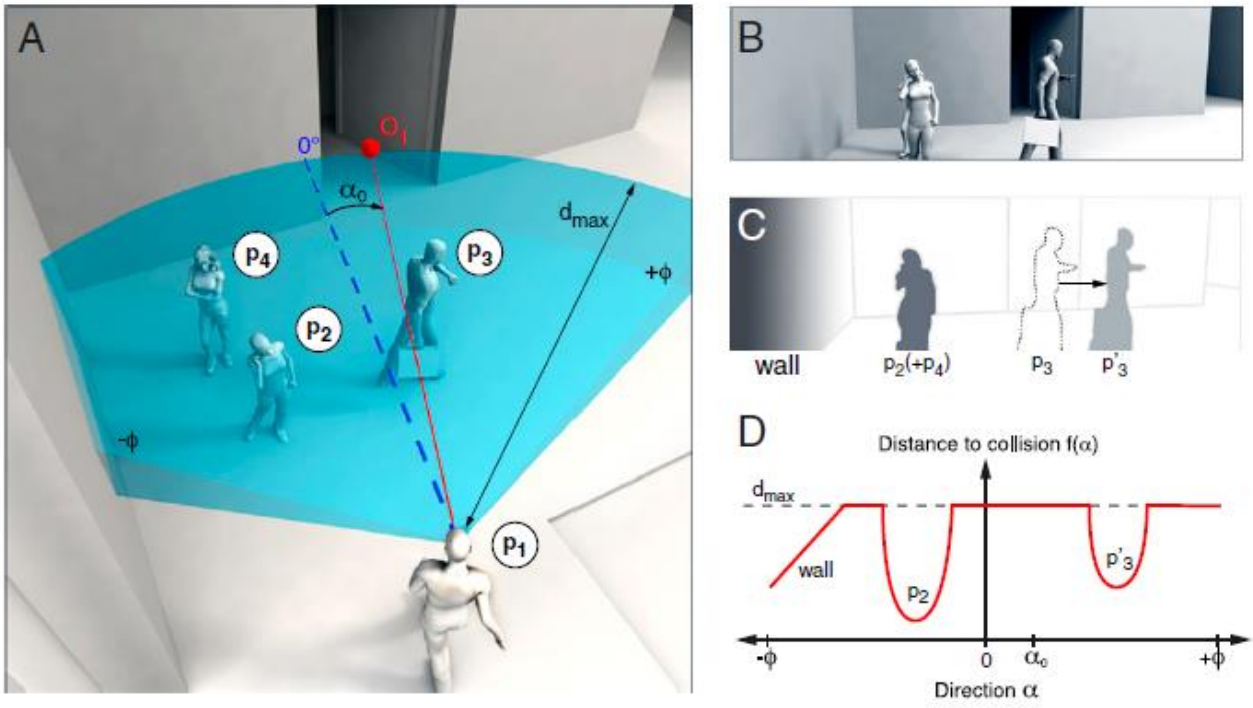

Figure 1.3 Model based on simple behavioral rules
(A): Representation of pedestrian p1 facing three other pedestrians and trying to reach the O1 destination (red). The blue dashed line corresponds to the line of sight.
(B): Representation of the same situation as shown by pedestrian p1.
(C): The same scene only in black and white colors, the darker areas represent shorter crash distance.
(D): Graphic representation of the function f (α) that reflects the distance from the collision in the direction a.

The left side of the field of vision is limited by a wall. The pedestrian p4 is hidden by pedestrian p2 and is therefore not visible. Pedestrian p3 is moving away, so a collision could occur in p'3, but only if p1 moved to the right.

2. Experimental analysis of pedestrian movement using video scenes.

2.1 Initial approach

At the beginning, we examined a variety of video scenes that captured the motion of pedestrian with different conditions and constraints. Our intention was to have an overall view of the information that different video recordings can provide. We started our examination with the motion of a single human inside a room from cameras placed in different level and positions. One problem that we came across was how we will study and process the human motion. We have chosen to track the individual with special video tracking tools. In this manner, we can obtain useful data for editing. We realized that the motion of a single person is simple for our case because there is absence of interactions. Thus, we continued with recordings that include more humans moving towards the exit of an indoor room from different levels of lateral positions. We understand that videos of this type will create great limitations due to overlapping between humans because of the limited sight vision. This will create gaps in the tracking procedure and thus our tracked motion data could be discontinuous.

In the view of the foregoing, more adequate video recordings that will have a more clear representation of the human's movement information were examined. We found that the format of the video recordings that captures continuously and without loss of information concerning the movement of the individuals and the crowd in total is the one which comes from cameras placed above. In these recordings, we can study the pedestrian motion without overlapping because the visual area is clear. Moreover, we can observe additional information about the motion and their interactions, such as the dynamical changes of the distance between them during their movement.

The dynamics of the pedestrian motion can be very complex and present a great variety of behaviors for different occasions. The next step in our work was to determine more specific details about the video recordings that we will examine. We found in the literature experiments with recordings in bottleneck, as well as corridors with unidirectional and bidirectional movement, T-junctions and corners. We have chosen to examine the corridors because they provide the most appropriate information for studying the human interactions in lower complexity. This happens because in corridors with unidirectional movement there is motion in one direction throughout the

whole recording. Thus, we diminish the parameters of the problem avoiding really complex behaviors and we are able to focus on specific crowd characteristics as a first step in our study.

The next step was to determine the flow density. When there is low density the pedestrians have more space during their movement and there is a long distance until the next pedestrian. Thus, they have more freedom and no obstructions are observed. The dynamics of their movement have attributes similar with these of gases. In these conditions, the interactions are very weak and it is maybe more difficult to capture and measure them. Additionally, when the flow density is very big, the pedestrians are getting so close to each other that there is physical contact. In these situations, individuals do not have enough free space around them, nor the option to choose their route. Newtonian mechanics describe the physical interactions that are developed among them, such as friction and repulsive forces. On the contrary, we wanted a medium flow density that will ensure that the physical interactions will not be the only and main forces to dictate crowd movement. In this case we will have the opportunity to analyze the non-physical interactions and their nature because the friction and the repulsive forces would be limited.

After the aforementioned constraints applied to the specific problem, we searched the literature and gathered a number of video recordings with pedestrian movement inside corridor. There was a variety of video with recordings from different heights and with different flow densities. We made a discrimination among those videos that satisfy our qualitative constraint about the flow density of the pedestrians. We came up with a very interesting observation in this process of collecting the most suitable videos that guided us through next steps of our research. Our observation was that when the pedestrians are walking in a corridor with a flow density that ensures that no strong interaction between the individuals will take place, some pedestrians synchronize their movement with the movement of their close neighbors for short periods of time. This apparent observation was our motivation to search for a quantitative explanation of this phenomenon that led the quest of analytical equations of the pedestrian’s movement.

2.2 Basic assumptions and constraints

As we mentioned before in order to continue our searching procedure we made some choices and put some constraints. Below, we present analytically these constraints:

1. We have chosen for the abovementioned reasons that we will analyze the movement of pedestrians in a unidirectional flow corridor

2. The first constraint was that we would focus our analysis on a specific part of the corridor. This means that we will not concern about the movement before and after our region of interest.

3. With our tracking procedure, we will obtain the useful data from the motion of the individuals and in particular we will track the heads of the individuals. Thus, the trajectory of the head represents the pedestrian's motion.

4. We examine our input data for oscillations and we observe the frequencies. With this approach, we include only indirectly the personal characteristics of each pedestrian such as gender, age, height, weight and volume.

5. The results of the tracking procedure will be directly associated with the dynamics of the tracked pedestrians. This means that our input data will be the time series of the coordinates, the velocity and the acceleration of each individual.

6. Another limitation of our approach is that we did not repeat the exact experiments with pedestrians that may have different social and cultural background and different walking habits.

2.3 Two level study

In order to search and reveal the relation of the individual motion, we examine the trajectory of the pedestrians in two different levels, i.e. microscopic and macroscopic. Below we describe these two approaches.

2.3.1. Microscopic approach

In the microscopic approach, we try to find and measure the interactions that are developed between individuals and thus determine their complex movement. These interactions originate from psychological and social factors and influence directly the crowd movement. In order to have an interaction we consider that we are in need of at least two people. In our microscopic analysis, we have chosen to examine also the interactions that are developed between three pedestrians. Our

choice is rational due to the width of the smallest corridor which was examined and equals to 1.80 meters. In this case, if we assign a minimum width for each person of 0.60 meters, we conclude that only three people can walk together side by side. In addition, we want to capture and quantify the effect of each pedestrian's movement on her two nearby neighbors. We present in Figure 2.1 the general search molecule that we will use. Our search molecule consists of three individuals, person 1, person 2 and person 3. The gray straight lines in Figure 2.1 represent the corridor boundaries.

Person1 is found slightly behind of the other two people, in this region between them. Person2 and person3 are in front with a short distance between them. The last pedestrian, i.e. Person1 has in her sight of vision the two neighbors in front of her, whether the front two pedestrians have in their sight of vision only their side neighbors. We also consider this formation to examine the differences of the interactions between the back and the front pedestrians.

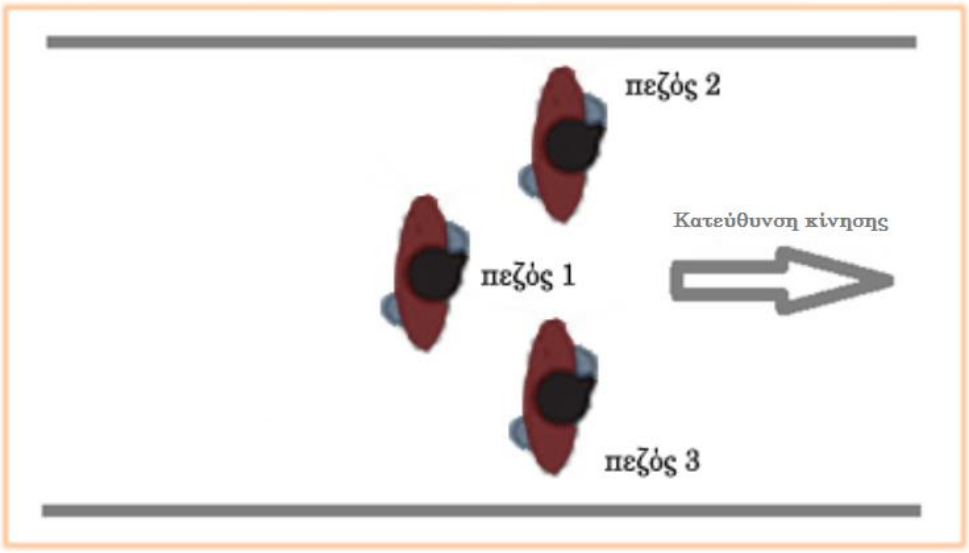

Figure 2.1 The basic search molecule of equations used in our microscopic approach

Additionally, we make the processing of the pedestrian's trajectories resulting to oscillations. In particular we analyze their frequencies, the amplitude and the equilibrium point of the trajectories-oscillations and then compare their results.

2.3.2. Macroscopic approach

In the macroscopic procedure, we want to examine the overall movement of the whole crowd among the space. Our intention is to model the movement of the crowd as a network of separate

individuals that interact. We measure the frequencies of the trajectories-oscillations of different individuals and we compare them with the average frequency of more pedestrians. In order to examine the macroscopic behavior of the crowd we create the concept of the flows. We divide the width of the corridor in three equal parts corresponding in general to the aforementioned three pedestrians able to be found side by side and assign one flow for each part. It is clear that the number of the selected zones is three for the same reason that was mentioned in the microscopic approach. In this way, we try to explain the movement of the whole crowd as a result of the microscopic interactions. We want to examine if the macroscopic complex movement of the whole crowd and our concept of flows can emerge from the massively parallel application of the microscopic simple interactions that exert among the individuals. In Figure 2.2 we see the corridor and inside it we observe the three different human flows that emerge.

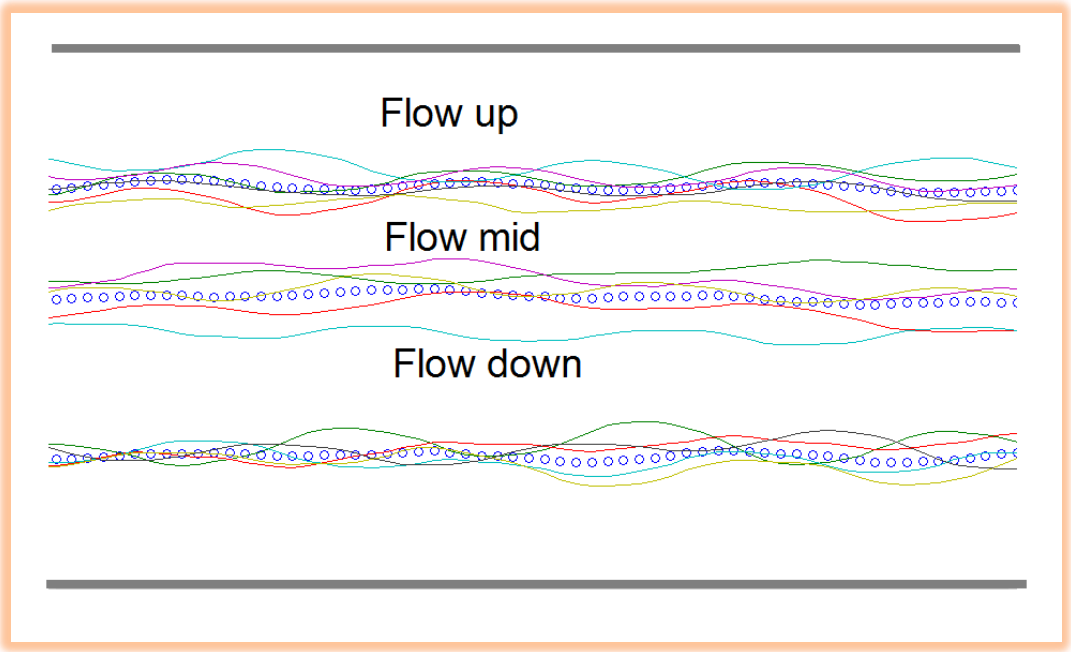

Figure 2.2 The trajectories created by the passing pedestrians and the corresponding flows created in each zone for a certain corridor width

2.4 Experimental Data

The experiments were performed within the project Hermes[1] and was funded by the Federal Ministry of Education and Research (BMBF) within the program “Research for Civil Security”.

At the beginning of the experiment, the participants were located inside a waiting area. They passed through a passage **Width in[m]** into a corridor **Width corridor[m]** and through another passage **Width out[m]** they went out (Figure 2.3). In the course of this experimental setup, the inflow, corridor and outflow widths varied.

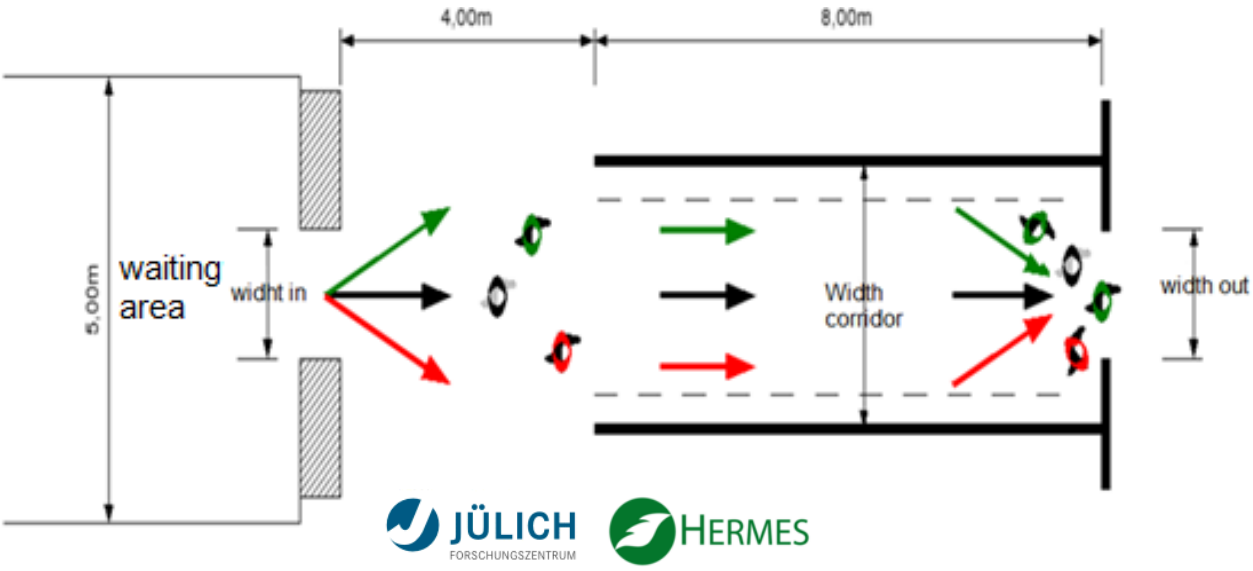

Figure 2.3 Representation of the experiment layout

[1] *Hermes Investigation of an evacuation assistant for use in emergencies during large-scale public events*

3. Search of equation with Genetic Algorithm

3.1 Introduction to Genetic Algorithms

Genetic Algorithms (GAs) are search algorithms based on the evolutionary ideas of natural selection and genetics. They are optimization algorithms which means they are used to find the optimal solution(s) to a given computational problem that maximizes or minimizes a particular function.

Genetic algorithms are considered one of the four components of Evolutionary computing a research area within the computer science. The other three components are evolution strategies, evolutionary programming and genetic programming. The last years they have begun to converge, although they started out as individual developments. The basic differences between them lie in the nature of the representation schemes, in the reproduction operators and the selection methods.

Evolutionary computing is based on the biological evolution. The theory of evolution first formulated in Darwin's book "On the Origin of Species" in 1859.This theory is the process by which organisms change over time as a result of changes in heritable physical or behavioral traits. Changes that allow an organism to better adapt to its environment will help it survive and have more offspring. [16].

Back in the 1950s and the 1960s several computer scientists independently studied evolutionary systems with the idea that evolution could be used as an optimization tool for engineering problems. Behind all these systems the main idea was to evolve a population of candidate solutions to a given problem, using operators inspired by natural genetic variation and natural selection. In the 1960s, Rechenberg introduced "evolution strategies", a method he used to optimize real−valued parameters for devices. Fogel, Owens, and Walsh developed "evolutionary programming," a technique in which candidate solutions to given tasks were represented as finite−state machines.

The father of GAs is John Holland who invented them in the 1960s. GAs was developed by Holland and his students and colleagues at the University of Michigan in the 1960s and the 1970s. In contrast with evolution strategies and evolutionary programming, Holland's original goal was not to design algorithms to solve specific problems, but rather to formally study the phenomenon of adaptation as it occurs in nature and to develop ways in which the mechanisms of natural

adaptation might be imported into computer systems. Holland presented the genetic algorithm as an abstraction of biological evolution [17].

Many researchers and scientists find the mechanism of biological evolution excellent to face computational problems of different fields. By this mean, biological evolution is an attractive source of inspiration for addressing problems that require searching among a huge number of possibilities for “solutions”. Furthermore, many search problems can gain advantage from the application of parallelism, in which simultaneously different possibilities are explored thus minimizing the necessary searching time. Another important benefit of genetic algorithms is that they have an adaptive nature, they can be used in different problems with small changes.

The basic elements of G use biological terms in analogy with real biology, though with attributes much simpler than the real biological ones. In real biology, all living organisms consist of cells, and each cell contains the same set of one or more chromosomes. Chromosomes are strings of DNA that serve as a "blueprint" for the organism. A chromosome can be divided into genes, each of which encodes a particular protein. The different possible "settings" for a trait are called alleles. Each gene is located at a particular locus (position) on the chromosome. The complete collection of genetic material (all chromosomes taken together) is called the organism's genome. The term genotype refers to the particular set of genes contained in a genome. During sexual reproduction, recombination (or crossover) occurs: in each parent, genes are exchanged between each pair of chromosomes to form a gamete (a single chromosome), and then gametes from the two parents pair up to create a full set of diploid chromosomes. Offspring are subject to mutation, in which single nucleotides (elementary bits of DNA) are changed from parent to offspring. The fitness of an organism is typically defined as the probability that the organism will live to reproduce (viability) or as a function of the number of offspring the organism has (fertility).

3.2 Elements of Genetic Algorithms

It seems that there is no strict definition accepted by all the evolutionary computation community that discriminates GAs from the other evolutionary computation components. Although, most of GAs have the following basic elements:

1. A population of chromosomes.

The term chromosome refers to a candidate solution to a problem. The chromosome consists of shorter blocks of symbols that called “genes” and encode a particular element of the candidate solution.

2. Selection of chromosomes.

With the term selection we mean the operator that is used to select chromosomes in the population for reproduction. The fitter the chromosome, the more possibilities it has to be selected to reproduce according to elitistic selection scheme.

3. A fitness function for optimization

The fitness function is a function that assigns a score (fitness) to each chromosome in the current population. The fitness of a chromosome depends on how well that chromosome solves the problem.

4. Crossover to produce next generation of chromosomes.

Crossover is a genetic operator used to vary the construction of a chromosome from one generation to the next. Crossover is a process of taking more than one parent solutions and producing a child solution from them.

5. Random mutation of new chromosomes.

Mutation replaces a symbol at a randomly chosen position with a randomly chosen new symbol. The mutation occurs during evolution according to a user-definable mutation probability. This probability should be set low. If it is set too high, the search will turn into a primitive random search.

6. Search space

In GAs, we call search space the collection of candidate solutions that solve with different ‘score’ our problem.

3.3 A simple genetic algorithm

A simple GA works as follows:

1. Start with a random population of chromosomes
2. Calculate the fitness $f(x)$ of each chromosome x in the population.
3. Repeat the following steps until *n* offspring have been created:
   a. Select a pair of parent chromosomes from the current population. The fittest chromosomes have bigger probability to be selected. Selection is done "with replacement," meaning that the same chromosome can be selected more than once to become a parent.
   b. With probability *pc* (the "crossover probability" or "crossover rate"), cross over the pair at a randomly chosen point (chosen with uniform probability) to form two offspring. If no crossover takes place, form two offspring that are exact copies of their respective parents.
   c. Mutate the two offspring at each locus with probability *pm* (the mutation probability or mutation rate), and place the resulting chromosomes in the new population. If *n* is odd, one new population member can be discarded at random.
4. Replace the current population with the new population.
5. Go to step 2.

Each iteration of the algorithm is called a 'generation'. A typical number of iterations for a GA is from 50 to 500 or more. The entire execution of iterations is called a run. At the end of a run, there are often one or more highly fit chromosomes in the population. Randomness plays such an important role in each run, that two runs with different random number seeds will generally produce different results. There are a number of details to fill in, such as the size of the population and the probabilities of crossover and mutation. The success of the algorithm often depends greatly on the values of these parameters.

3.1 Search of equations

The purpose of this thesis is to find the analytical equations that describe the movement and the interactions of pedestrians. In order to achieve that, we approximate the human motion with the characteristics of the periodic motion of a pendulum. The characteristics of a pendulum are the amplitude and the period or frequency. In the situation of human motion, there is a two dimensional movement. In this thesis we focus on the attributes of the vertical motion of the pedestrian walking

direction because we suppport that the vertical motion includes more information. Due to the absence of a fixed point of equilibrium we are more interested on the variations of the amplitude rather than its absolute values. The other useful periodic dimension that we examine is the frequency. The complex human motion insinuates that our approximation will be more similar with a composite oscillation. This means that it is possible to have more than one characteristic frequencies in the formation of the equations. Microscopically, we are trying to examine the frequencies of the movement of one pedestrian and compare them with the frequencies of the movement of its neighbor pedestrians. In this way, we want to reveal the existence of socio-psychological interactions that act among group of neighbor pedestrians and intervene in the trajectory of their movement.

In our macroscopic point of view we are making a more abstract examination about the behavior of the whole crowd. We introduce the concept of flows which divides the width of the corridor in three equal lanes and thus we examine the whole crowd as a movement of three separate flows. Moreover, we compute the average trajectories and we calculate the average frequency of more pedestrians in each flow as representative data for the behavior of the whole crowd

Moreover, we consider specific scenarios and we edit in different ways the input data from real video recordings, in order to construct the analytical equations of the pedestrian movement. These equations would include the microscopic interactions among the neighbor pedestrians and would describe the trajectory of a walking individual. We assume and we want to confirm that the equations are composed of some basic independent variables that in our case are the variables of dynamics of the pedestrian movement. This means that the relevant position, the velocity and the acceleration among neighbor pedestrians plays a significant role in the formation of the pedestrian's trajectory. For example, the acceleration or deceleration of an individual person can be caused by the acceleration or deceleration of a nearby individual person. In addition, the greater velocity that may have an individual from its nearby pedestrians will create an empty space behind him that in turn can provoke the growth of the velocity of his neighbor who has the choice now to walk faster. Thus, we try to construct the equations with the suitable combination of the pedestrian dynamics variables. We want also to examine whether there is a universal form of equation that is repeated and approximates the trajectories of the pedestrians. Moreover, we construct a macroscopic case of research. The additional data of the average trajectories and frequency will guide us to proceed in the calculation of the analytical equations that describe the average movement behavior. These equations introduce a universal behavior and the comparison of the macroscopic with the microscopic results will reveal many useful information and conclusions about the crowd behavior.

3.2 Main constraints

One of the most important issues is the formation of the input data. The formation of the input data is the first step of searching our equations of pedestrian movement. This procedure resembles the basic assumptions and it is a direct modeling of the equation's form. We create a physical explanation and we specify the list of the independent variables of the equation. In our case of searching equations, our results and their universality are greatly dependent on the way that we will import the independent variables. The independent variables are time series that have come up from real video recordings.

The second issue we have to deal with is the enormous search space of equations. There is a huge number of equations with different components and forms that can approximate the trajectory of the pedestrian. We should choose from these equations the ones that have not only a significant fitting with the real data but also a physical explanation.

The third issue is related to our purpose that is to detect any underline physical law among the trajectories. In other words, we search for equations with a physical meaning. We want to find a universal form of equation that would be able with the suitable calibration to simulate the movement of the pedestrian.

In order to overcome all the issues, we develop our methodology. First of all, we create three different cases of search. In this way we examine and edit our input data taking into account different aspects in order to construct the analytical equations of the pedestrian trajectory. Secondly, we use a specific genetic algorithm that uses symbolic regression in order to guide our procedure among the search space and is able to achieve its predictive ability for physical laws with the use of partial derivatives.

3.2.1. First microscopic search case

In the first case of search we are trying to find the vertical coordinate of the pedestrian movement as a function of time, Euclidian distance among the individuals namely the difference of their coordinates, velocity and acceleration of their movement. We are focusing our interest in the person found in the middle position. This person has in her sight of view the other two individuals in front of her. Our intention is to prove that among the movement of the pedestrian exist forces that are dependent from the distance. This case is inspired from empirical observations. These observations dictate that the motion of the pedestrians has some similarities with the motion of

charged particles. We know from electrostatics that charged particles exert forces on each other [18]. According to Coulomb's law the magnitude of the electrostatic force between two particles is inversely proportional with the square of their intermediate distance. This means that the force is greatly decreasing as the distance is rising. Similarly, we want during this case to examine whether the pedestrian movement appears to have the same attributes namely large interaction forces when the individuals are close enough and a fast decrease of those forces as the intermediate distance is rising. Similarly, in this case we want to examine whether pedestrian movement has similar properties namely great interaction forces when individuals are close enough and a small interactions as the intermediate distance increases.

The general form of the search equation is:

$$y_1 = f\left(t, x1, V_{x1}, V_{y1}, a_{x1}, a_{y1}, x_1 - x_2, y_1 - y_2, x_1 - x_3, y_1 - y_3\right) \qquad (3.1)$$

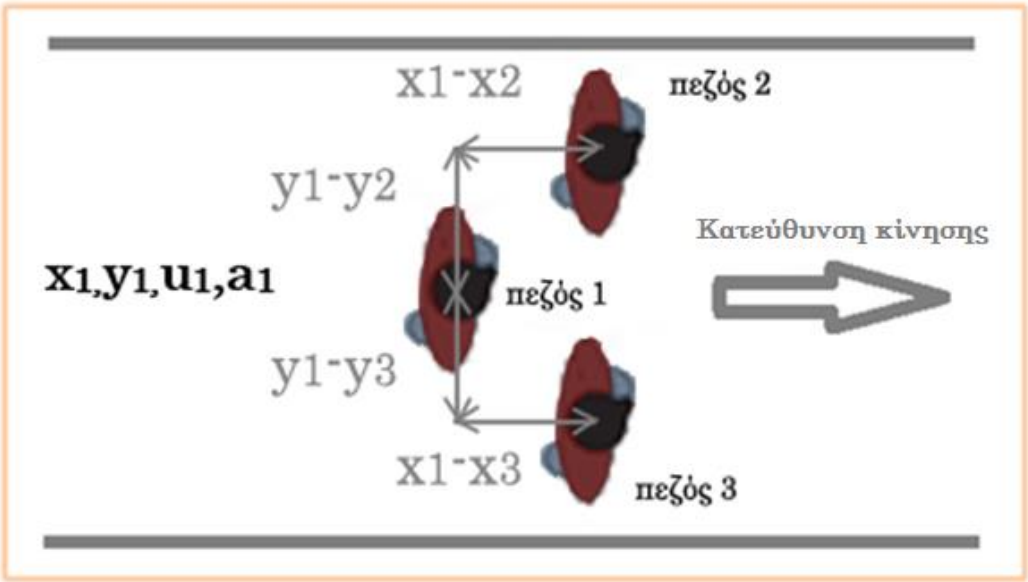

Figure 3.1 The quest process of corresponding equations for the first microscopic search case

We can see in the above equation, the list of the candidate independent variables (input variables). In the formation of the equation it is not necessary to participate the whole list. The final equations will be constructed from the most adequate variables that describe the behavior of the pedestrians from the video recordings with the more accurate way.

3.2.2. Second microscopic search case

In the second examined case, we are trying to find the vertical coordinate of the pedestrian movement as a function of time, velocity and acceleration of all the three people of the initial microscopic formation. We are not focusing our examination only in the middle individual but we try to correlate each person of the initial formation with the behavior of the other two. In this case the concept is same as the previous one but we introduce different candidate independent variables for the searching procedure. The candidate variables in this situation are those that describe the pedestrian dynamics of each individual. This case is also inspired from empirical observations. The difference with the previous case is that there are more candidate variables for the formation of the equation and we there is more freedom for the formation of the final equations. Additionally, we examine the behavior of all the three people of the molecular structure because we want to make comparisons among the corresponding results.

The general forms of the search equations are:

$$y_1 = f(Dynamics_{person1}, Dynamics_{person2}, Dynamics_{person3}) \qquad (3.2)$$

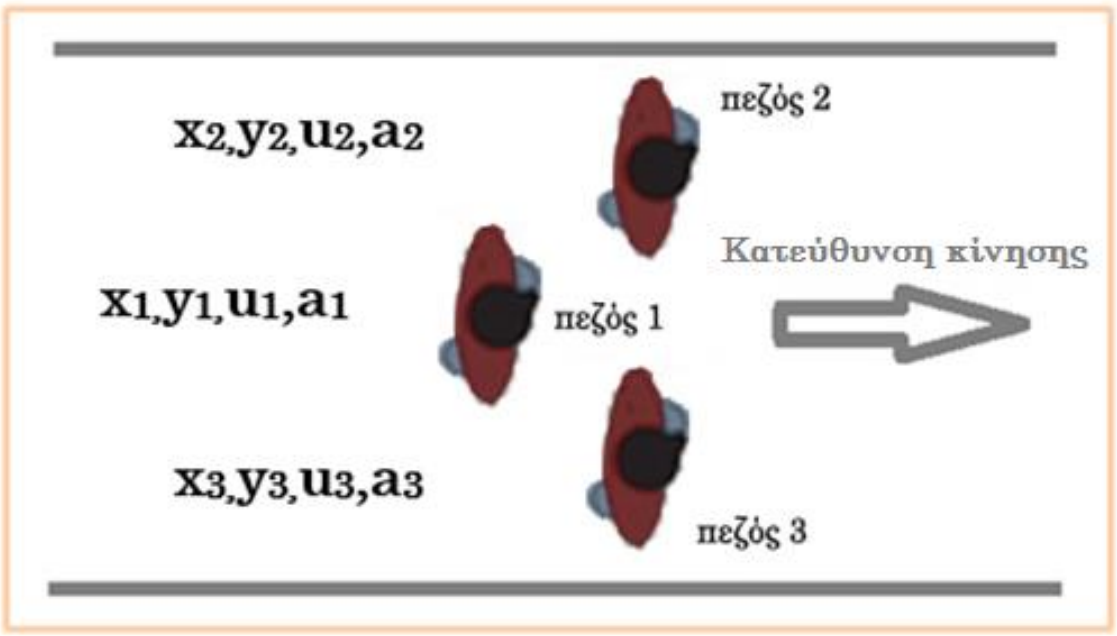

Figure 3.2 The quest process of corresponding equations for the second microscopic search case

Or more detailed

Person 1 **Person 2** **Person 3**

$$y_1 = f(t, x_1, V_{x1}, V_{y1}, a_{x1}, a_{y1}, x_2, y_2, V_{x2}, V_{y2}, a_{x2}, a_{y2}, x_3, y_3, V_{x3}, V_{y3}, a_{x3}, a_{y3}) \quad (3.3)$$

Similarly, we have the equations for the other two persons:

$$y_2 = f(t, x_1, y_1, V_{x1}, V_{y1}, a_{x1}, a_{y1}, x_2, V_{x2}, V_{y2}, a_{x2}, a_{y2}, x_3, y_3, V_{x3}, V_{y3}, a_{x3}, a_{y3}) \quad (3.4)$$

$$y_3 = f(t, x_1, y_1, V_{x1}, V_{y1}, a_{x1}, a_{y1}, x_2, y_2, V_{x2}, V_{y2}, a_{x2}, a_{y2}, x_3, V_{x3}, V_{y3}, a_{x3}, a_{y3}) \quad (3.5)$$

3.2.3. Third macroscopic search case

The third case of search is an examination of the crowd behavior. We are trying to find the vertical coordinate of the flow movement as a function of time, velocity and acceleration. Each of the three flows is a signal-oscillation that is calculated by the average trajectory of 6 pedestrians. Additionally, we compute the average position coordinates, velocity and acceleration for each flow. The candidate independent variables are the average position, velocity and acceleration. We are trying to correlate the three different flows and compare the results. At the end, we want to compare the macroscopic case equation with those of the microscopic cases. This comparison will be very

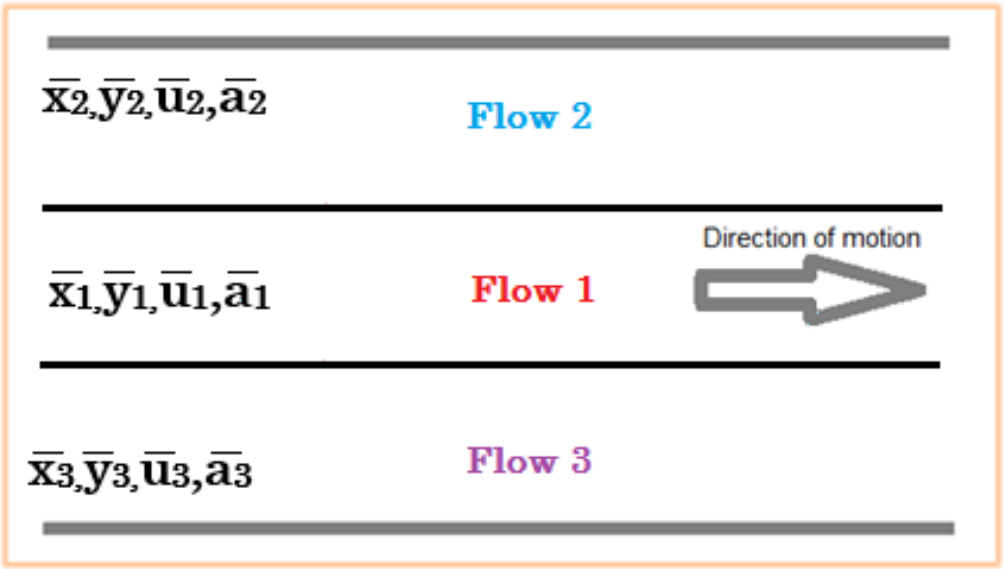

Figure 3.3 The quest process of corresponding equations for the third macroscopic search case

useful for our conclusions about the movement and the interaction that exert among the walking

individuals. This comparison will be very useful for our conclusions relating to the movement and interactions among the walking people.

The general forms of the search equations are:

$$y_{flow\_1} = f(Dynamics_{flow\_1}, Dynamics_{flow\_2}, Dynamics_{flow\_3}) \quad (3.6)$$

Or more detailed

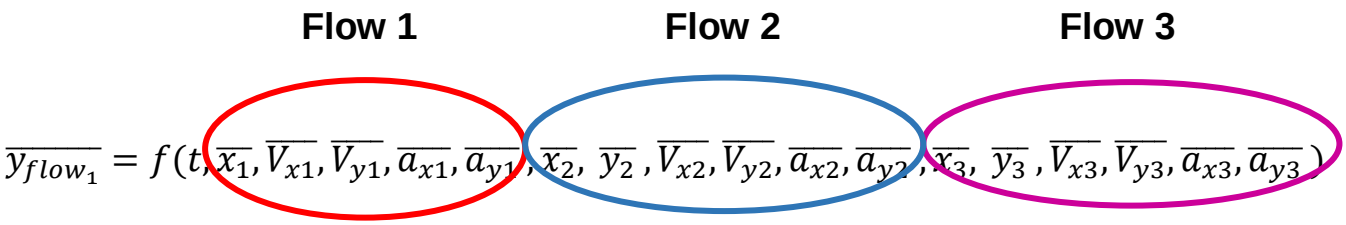

$$\overline{y_{flow_1}} = f(t, \overline{x_1}, \overline{V_{x1}}, \overline{V_{y1}}, \overline{a_{x1}}, \overline{a_{y1}}, \overline{x_2}, \overline{y_2}, \overline{V_{x2}}, \overline{V_{y2}}, \overline{a_{x2}}, \overline{a_{y2}}, \overline{x_3}, \overline{y_3}, \overline{V_{x3}}, \overline{V_{y3}}, \overline{a_{x3}}, \overline{a_{y3}}) \quad (3.7)$$

Similarly, we have the equations for the two other flows:

$$\overline{y_{flow_2}} = f(t, \overline{x_1}, \overline{y_1}, \overline{V_{x1}}, \overline{V_{y1}}, \overline{a_{x1}}, \overline{a_{y1}}, \overline{x_2}, , \overline{V_{x2}}, \overline{V_{y2}}, \overline{a_{x2}}, \overline{a_{y2}}, \overline{x_3}, \overline{y_3}, \overline{V_{x3}}, \overline{V_{y3}}, \overline{a_{x3}}, \overline{a_{y3}}) \quad (3.8)$$

$$\overline{y_{flow_3}} = f(t, \overline{x_1}, \overline{y_1}, \overline{V_{x1}}, \overline{V_{y1}}, \overline{a_{x1}}, \overline{a_{y1}}, \overline{x_2}, \overline{y_2}, \overline{V_{x2}}, \overline{V_{y2}}, \overline{a_{x2}}, \overline{a_{y2}}, \overline{x_3}, \overline{V_{x3}}, \overline{V_{y3}}, \overline{a_{x3}}, \overline{a_{y3}}) \quad (3.9)$$

3.3 The GA of searching equations

The GA for searching the equations is a specific GA that uses symbolic regression in order to construct the candidate equations. The GA consist of two basic procedures.

- The first one is the core of the algorithm. It is a procedure named “symbolling regression” [2]

  “*Symbolic regression is an established method based on evolutionary computation for searching the space of mathematical expressions by calculating both the parameters and the form of equations simultaneously while it minimizes various error metrics* [19]." Symbolic regression is the procedure of finding a mathematical expression in symbolic form that is fitting with the best way to a given finite set of sample values. Symbolic regression differs from conventional linear, quadratic, or polynomial regression, which merely involve finding the numeric coefficients for a function whose form (linear, quadratic, or polynomial) has been prespecified. Thus, symbolic regression involves finding a model that fits a given sample of data. In the case of data from the real world, this problem of finding the model from the data is often called empirical discovery.
  In the following paragraph we describe in detail the procedure of symbolic regression that we use in our situation in order to discover the equations that represent the pedestrian’s movement. We start with some initial expression that consist of randomly combined mathematical building blocks algebraic operators {+, –, ÷, ×}, analytical functions (for example, sine and cosine), constants, and state variables. New equations are formed by recombining previous equations and probabilistically varying their subexpressions in an evolutionary way using the operators of crossover and mutation. The algorithm retains equations that model the experimental data better than others and abandons unpromising solutions making use of a metric. At the end, we keep only a subset with equations that have the biggest probability of correspondence to underlying physical laws.

- The second one is a metric that is suitable for our purpose. We use this metric as a way to distinguish good candidate equations that may represent physical laws from those that don’t. The metric uses the idea that the candidate equations may represent physical laws only if they are able to predict connections between dynamics of subcomponents of the system. We make use of the partial derivative between pairs of variables for the role of this metric*. This means that our candidate equations may represent physical laws only if they are able to have an adequate fitting with the partial derivative of the two variables from the input tracked data when they are partially differentiated with the same variables.*

[2] Michael Schmidt and Hod Lipson **Distilling Free-Form Natural Laws from Experimental Data** *Science* 324, 81(2009)

3.4 The overall procedure of searching equations

In total, the proposed procedure of searching equation is as follows:

At start, we import the time series with the tracking procedure from the trajectories of the pedestrians. The time series are different for each case of search. The time series may be for example *x(t)* and *y(t)* in correspondence with the Cartesian coordinates of the pedestrians . Then, we calculate numerically the partial derivatives of those time series data as is shown below:

$$\frac{x'}{y'} = \frac{\frac{dx}{dt}}{\frac{dy}{dt}} \approx \frac{\Delta y}{\Delta x} \qquad (3.10)$$

With the use of the GA we construct a population of candidate equations. Subsequently, we differentiate each candidate equation *f* and we store those values:

$$\frac{\frac{\delta f}{\delta y}}{\frac{\delta f}{\delta x}} \approx \frac{\delta y}{\delta x} \quad (3.11) \quad and \quad \frac{\frac{\delta f}{\delta x}}{\frac{\delta f}{\delta y}} \approx \frac{\delta x}{\delta y} \quad (3.12)$$

Now we can compare $\frac{\Delta y}{\Delta x}$ values from the experimental data with $\frac{\delta y}{\delta x}$ values from a candidate equation and measure with this way how well they present intrinsic relations in the system.

We keep from these equations the ones which minimize the error: $\frac{\Delta x}{\Delta y} - \frac{\delta x}{\delta y}$

The equations that achieve better scores are highly rated. After the use of the evolution operators of crossover and mutation of different mathematical expressions we derive new candidate equations and evaluate them. The most highly rated equations are forming the population of the next generation and the GA is continuing to the next iteration. After, several iterations we have some of the best scored equations.

4. Processing of pedestrian movement data

We have mentioned that we are approaching the trajectories of the pedestrian as if they are oscillations. This assumption gives us the opportunity to use a variety of mathematical tools. Thus, we can see from another point of view our trajectories and take additional results that may lead us to additional conclusions. Furthermore, we can evaluate our previous results from the search of analytical equations and examine whether they are in agreement.

We use two signal processing functions: cross-correlation and autocorrelation. We make some calculations with these two functions and thus we can have a clearer and deeper insight about the behavior of the pedestrians. The purpose of this chapter is to obtain an analytical knowledge concerning the frequency spectrum of the pedestrians' movement-oscillation.

4.1 Cross-correlation

The mathematical definition of cross correlation for discrete functions is the following:

$$(\boldsymbol{f} * \boldsymbol{g})[\boldsymbol{n}] \stackrel{\text{def}}{=} \sum_{\boldsymbol{m}=-\infty}^{\infty} \boldsymbol{f}^{*}[\boldsymbol{m}]\boldsymbol{g}[\boldsymbol{m}+\boldsymbol{n}] \quad (4.1)$$

In signal processing, cross-correlation is a measure of similarity of two series as a function of the

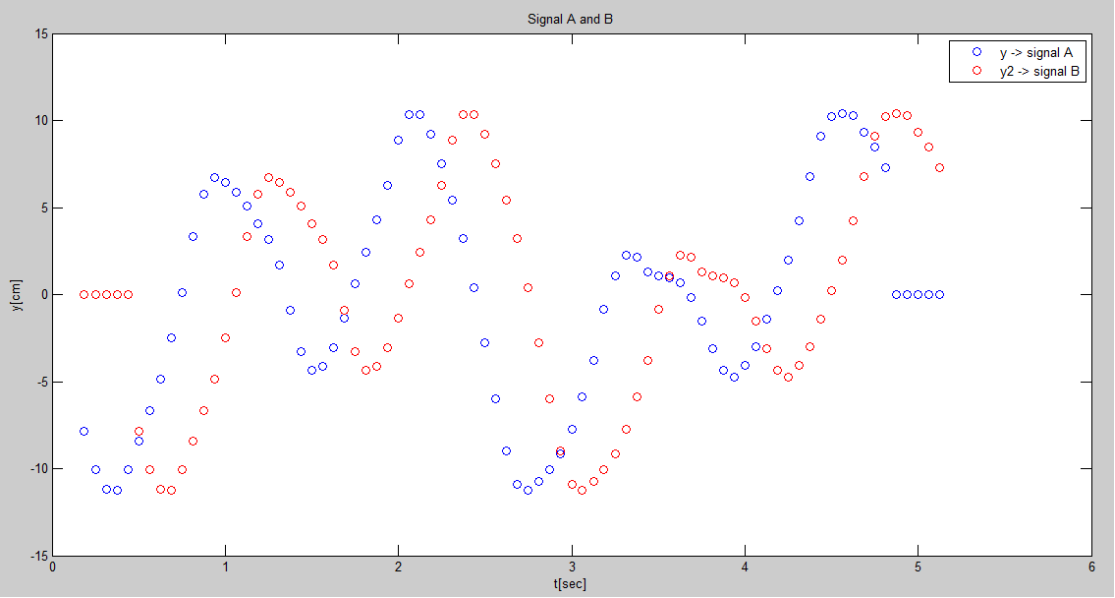

Figure 4.1 Two signals A and B to demonstrate cross-correlation function

displacement of one relative to the other. The cross-correlation of the two measurements has a maximum at a point in the time axis equal to the delay. In our situation, cross-correlation give us

the displacement between two pedestrians. In order to clarify the operation of the function we present an example. In Figure 4.1 we can see two signals A and B. Signal B is a lagged copy of signal A by 0.3125 seconds.

In Figure 4.2 we can see the result of cross correlation of signal A and B. We observe that the highest peak of the plot is pointing on the value -0.3125 sec. This value as mentioned before corresponds to the lag between the two signals. The sign of the value is minus and indicates that the signal A is before the signal B.

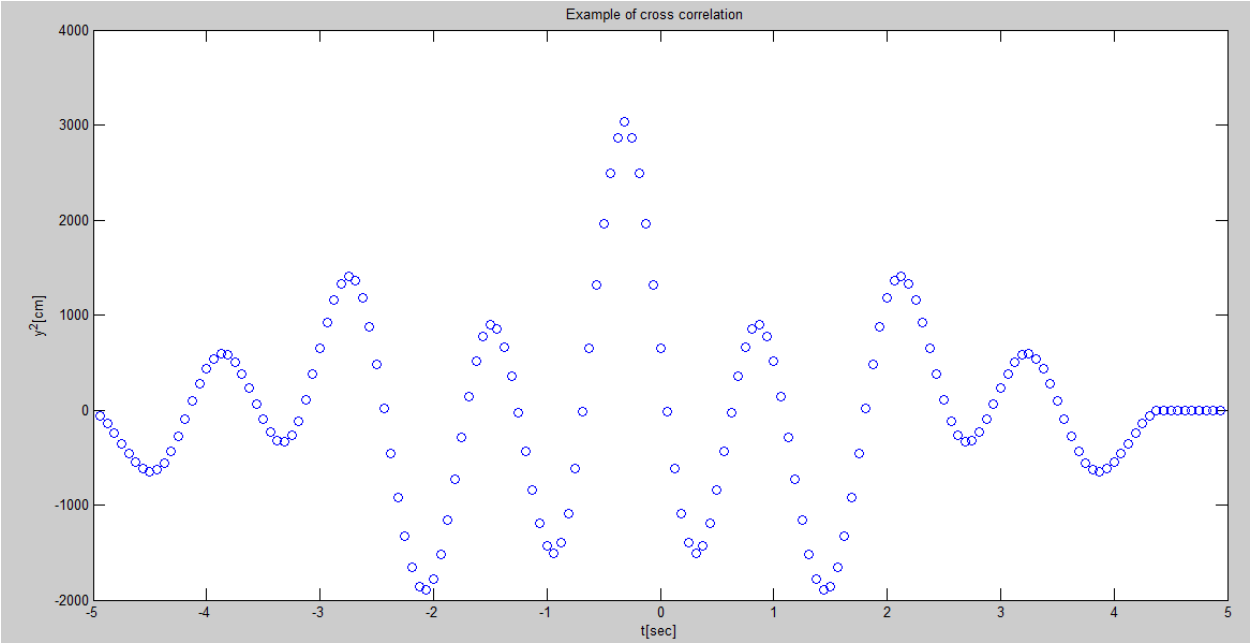

Figure 4.2 The result of the cross-correlation for the A and B signals. The highest peak is observed at the value corresponding to the relative displacement of the two signals.

In our problem the function of cross-correlation will give us the information about the displacement between the pedestrians. This information is very useful for our research because it provides us with the magnitude of the distance among the individuals. The distance would help us in our examination to have a deeper analysis in the nature of the interactions and for their more accurate future modeling.

4.2 Autocorrelation

The mathematical definition of autocorrelation for discrete functions is the following:

$$\boldsymbol{R_{ff}[n]} = \boldsymbol{(f * f)[n]} \stackrel{\text{def}}{=} \sum_{\boldsymbol{m=-\infty}}^{\infty} \boldsymbol{f^*[m] f[m+n]} \qquad (4.2)$$

Autocorrelation is the correlation of a signal with a delayed copy of itself as a function of delay. The analysis of autocorrelation is a mathematical tool for finding repeating patterns, such as the presence of a periodic signal obscured by noise, or identifying the missing fundamental frequency in a signal implied by its harmonic frequencies. It is often used in signal processing for analyzing functions or series of values, such as time domain signals.

Autocorrelation has greater resolution for low frequency signals. From empirical observations we know pedestrian movement is made up of low frequencies, so this function is appropriate for our examination.

4.3 Results of cross-correlation and autocorrelation

At this point, we need to highlight some important details about the conditions of the time series we use in the signal processing process.

- Place the oscillation reference to zero.

  Our oscillation has an offset value (dc) due to the arbitrary placement of the reference of the axis system during the tracking process. The function we use needs to eliminate this offset in order to take useful results.

We apply cross-correlation and autocorrelation to data from video recordings. First, we process the data from the microscopic procedure namely the oscillation-orbits derived from separate individuals. Then we apply the same functions to data derived from the macroscopic procedure, namely the average orbit from six different individuals. Also, by using spectrum analysis functions we will investigate the oscillation frequencies that can lead us to useful conclusions. That's why

we're studying 6 different video recordings with different corridor widths and different crowd densities. Pedestrian traffic is studied and results in one direction only.

4.3.1. Cross correlation and auto correlation to individuals

1. First video recording

In figure 4.3 we can observe the trajectories of the individuals from a part of a video from Hermes, namely uo-145-180-180_cam2. The waveforms result directly from the tracking procedure..

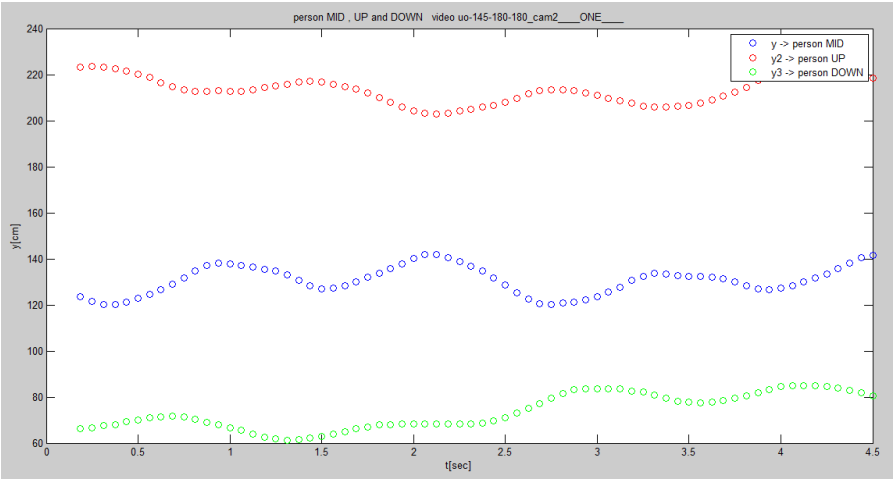

Figure 4.3 Pedestrian trajectories as recorded by video uo-145-180-180_cam2

Note that the recording process does not take into account the horizontal relative shift between individuals. This means that in Figure 4.3 we observe the vertical trajectory on the walking direction of the pedestrian. This depicts the head's motion of each pedestrian without including the relative horizontal displacement between the tracks due to their different initial position.
In Figure 4.4, we see the same people's trajectories from the same part of the video uo-145-180-180_cam2 only that in this case we have removed the mean value and the oscillations have their reference to zero.

Figure 4.5 shows the result from the application of the cross-correlation function for each combination of the three oscillation-signals presented above. As we have previously mentioned, cross-correlation gives us the relative displacement between the waveforms for each pair of individuals if we observe the value of the highest peak for each waveform.

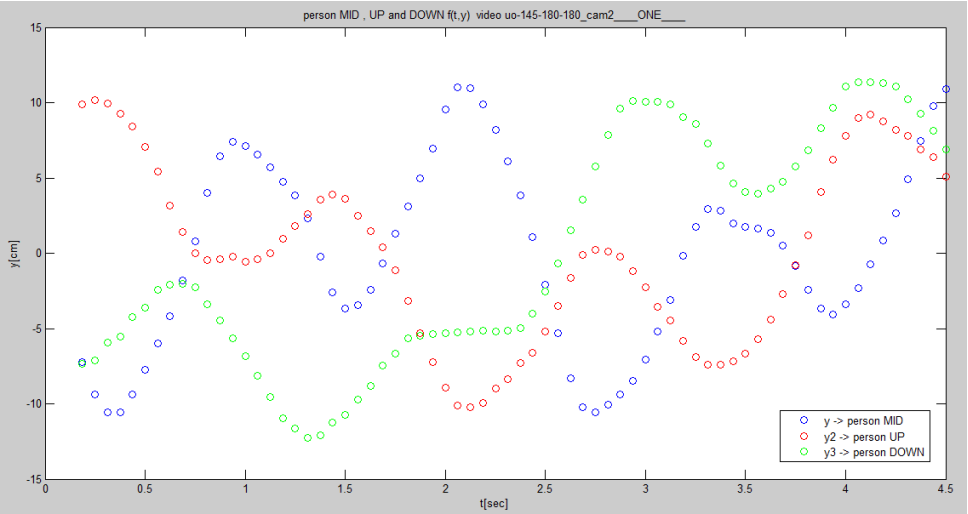

Figure 4.4 Pedestrian trajectories as recorded having removed the average value

Figure 4.5 shows the result from the application of the cross-correlation function for each combination of the three oscillation-signals presented above. As we have previously mentioned, cross-correlation gives us the relative displacement between the waveforms for each pair of individuals if we observe the value of the highest peak for each waveform. Thus, according to the results the distance between the middle and the lower individual is 2 [sec] while the middle precedes. The distance of the middle with the upper individual is 0.8 [sec] and the upper one precedes. The distance between the upper and the lower individual is 1.1 [sec]. These results were expected due to the alignment of the individuals in the search process that has been presented in previous chapter

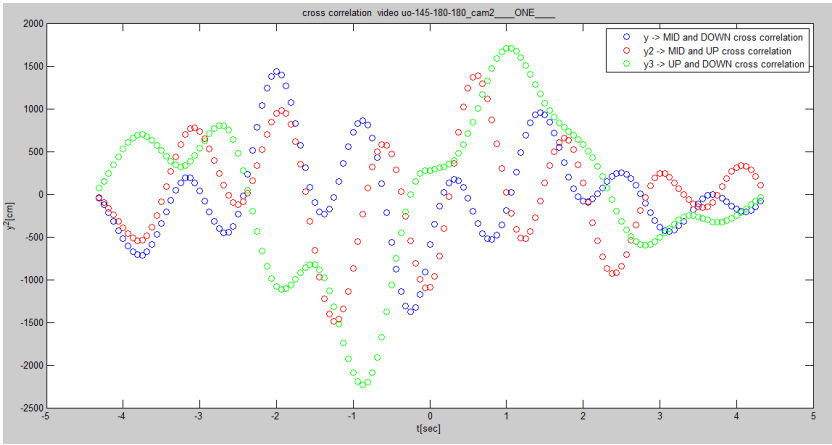

Figure 4.5. The waveforms of the cross-correlation application for each pair between the three input waveforms.

In Figure 4.6 we see the result from the application of the autocorrelation function for each combination of the three oscillation signals. We observe that the waveforms are symmetrical and the highest peak at zero corresponds to the energy of the signal. From the remaining peaks we can extract the basic frequencies that appear in the oscillation movements.Due to the fact that the initial signals have finite length, eventhough we can calculate the basic frequencies, our estimation of the energy distribution is limited. The sampling period is T=0.0625[sec] and the sampling frequency $f = \frac{1}{0.0625} = 16$[Hertz] . The frequencies are calculated by the equation $f = \frac{f_S}{mi} = \frac{16}{mi}$, where mi is the number of samples after which the signal is repeated, or differently the samples that correspond to each peak. Thus, for the middle individual we have: mi =19[samples] or 19*0.0625[sec]=1,18[sec], mi =38 [samples] and mi =56[samples] for each peak corresponding to $f = 0.84$[Hz] , $f = 0.42$[Hz] and $f = 0.28$[Hz].

For the upper individual we have: mi =19[samples] , mi =42[samples] and mi =61[samples] for each peak corresponding to $f = 0.84$[Hz] , $f = 0.38$[Hz] and $f = 0.26$[Hz].

For the lower individual we have: mi =35[samples] for each peak corresponding to $f = 0.46$[Hz]

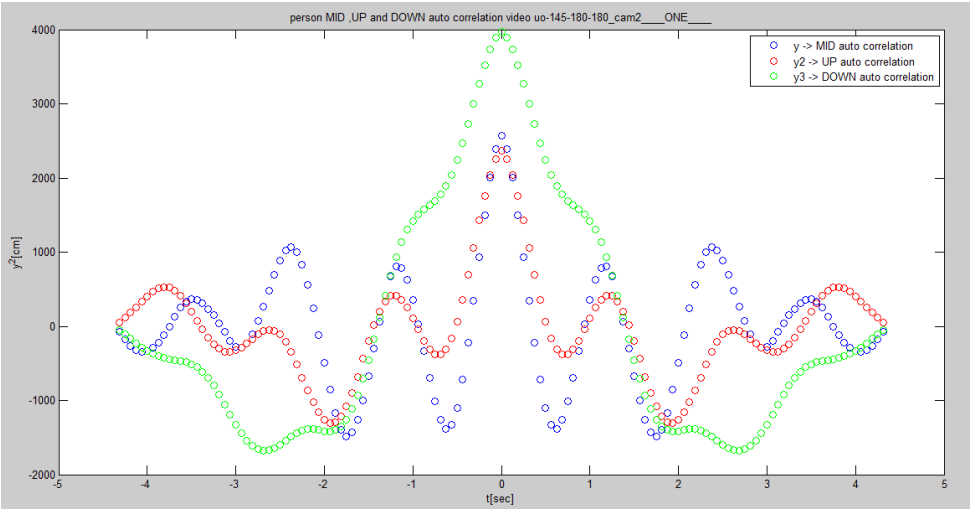

Figure 4.6. The result of autocorrelation between the three input waveforms

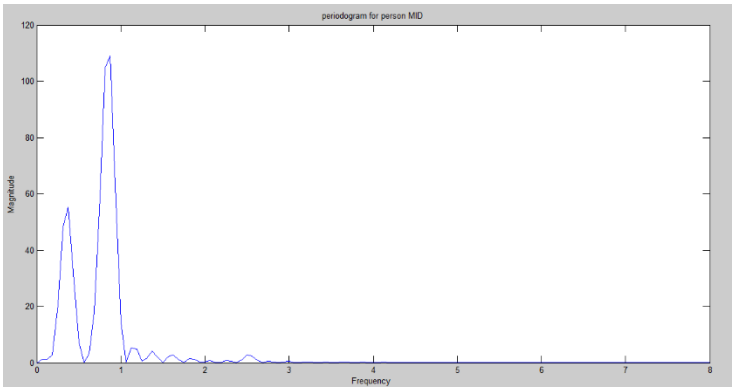

(a)

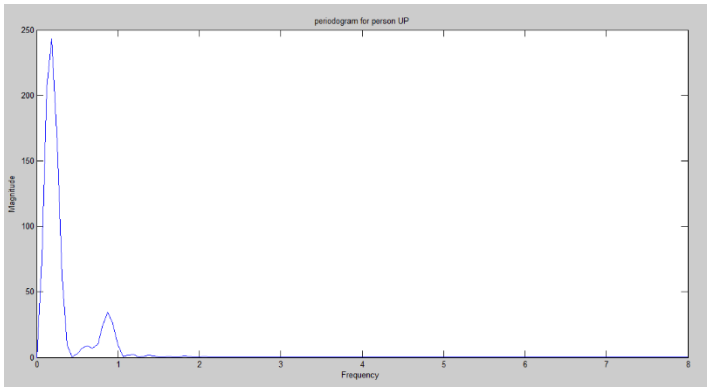

(b)

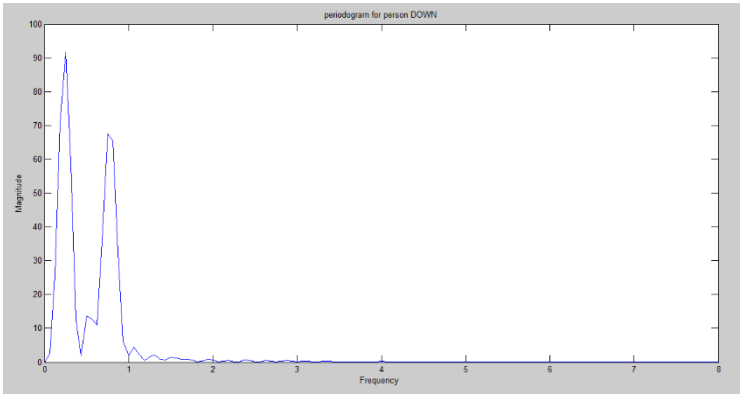

(c)

Figure 4.7 Spectral analysis of the trajectories: (a) of the middle individual (b) of the upper individual and (c) of the lower individual

In Figure 4.7 we have presented the graphical representations of the spectral analysis of the signals where the previous calculations are confirmed. We observe that the frequencies for each individual-oscillation consist of almost the same frequencies as small deviations.

2. Second video recording

In figure 4.8 we can observe the trajectories of the individuals from a part of a video from Hermes, namely video uo-180-180-180_cam2. The waveforms are directly from the tracking procedure

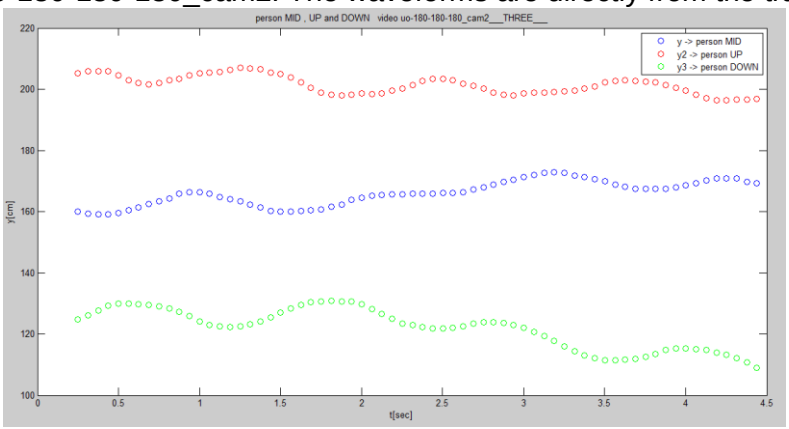

Figure 4.8 Pedestrian trajectories recorded as by video uo-180-180-180_cam2

In Figure 4.9 there are trajectories of individuals from the same part of the video uo-180-180-180_cam2 only that in this case we have removed the average value.

In Figure 4.10 we see the result from the application of the cross-correlation function for each combination of the three oscillation-signals. According to the results the distance between the middle and the lower individual is 2.4[sec] and the lower one precedes. The distance of the middle with the upper individual is *2.8* [sec] and the upper one precedes.

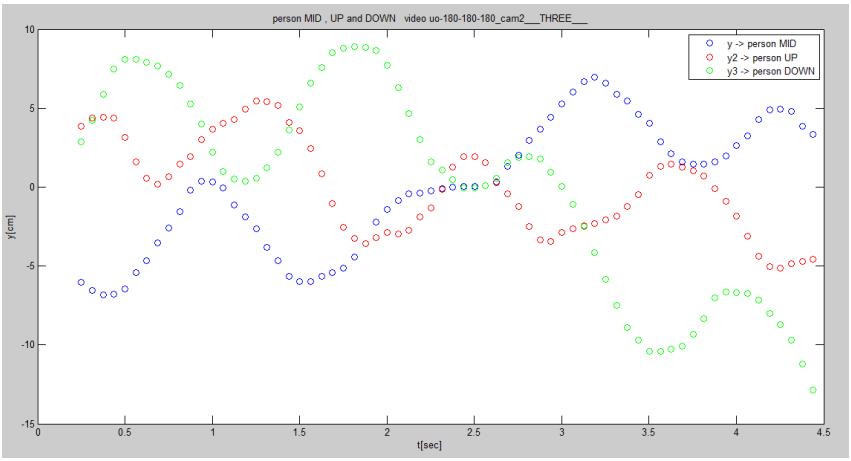

Figure 4.9 Pedestrian trajectories as recorded having removed the average value

The distance between the upper and the lower individual is 0.3 [sec] and the upper one precedes.

In Figure 4.11 we see the result from the application of the autocorrelation function for each

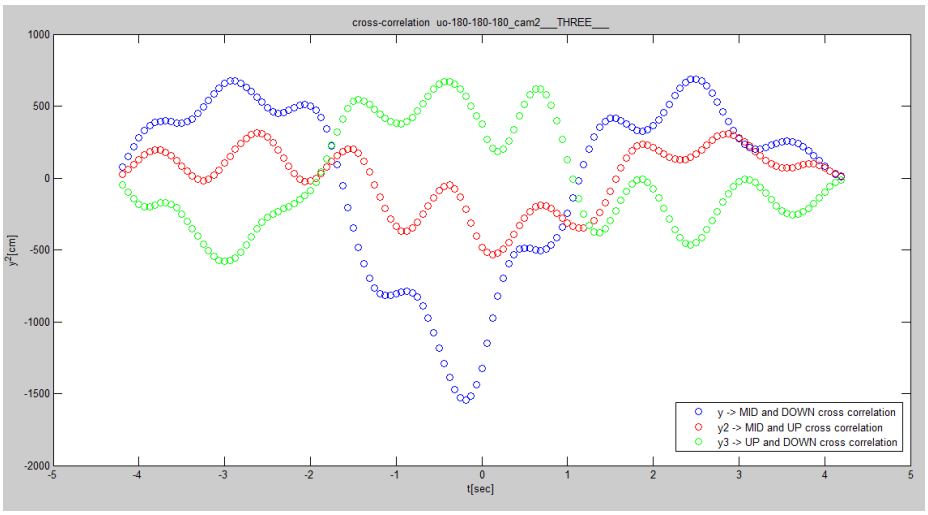

Figure 4.10. The waveforms of the cross-correlation application for each pair between the three input waveforms.

combination of the three oscillation signals. From the waveforms we have the following results: For the middle individual we have: mi =15[samples] , mi = 33[samples] and mi =54[samples] for each peak corresponding to $f = 1.06$ [Hz] , $f = 0.48$[Hz] and $f = 0.3$[Hz].

For the upper individual we have: mi =18[samples] , mi =36 [samples] and mi =56[samples] for each peak corresponding to $f = 0.9$[Hz] , $f = 0.44$[Hz] and $f = 0.28$[Hz].

For the lower individual we have: mi =34[samples] for each peak corresponding to $f = 0.47$[Hz] .

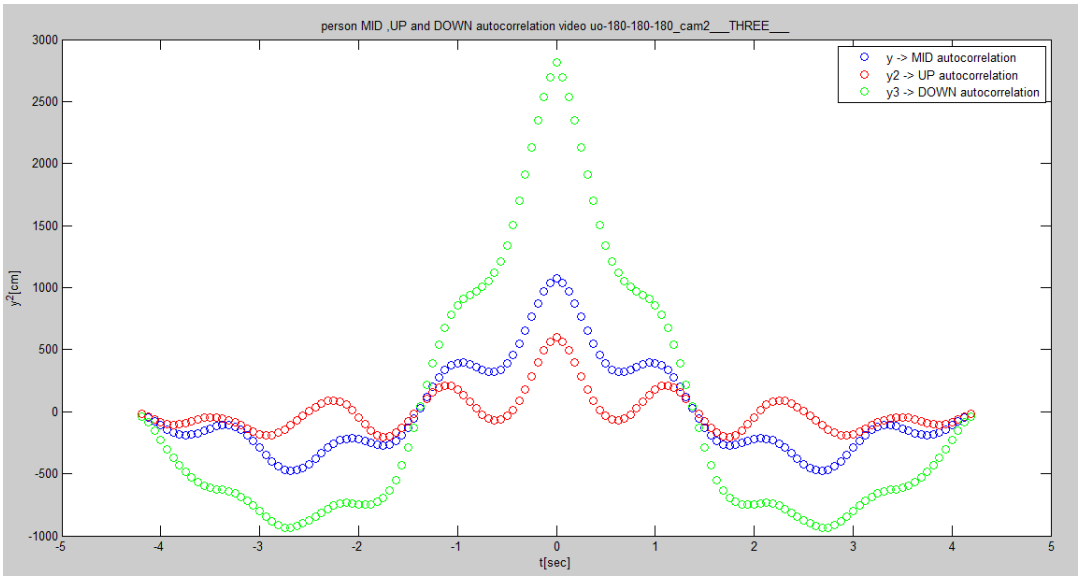

Figure 4.11. The result of autocorrelation between the three input waveforms

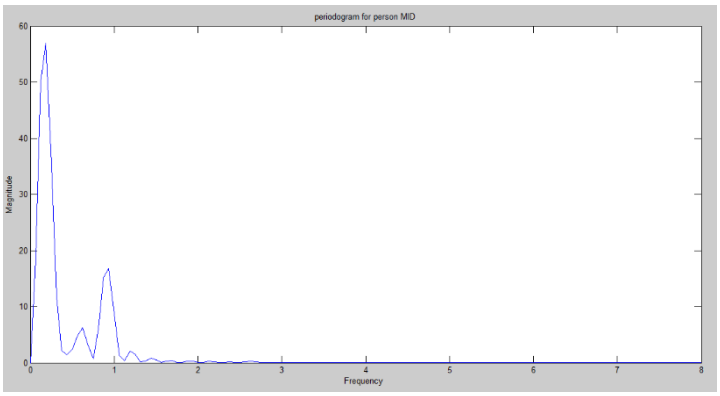

(a)

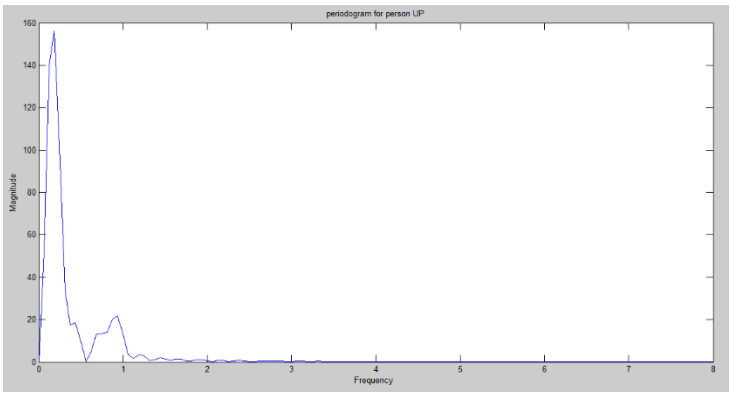

(b)

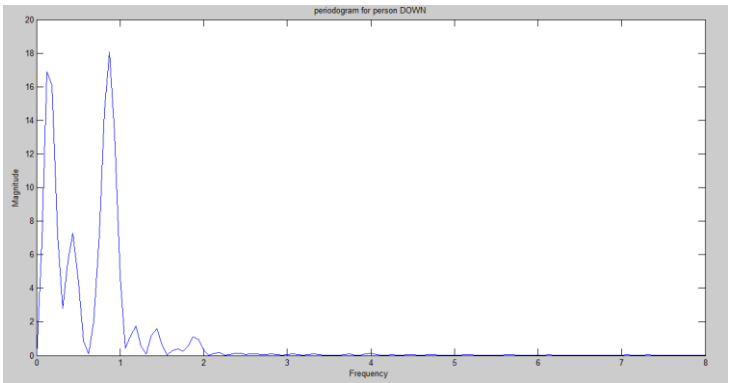

(c)

Figure 4.12 Spectral analysis of the trajectories: (a) of the middle individual (b) of the upper individual and (c) of the lower individual

In Figure 4.12 we have presented the graphical representations of the spectral analysis of the

signals where the previous calculations are confirmed. We observe that the frequencies for each individual-oscillation consist of almost the same frequencies with small deviations.

3. Third video recording

In figure 4.13 we can observe the trajectories of the individuals from a part of the same video uo-180-180-180_cam2 like before.

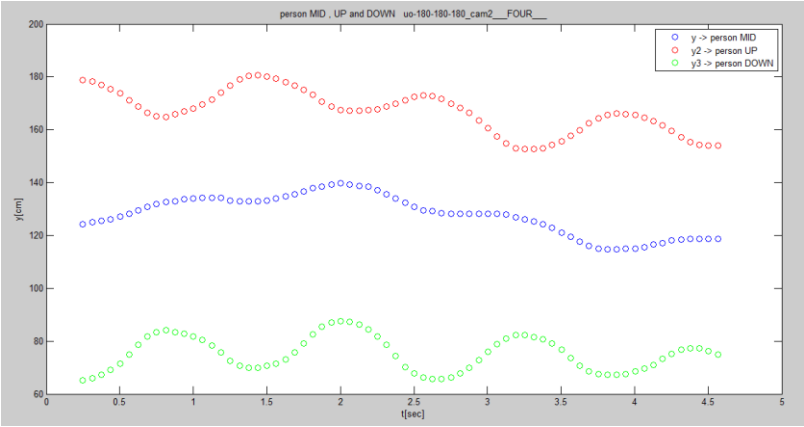

Figure 4.13 Pedestrian trajectories as recorded by video uo-180-180-180_cam2

In Figure 4.14 there are trajectories of individuals from the same part of the video uo-180-180-

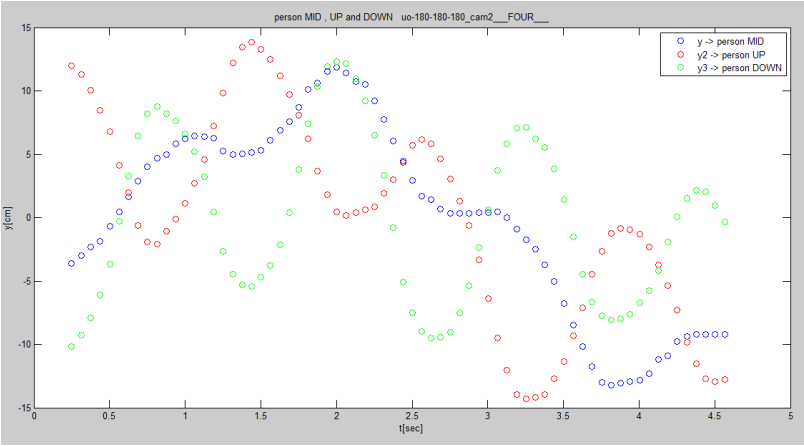

Figure 4.14 Pedestrian trajectories as recorded having removed the average value

180_cam2 only in this case we have removed the average value.

In Figure 4.15 we see the result from the application of the cross-correlation function for each combination of the three oscillation-signals. According to the results, the distance between the middle and the lower individual is 0.1[sec] and the lower one precedes. The distance of the middle with the upper individual is 0.8[sec] and the upper one precedes and the distance between the upper and the lower individual is 0.8[sec] and the lower one precedes.

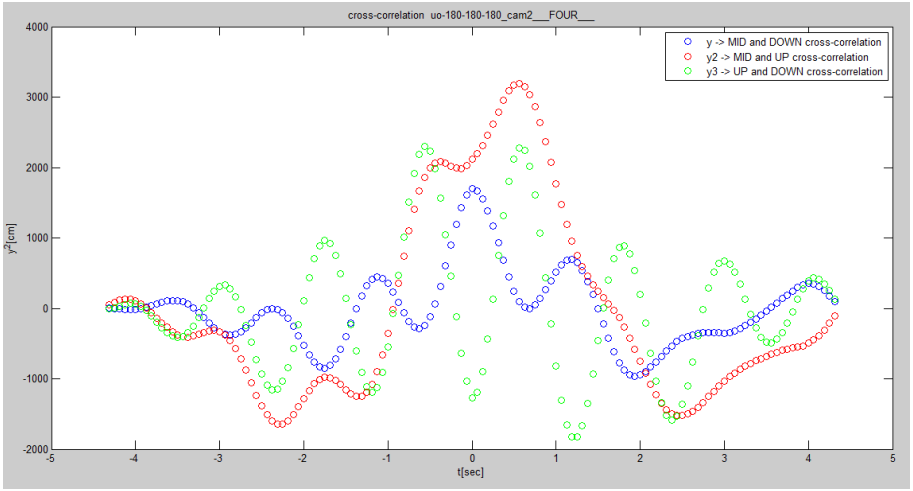

Figure 4.15 Cross-correlation waveforms for each pair between the three input waveforms.

In Figure 4.16 we see the result from the application of the autocorrelation function for each combination of the three oscillation signals. From the waveforms we have the following results:

For the middle individual we have: mi =65[samples], for each peak corresponding to $f = 0.25$[Hz].

For the upper individual we have: mi =18[samples], mi =38[samples] and mi =57[samples] for each peak corresponding to $f = 0.88$[Hz], $f = 0.42$[Hz] and $f = 0.26$[Hz]. For the lower individual

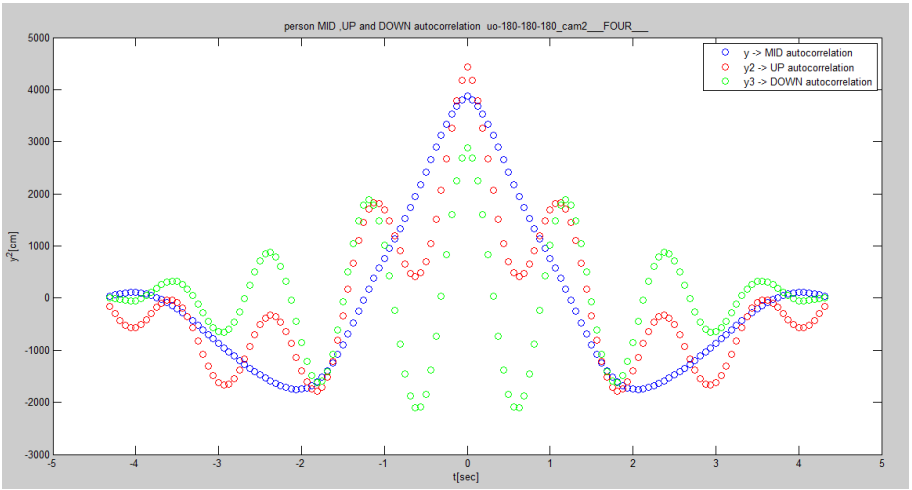

Figure 4.16 The result of autocorrelation between the three input waveforms

we have: mi =19[samples], mi =38[samples] and mi =57[samples] for each peak corresponding to $f = 0.84$[Hz] , $f = 0.42$[Hz] and $f = 0.26$[Hz].

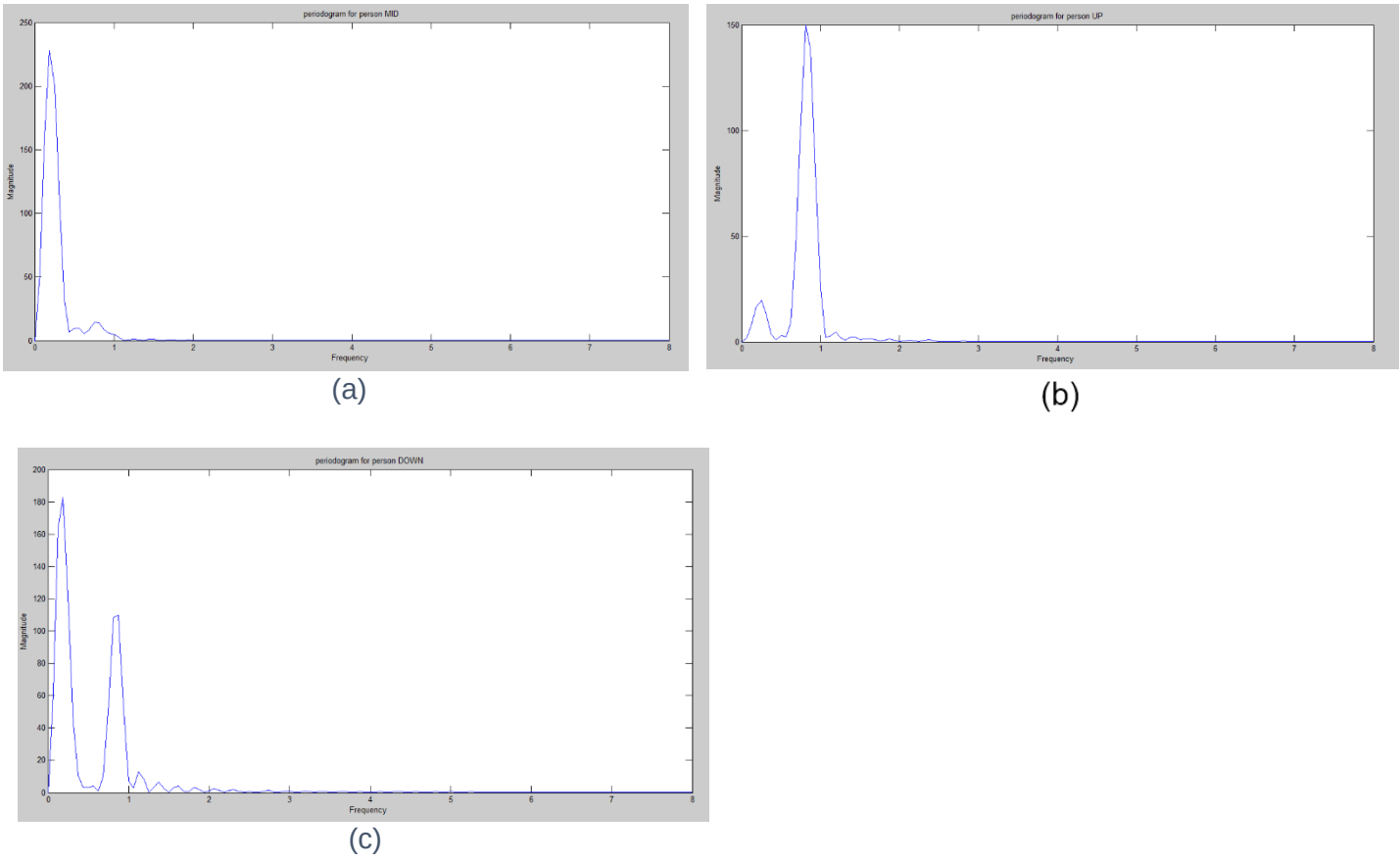

Figure 4.17 Spectral analysis of the trajectories: (a) of the middle individual (b)of the upper individual and (c) of the lower individual

In Figure 4.17 we have presented the graphical representations of spectral analysis of signals. Although we were unable to calculate the frequencies for the lower individual through autocorrelation, the spectral analysis gives us its spectrum. We again observe that the frequencies for each individual -oscillation consist of similar frequencies.

4. Fourth video recording

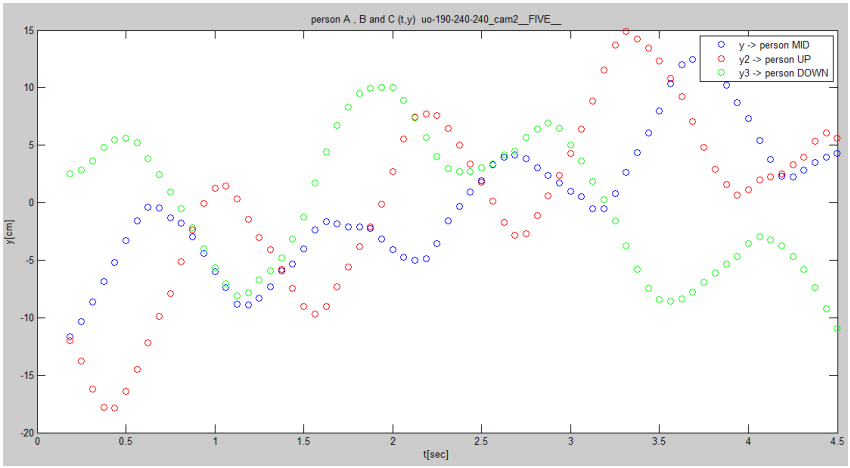

Figure 4.18 Pedestrian trajectories as recorded by video uo-180-180-180_cam2

In figure 4.18 we can observe the trajectories of the individuals from a part of a video from Hermes, namely uo-190-240-240_cam2. The waveforms are directly from the tracking procedure.

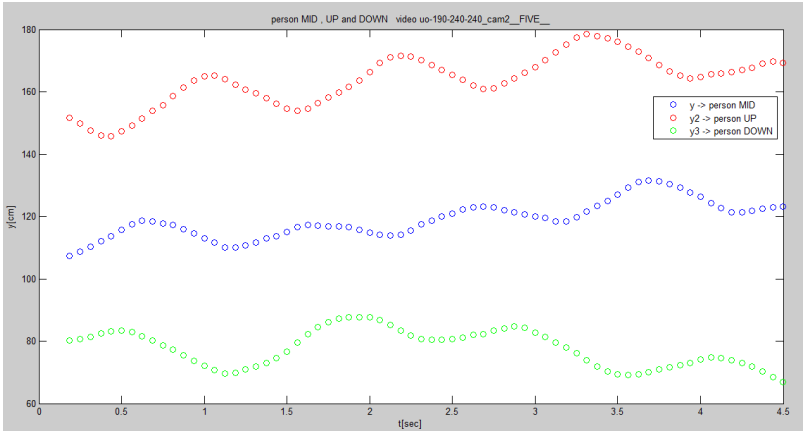

Figure 4.19 Pedestrian trajectories as recorded having removed the average value

In Figure 419 there are trajectories of individuals from the same part of the video uo-190-240-240_cam2 only that in this case we have removed the average value.

In Figure 4.20 we see the result from the application of the cross-correlation function for each combination of the three oscillation-signals. According to the results the distance between the middle and the lower individual is 0.1[sec] and the lower one precedes. The distance of the middle with the upper individual is 0.8[sec] and the upper precedes. The distance between the upper and the lower individual is 0.8[sec] and the lower one precedes.

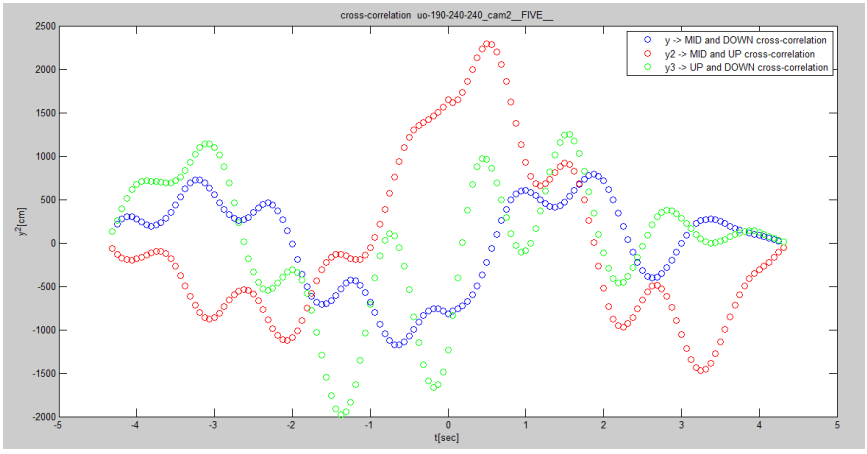

Figure 4.20 The cross-correlation waveforms for each pair between the three input waveforms.

In Figure 4.21 we see the result from the application of the autocorrelation function for each combination of the three oscillation signals. From the waveforms we have the following results:

For the middle individual we have: mi=14[samples], mi=29 [samples], mi=47[samples] and mi=64[samples] for each peak corresponding to $f = 1.14$ [Hz] , $f = 0.55$[Hz] and $f = 0.34$[Hz] $f = 0.25$[Hz].

For the upper individual we have: mi =18[samples] , mi =37 [samples] and mi =57[samples] for each peak corresponding to $f = 0.88$[Hz] , $f = 0.43$[Hz] and $f = 0.28$[Hz].

For the lower individual we have mi =17[samples], mi = 39[samples] and mi =52[samples] for each peak corresponding to $f = 0.94$[Hz] , $f = 0.41$[Hz] and $f = 0.59$[Hz]

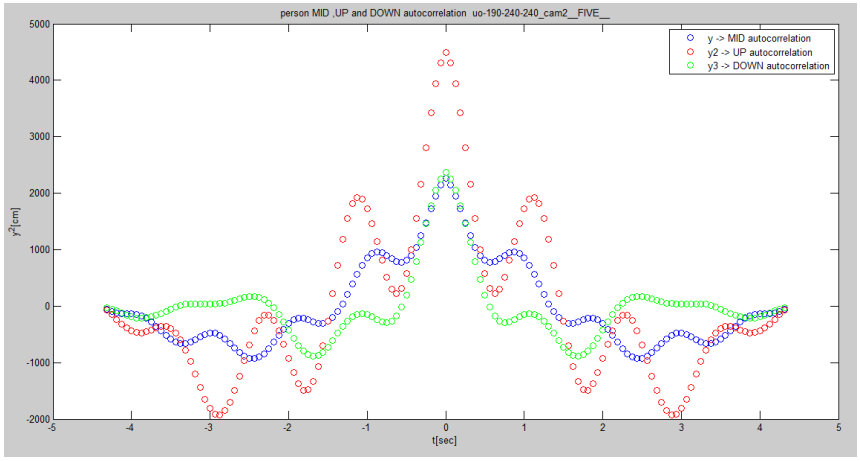

Figure 4.21. The result of autocorrelation between the three input waveforms.

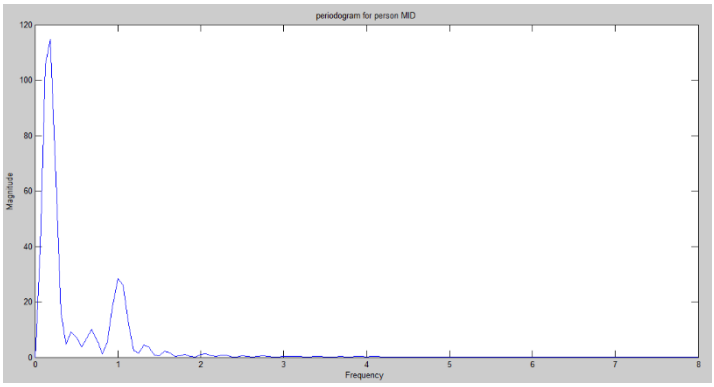

(a)

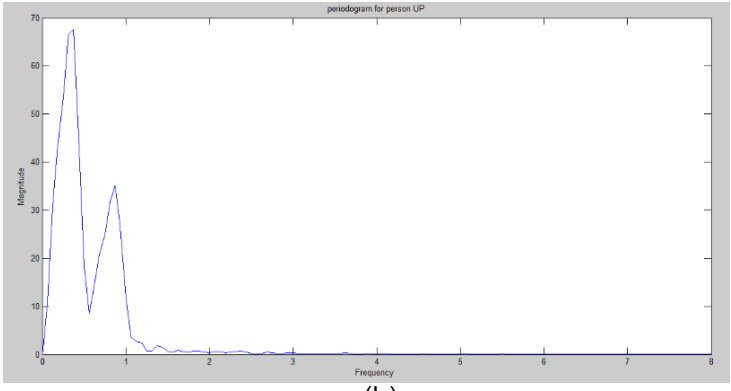

(b)

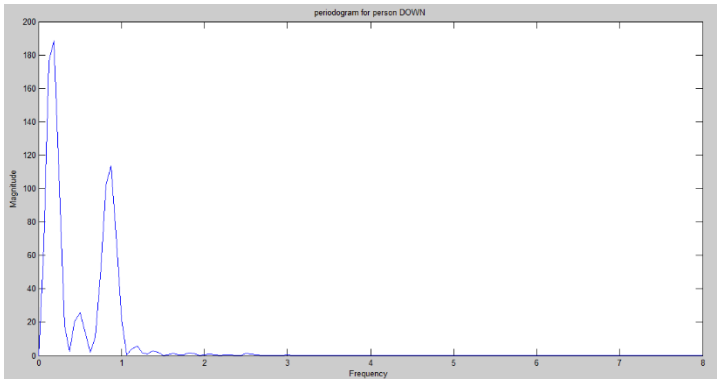

(c)

Figure 4.22 Spectral analysis of the trajectories: (a) of the middle individual (b) of the upper individual and (c) of the lower individual

In Figure 4.22 we have presented the graphical representations of the spectral analysis of the signals.

5. Fifth video recording

In figure 4.23 we can observe the trajectories of the individuals from a part of a another video from Hermes, i.e. uo-300-300-300_cam2

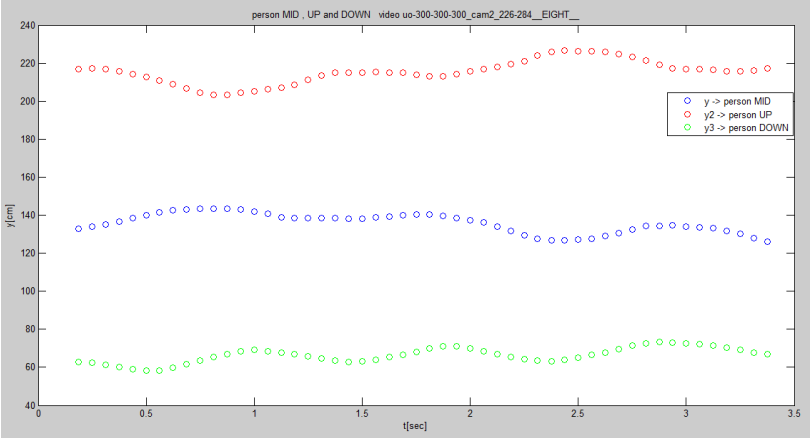

Figure 4.23 Pedestrian trajectories as recorded by video uo-300-300-300_cam2

In Figure 4.24 there are represented the trajectories of individuals from the same part of the video

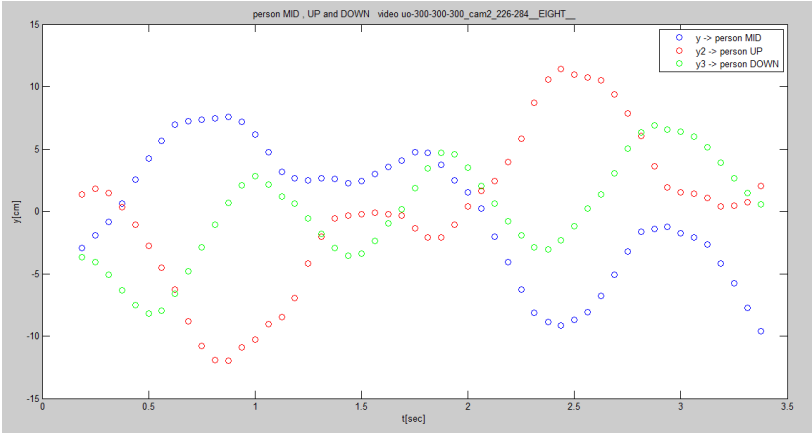

Figure 4.24 Pedestrian trajectories as recorded having removed the average value

uo-300-300-300_cam2 only that in this case we have removed the average value.

In Figure 4.25 we see the result from the application of the cross-correlation function for each combination of the three oscillation-signals. According to the results the distance between the

middle and the lower individual is 2[sec] and the lower one precedes. The distance of the middle with the upper individual is 1.5[sec] and the upper one precedes and the distance between the upper and the lower individual is 0.5[sec] and the lower one precedes.

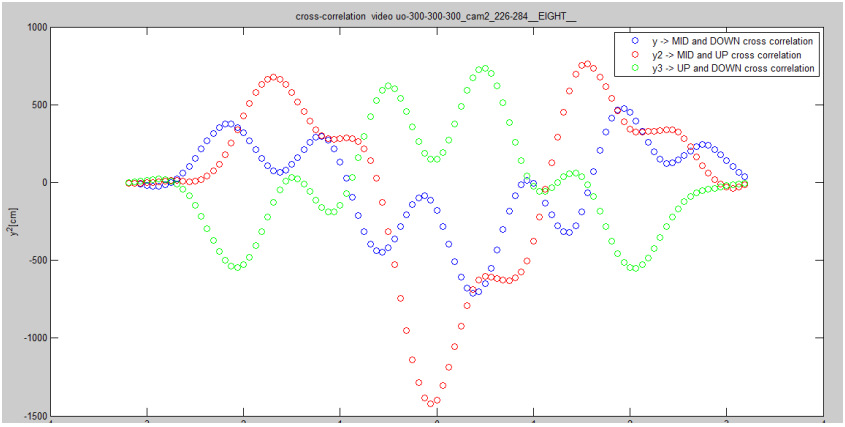

Figure 4.25 Cross-correlation waveforms for each pair between the three input waveforms.

In Figure 4.26 we see the result from the application of the autocorrelation function for each combination of the three oscillation signals. From the waveforms we have the following results:

For the middle individual we have: mi =14[samples], mi =36[samples] and mi =50[samples] for each peak corresponding to $f = 1.14$ [Hz] , $f = 0.44$ [Hz] and $f = 0.32$[Hz].

For the upper individual we have: mi =49[samples] for each peak corresponding to $f = 0.33$[Hz].

For the lower individual we have: mi =15[samples], mi =30[samples] for each peak corresponding to $f = 1.06$[Hz] , $f = 0.53$[Hz]

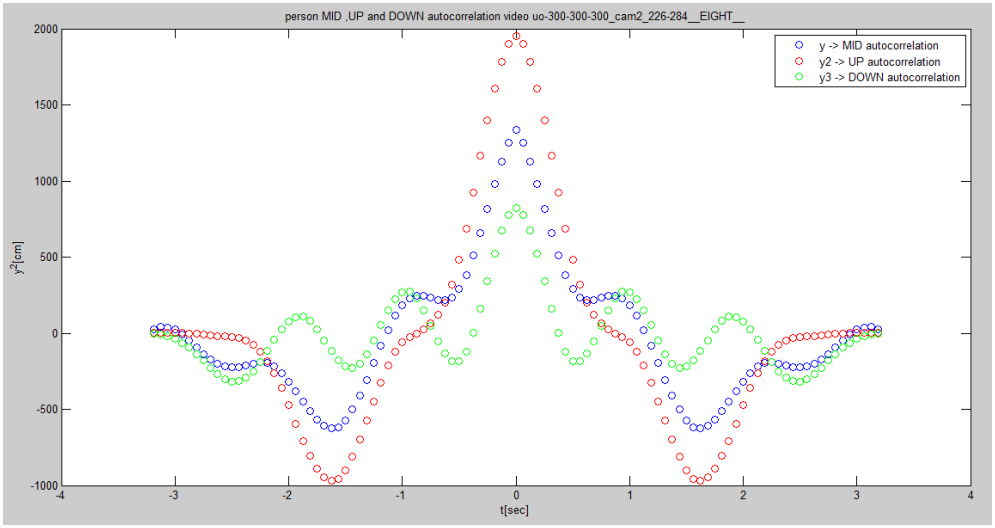

Figure 4.26. The result of autocorrelation between the three input waveforms

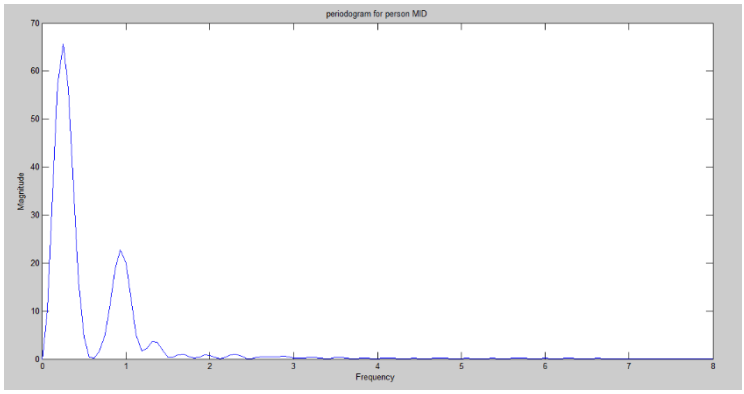

(a)

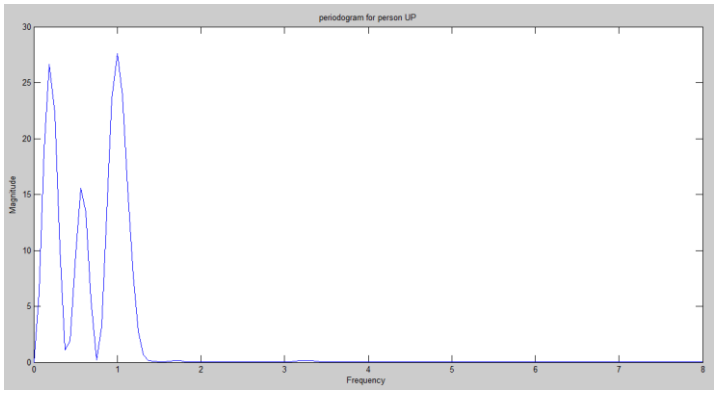

(b)

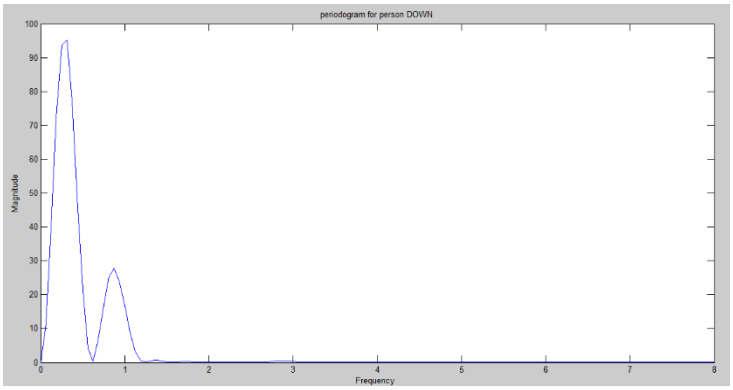

(c)

Figure 4.27 Spectral analysis of the trajectories: (a) of the middle individual (b) of the upper individual and (c) of the lower individual

In Figure 4.27 we have presented the graphical representations of the spectral analysis of the signals

6. Sixth video recording

In figure 4.28 we can observe the trajectories of the individuals from a part of the previous video uo-300-300-300_cam2.

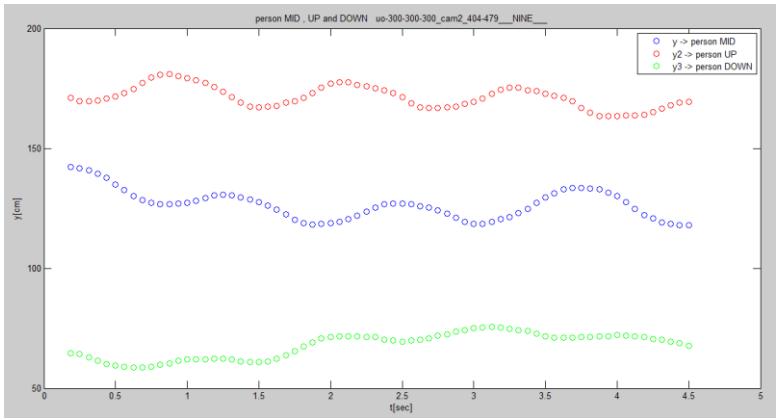

Figure 4.28 Pedestrian trajectories as recorded by video uo-300-300-300_cam2

In Figure 4.29 there are trajectories of individuals from the same part of the video uo-300-300-300_cam2 only that in this case we have removed the average value.

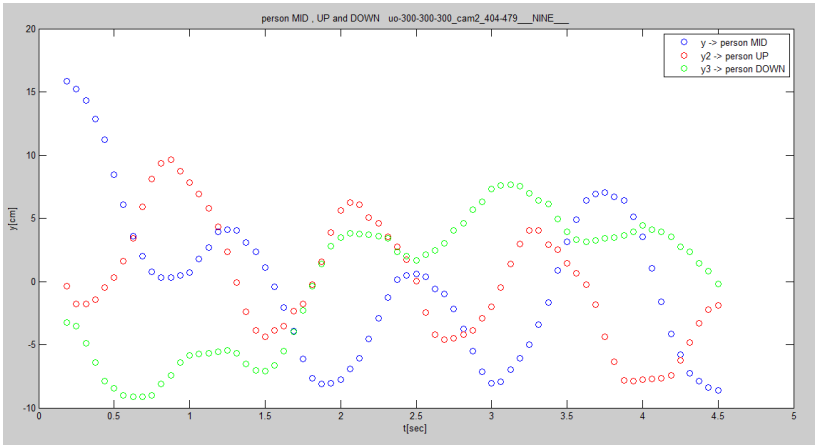

Figure 4.29 Cross-correlation waveforms for each pair between the three input waveforms.

In Figure 4.30 we see the result from the application of the cross-correlation function for each combination of the three oscillation-signals. According to the results the distance between the middle and the lower individual is *1.5[sec]* and the lower one precedes. . The distance of the middle with the upper individual is *0.5[sec]* and the upper one precedes and the distance between the upper and the lower individual is *3.5[sec]* and the lower one precedes.

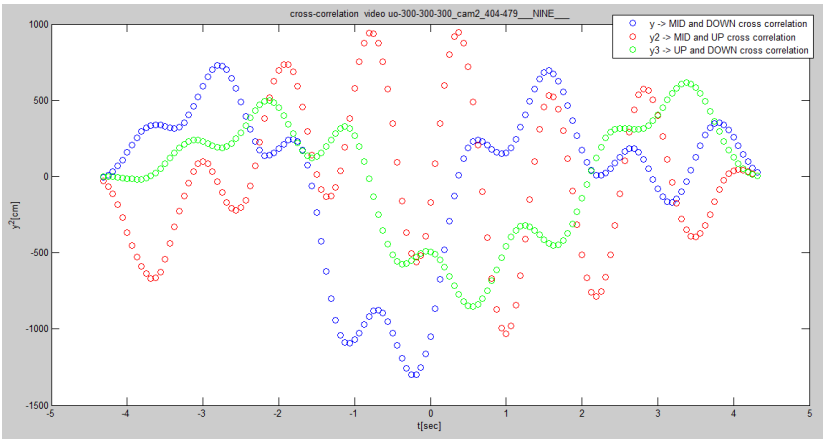

Figure 4.30 Cross-correlation waveforms for each pair between the three input waveforms.

In Figure 4.31 we see the result from the application of the autocorrelation function for each combination of the three oscillation signals. From the waveforms we have the following results:

For the middle individual we have: mi =18[samples] , mi =37[samples] and mi =65[samples] for each peak corresponding to $f = 0.9$ [Hz] , $f = 0.41$[Hz] $f = 0.28$[Hz].

For the upper individual we have: mi =20[samples] , mi =39[samples] mi =63[samples] for each peak corresponding to $f = 0.83$ [Hz] , $f = 0.4$[Hz] and $f = 0.27$[Hz].

For the lower individual we don't have peaks except from zero.

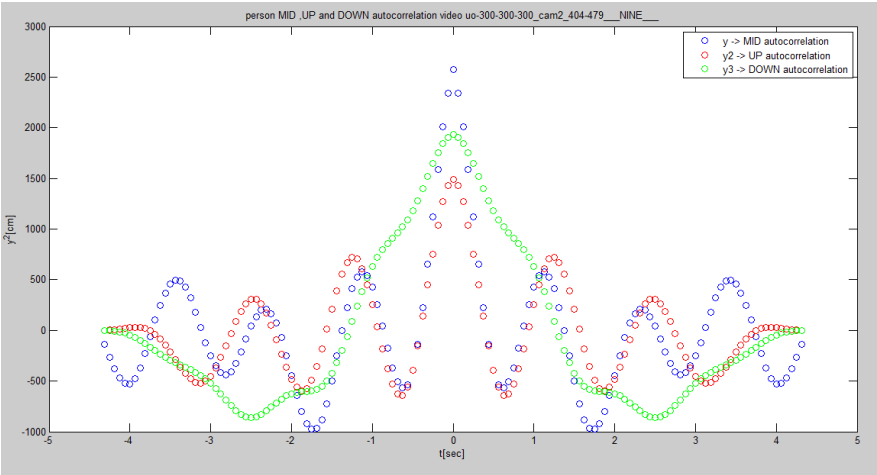

Figure 4.31 The result of autocorrelation between the three input waveforms

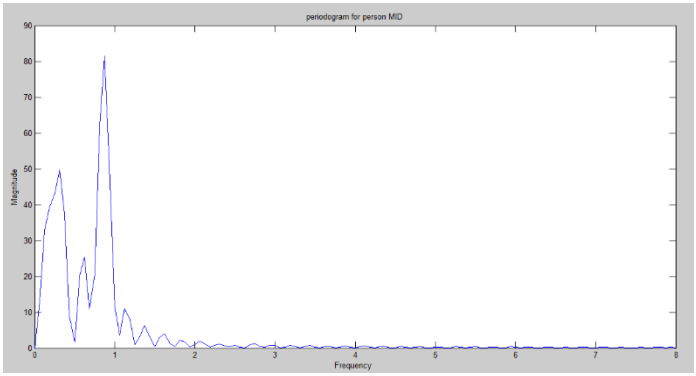

(a)

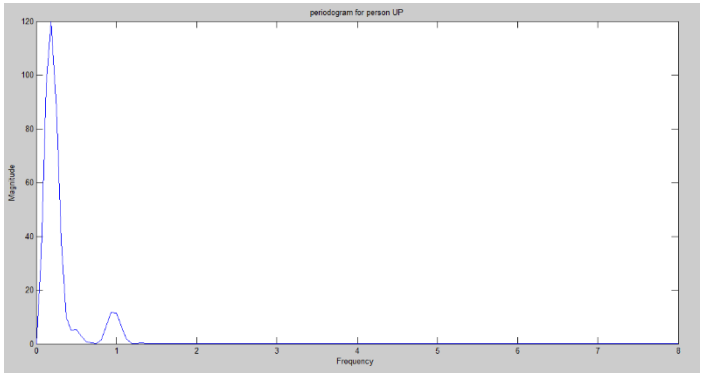

(b)

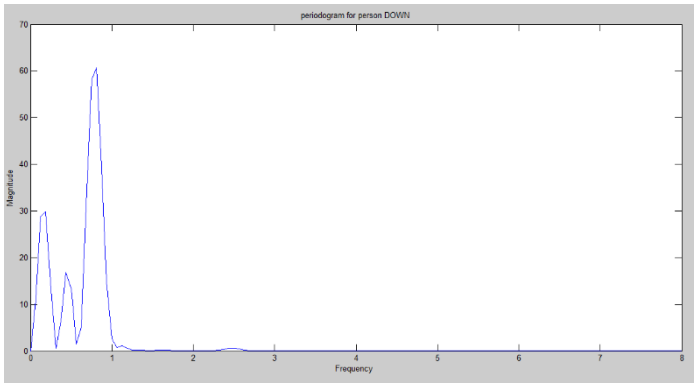

(c)

Figure 4.32 Spectral analysis of the trajectories: (a) of the middle individual (b)of the upper individual and (c) of the lower individual

In Figure 4.32 we have presented the graphical representations of the spectral analysis of the signals

4.3.2. Application of cross-correlation and autocorrelation to crowd flows

In the case of flows, the implementation of the cross-correlation and autocorrelation functions is done in the same way. The only difference is that the data does not represent the movement of individuals but the average of the movement of more people. Thus, we have a more generic picture of the range of motion of the crowd as a whole.

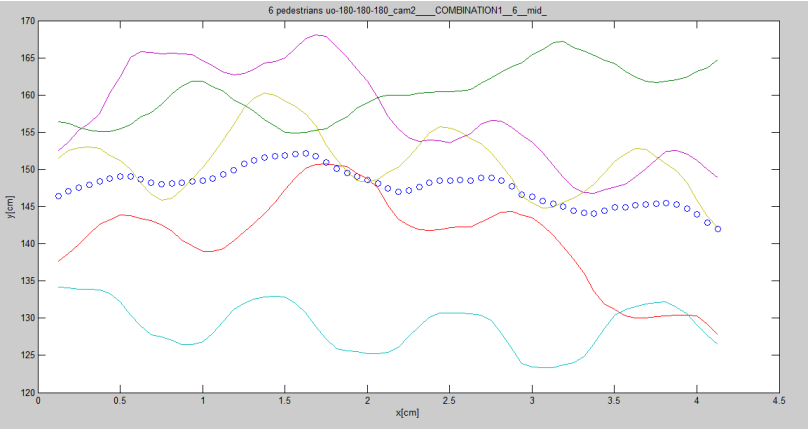

Figure 4.33 The crowd flow of the middle zone which is essentially the average of six different individuals

In Figure 4.33 we see how the average is calculated from the six individual trajectories for the middle flow.

In the same way, in Figure 4.34 we see how the average is calculated from the six individual trajectories for the upper flow.

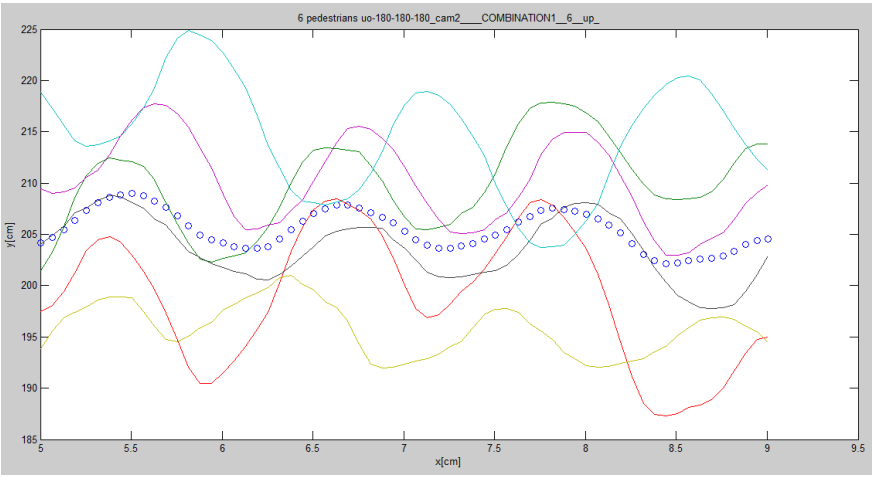

Figure 4.34 The crowd flow of the upper zone, which is essentially the average of six different individuals

In Figure 4.34 we see how the average is calculated from the six individual trajectories for the lower flow.

Figure 4.36 summarizes the three flows after the average value from each one (dc component) has

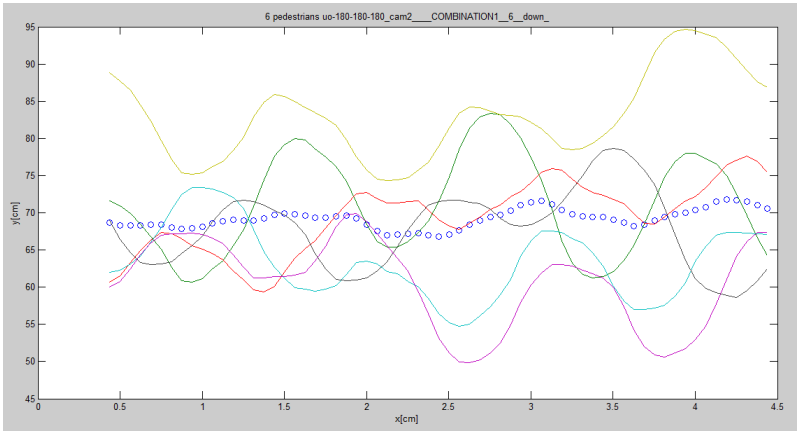

Figure 4.35 The crowd flow of the lower zone which is essentially the average of six different individuals

been subtracted.

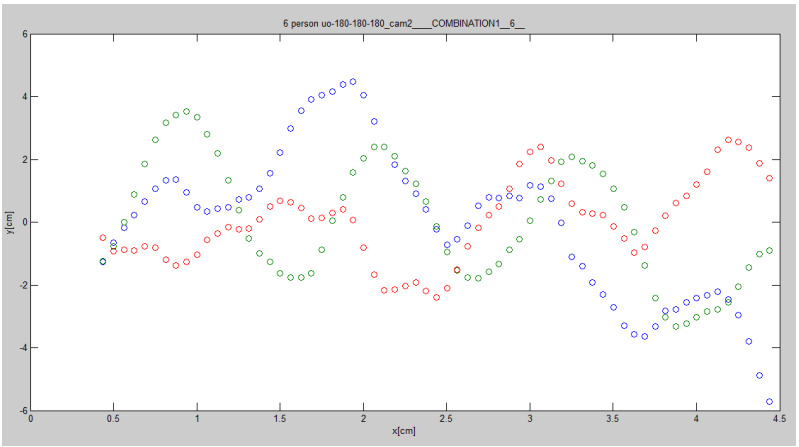

Figure 4.36 The three flows middle, upper and lower after the average has been subtracted

In Figure 4.37 we see the result from the application of the cross-correlation function for each combination of the three oscillation-signals. The results are:

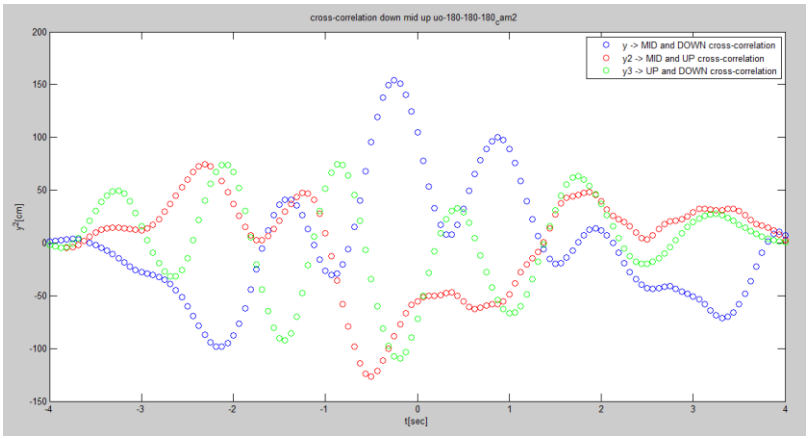

Figure 4.37 The result of the application of cross-correlation for the three crowd flows

Middle with lower flow is *0.2[sec]* and the upper one precedes.

Middle with upper flow is *2.2[sec]* and the middle one precedes

Upper with lower flow is 1[sec] and the upper one precedes.

In Figure 4.38 we see the result from the application of the autocorrelation function for each combination of the three oscillation signals. From the waveforms we have the following results:

For the middle flow we have: mi =53[samples] , mi =63[samples] for each peak corresponding to $f = 0.3$ [Hz] , $f = 0.25$[Hz]

For the upper flow we have: mi =19[samples] , mi =39[samples] mi =61[samples] for each peak corresponding to $f = 0.84$ [Hz] , $f = 0.41$[Hz], $f = 0.26$[Hz].

For the lower flow we have: mi =20[samples] , mi =44[samples] for each peak corresponding to $f = 0.8$[Hz] , $f = 0.36$[Hz].

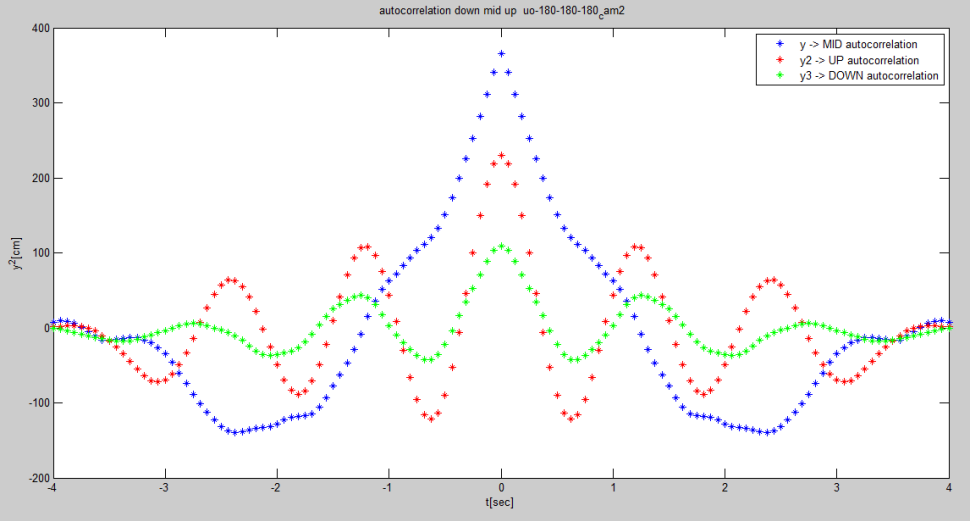

Figure 4.38 The result of the application of auto-correlation for the three crowd flows

In Figure 4.39 we have presented the graphical representations of the spectral analysis of the signals. A great observation that has been observed by the spectrum analysis of the individuals and flows is that their spectrum shows similarities. They consist of two or three frequencies, which exhibit small deviations from the same values.

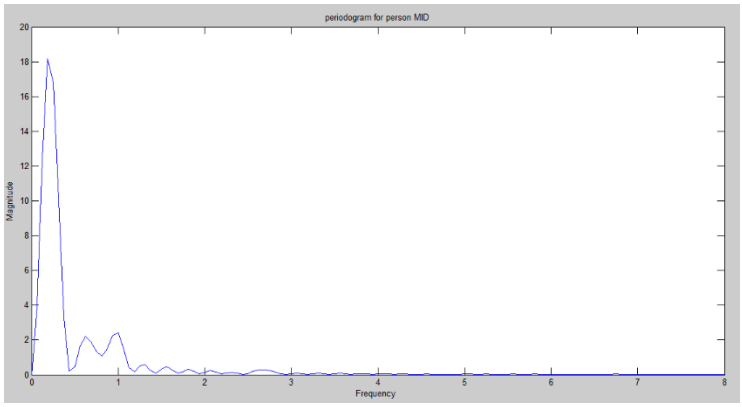

(a)

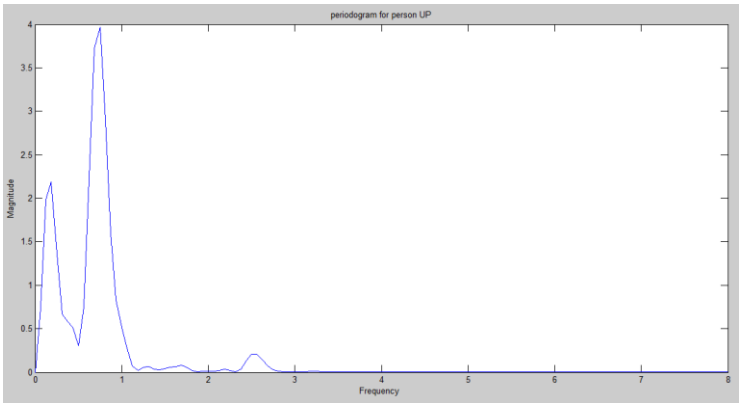

(b)

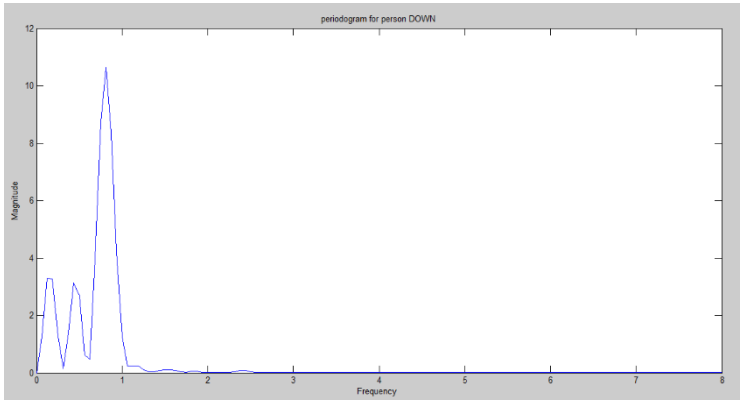

(c)

Figure 4.39 Spectral flow analysis: (a) middle flow (b) upper flow (c) lower flow

The function that calculates the power spectral density of the oscillations through Fast Fourier Transform (FFT) has low resolution for low frequencies. Thus, the deviations between this and autocorrelation are justified.

Furthermore, due to the time series being finite, which means that before and after the time series the samples are zero, an error is created during the calculation of both autocorrelation and FFT.

5. Results of equation search

In this chapter the results of the equations search procedure are presented. Initially, the method of the equations evaluation is shown. Latter, the equations that collected with their evaluation are presented and discussed. We recall that our goal is to extract equations that approach precisely but also to highlight the existence of laws governing pedestrian movement. In addition, we comment on the results and enter some conclusions.

5.1 Evaluation method of equations

In order to achieve our purpose we evaluate the equations in two different ways. Initially, in order to calculate the accuracy of the equations, we study them in the time domain. We compare directly the data we have recorded from the recording process to those resulting from the equations. We have chosen to take the absolute point-to-point error as a representative metric of accuracy. Thus, if *y (t)* is the time series that has been derived from the logging process and *f (t)* is the time series that has been derived from the equation we have found, then the absolute error *e(t)* will be:

$$\mathbf{e(t)} = |\mathbf{y(t)} - \mathbf{f(t)}| \quad (\mathbf{5.1})$$

In addition, in order to examine if the equations describe some “physical” laws governing the pedestrian movement, we process the equations in the frequency domain. This is achieved with the help of the cross-correlation and autocorrelation signal processing functions that were described and used in the previous chapter. The data from the real recordings were compared with the results of the equations in terms of their spectrum. The approach of pedestrian movement through oscillations provided us with the opportunity to extract useful information and conclusions from the analysis of the spectrum of these approximate periodic movements. We want to compare which frequencies collect the most energy but also what is their physical meaning.

Our purpose is to investigate the movement attributes of crowd through the equations we have obtained. For this reason we're studying 6 different video recordings with different corridor widths and different crowd densities. This means that for each search we have created, we will have 6 different video clips. Pedestrian motion is done in one direction only. In the table below we summarize the features of each snippet we studied.

Table 1 The attributes of each video recording examined

Video Recording	Width In [m]	Corridor Width [m]	Width Out [m]	Number of pedestrian N	Time t[s]
First	1,45	1,8	1,8	150	1:29
Second	1,8	1,8	1,8	200	1:17
Third	1,8	1,8	1,8	200	1:10
Fourth	1,9	2,4	2,4	200	1:21
Fifth	3	3	3	>350	1:21
Sixth	3	3	3	>350	1:21

We also want to emphasize that the sampling period when recording videos is 0.0625 [sec] and sampling frequency is 16 [Hertz].

5.2 First microscopic search case

In this section it is presented the equations found for each one of the video recordings according to the first microscopic search case and describe the movement of the middle person from the basic search molecule. In chapter three, we showed that the quest process consists of three pedestrians and in this case we focus only on the behavior of a pedestrian in the middle. The general form of the equation is:

$$\boldsymbol{y_1 = f\left(t, x1, V_{x1}, V_{y1}, a_{x1}, a_{y1}, x_1 - x_2, y_1 - y_2, x_1 - x_3, y_1 - y_3\right)} \quad \boldsymbol{(5.2)}$$

We observe, that in this case we search for the equation between the trajectory of the middle man and the Euclidean difference of the coordinates of herself with the other two neighbors. Below the results are presented for the evaluation of the six different video clips.

5.2.1. First video recording

The equation with the best score for the first video clip is:

$$f(\ldots) = 137. + 0.320\, y1\text{-}y_3 + 0.320 \exp\left(0.160\, t^2\right) + 1.32 \cos\left(6.06\, t\right) - 0.565\, t \sin\left(t\right) - 0.320\, y1\text{-}y_2$$

We notice that in the description of the vertical trajectory of the middle man exists the distance with the upper person $y_1 - y_2$ and with the lower person $y_1 - y_3$. Furthermore, there are two frequencies that are described from the sine and cosine functions with frequencies $f_1 = 0.16$ [Hz] and $f_2 = 1$ [Hz] respectively. It exists also a constant term due to the arbitrary placement of the axes during the video recording process.

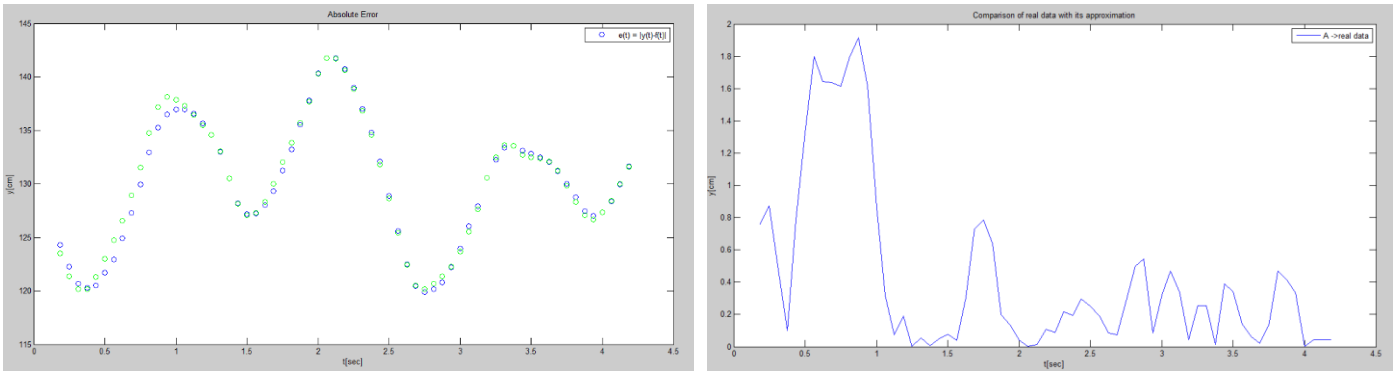

(a) (b)

Figure 5.1 Comparison of the equation and the real data in the time domain
(a) Representation of the trajectories of the equation and the real data
(b) The absolute error between the two trajectories

The equation has an absolute error less than < 2[cm] and describes with great accuracy the real pedestrian movement.

5.2.2. Second video recording

The equation with the best score for the second video clip is:

$$f(\ldots) = 133. + 13.9\log(y1\text{-}y_3) - \exp(0.453\,t) - 0.430\,y1\text{-}y_2$$

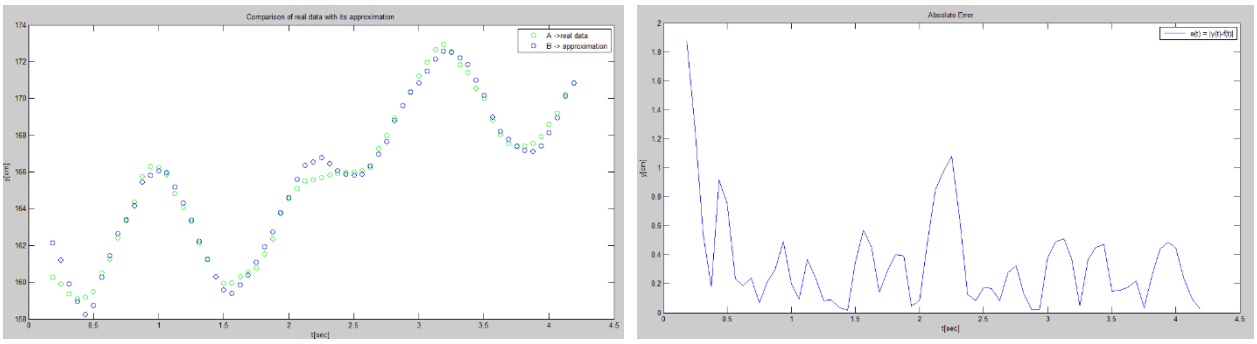

(a) (b)

Figure 5.2 Comparison of the equation and the real data in the time domain
(a) Representation of the trajectories of the equation and the real data
(b) The absolute error between the two trajectories

5.2.3. Third video recording

The equation with the best score for the third video clip is:

$$f(\ldots) = 140. + 1.49t\cos(3.69 + 1.84t) + 3.50\,t\sin(t) - 0.286\,y1\text{-}y_2$$

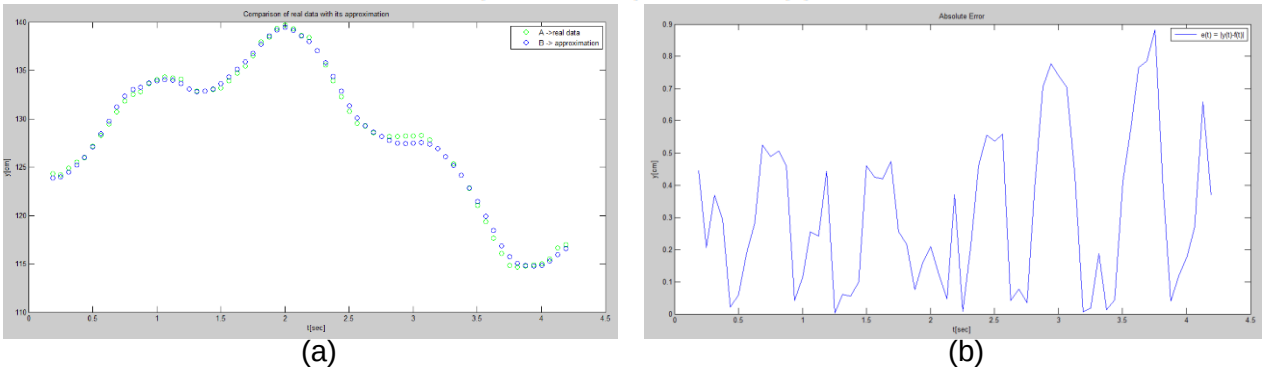

(a) (b)

Figure 5.3 Comparison of the equation and the real data in the time domain
(a) Representation of the trajectories of the equation and the real data
(b) The absolute error between the two trajectories

5.2.4. Fourth video recording

The equation with the best score for the forth video clip is:

$$f(...) = 133. + 0.263\,y1\text{-}y_3 - 6.21\cos(t) - 3.05\sin(5.18\,t) - 0.584\,y1\text{-}y_2$$

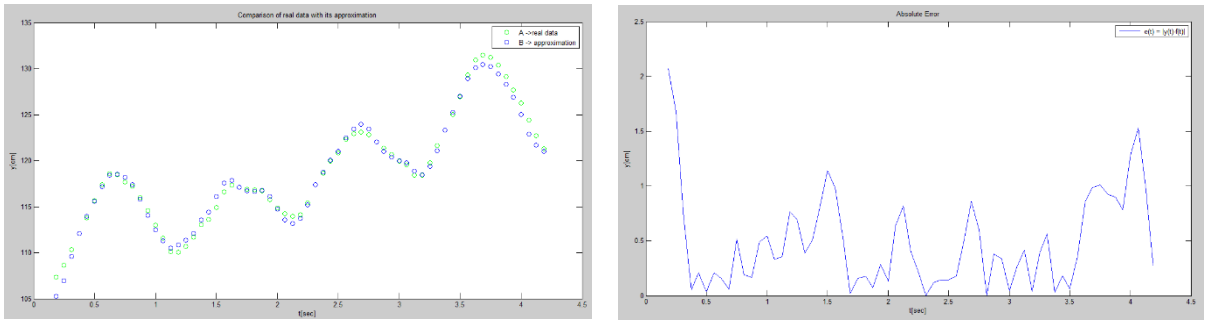

(a) (b)

Figure 5.4 Comparison of the equation and the real data in the time domain
(a) Representation of the trajectories of the equation and the real data
(b) The absolute error between the two trajectories

5.2.5. Fifth video recording

The equation with the best score for the fifth video clip is:

$$f(...) = 169. + 1.39\sin(5.40\,t - 0.939) + t\sin(1.11\,t) - 0.427\,y1\text{-}y_2 - 0.00365\,a\_\{y\}$$

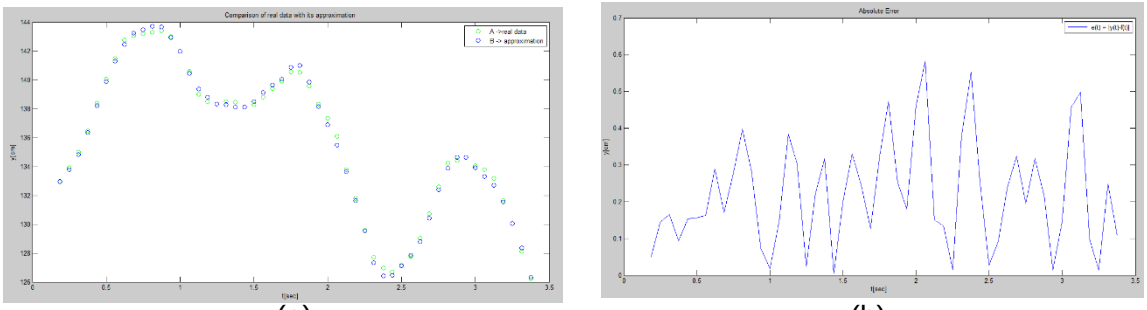

(a) (b)

Figure 5.5 Comparison of the equation and the real data in the time domain
(a) Representation of the trajectories of the equation and the real data
(b) The absolute error between the two trajectories

5.2.6. Sixth video recording

The equation with the best score for the sixth video clip is:

$$f(...) = 80.0 + 0.740\,y1\text{-}y_3 + 1.34\sin(6.73\,t) - \cos(t)\log(y1\text{-}y_3)\log(2.25\,t)$$

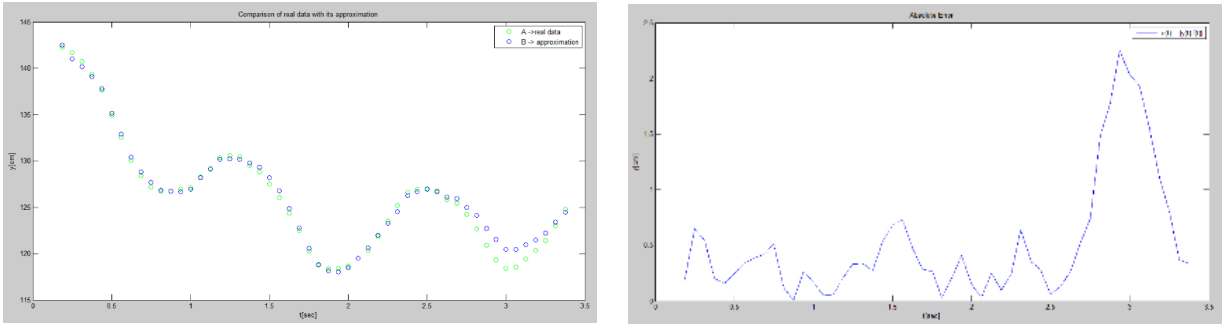

(a) (b)

Figure 5.6 Comparison of the equation and the real data in the time domain
(a) Representation of the trajectories of the equation and the real data
(b) The absolute error between the two trajectories

5.3 Second microscopic search case

In this section we will present the equations for the second microscopic search case and we will describe the movement of all three pedestrians that appear in the quest structure. We mentioned that our microscopic approach consists of three pedestrians and thus our results will be presented in groups of three. The general form of the equation is:

$$\boldsymbol{y_i = f(t, x_1, V_{x1}, V_{y1}, a_{x1}, a_{y1}, x_2, y_2, V_{x2}, V_{y2}, a_{x2}, a_{y2}, x_3, y_3, V_{x3}, V_{y3}, a_{x3}, a_{y3})} \quad (5.3)$$

,where i=1,2,3. We observe that in this case we are interested to find the relationship of each person's vertical coordinate with the dynamics variables of himself and the other two neighbors. Below we present the results and the evaluation for the six different video clips.

5.3.1. First video recording

a) The equation for the middle pedestrian with the best score is:

$$f(\ldots) = 134. + 0.658\,t + 5.61\cos(5.03 - 5.20\,t) + \cos(3.40\,t - 101.) - 8.84\cos(t)^2 - 0.00753\,a\_\{y\}$$

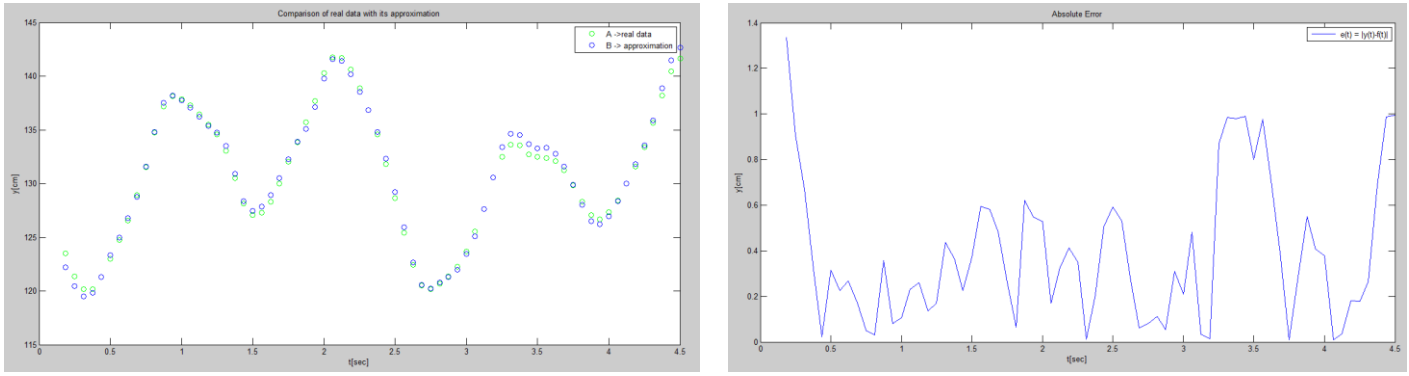

(a) (b)

Figure 5.7 Comparison of the equation and the real data in the time domain for the middle pedestrian
(a) Representation of the trajectories of the equation and the real data
(b) The absolute error between the two trajectories

b) The equation for the upper pedestrian with the best score is:

$$f(\ldots) = 220. + 4.92\cos(1.20 - 4.93\,t) - 3.04\,t\sin(t - 0.320) - 0.685\cos(3.45\,t) - 2.57\,t$$

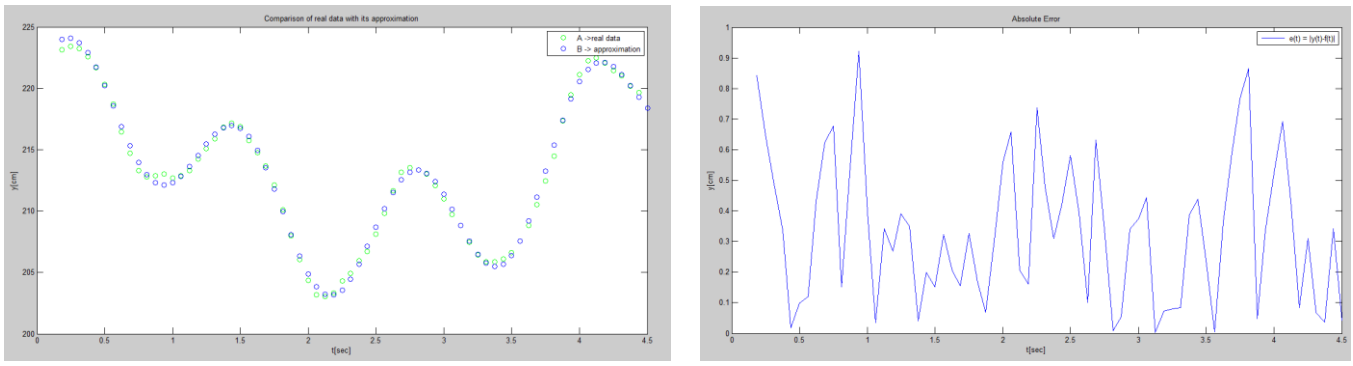

(a) (b)

Figure 5.8 Comparison of the equation and the real data in the time domain for the upper pedestrian
(a) Representation of the trajectories of the equation and the real data
(b) The absolute error between the two trajectories

$$f(\ldots) = 72.2 + 2.21\cos(3.00\,t - 2.20) - 1.82\,t\sin(1.28 + t) - 5.87\sin(0.291 + t) - 0.0265\,a3\_\{y\}$$

c) The equation for the lower pedestrian with the best score is:

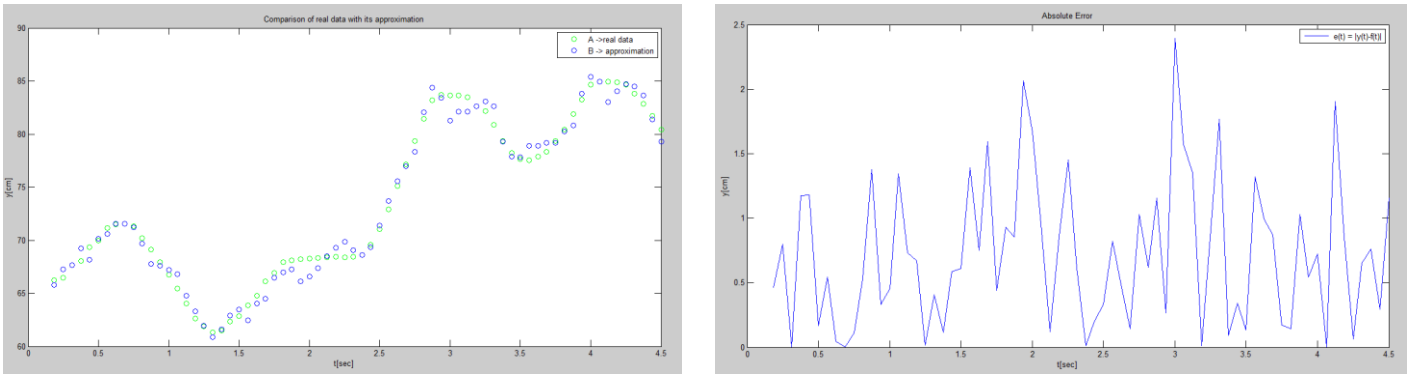

(a) (b)

Figure 5.9 Comparison of the equation and the real data in the time domain for the lower pedestrian
(a) Representation of the trajectories of the equation and the real data
(b) The absolute error between the two trajectories

5.3.2. Second video recording

a) The equation for the middle pedestrian with the best score is:

$$f(\ldots) = 159. + 3.15\,t + 1.84\cos(5.86 - 5.76\,t) - 2.59\cos(1.08 + 2.79\,t)$$

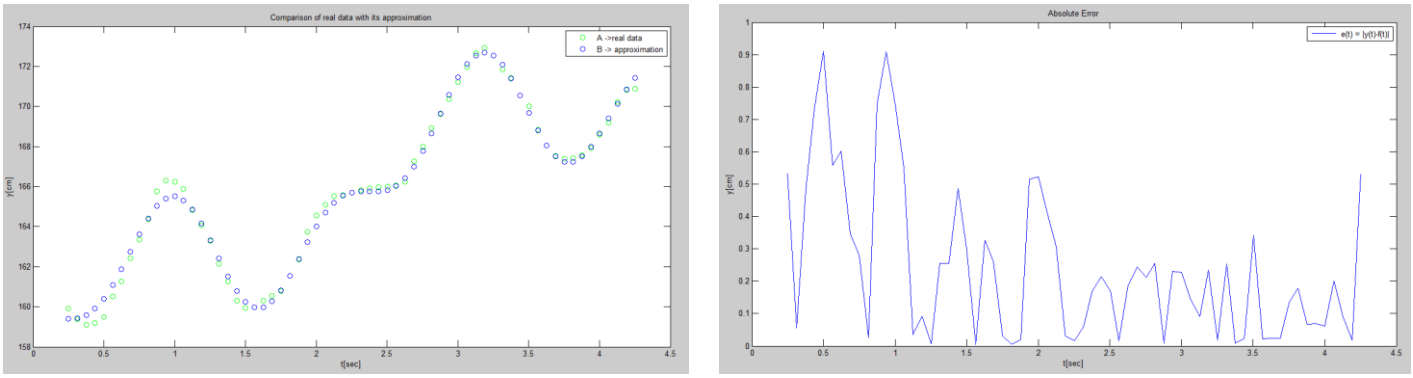

(a) (b)

Figure 5.10 Comparison of the equation and the real data in the time domain for the middle pedestrian
(a) Representation of the trajectories of the equation and the real data
(b) The absolute error between the two trajectories

b) The equation for the upper pedestrian with the best score is:

$$f(\ldots) = 205. + 2.77\sin(0.975 + 5.29t) + 1.35\sin(2.07t) - 1.62t$$

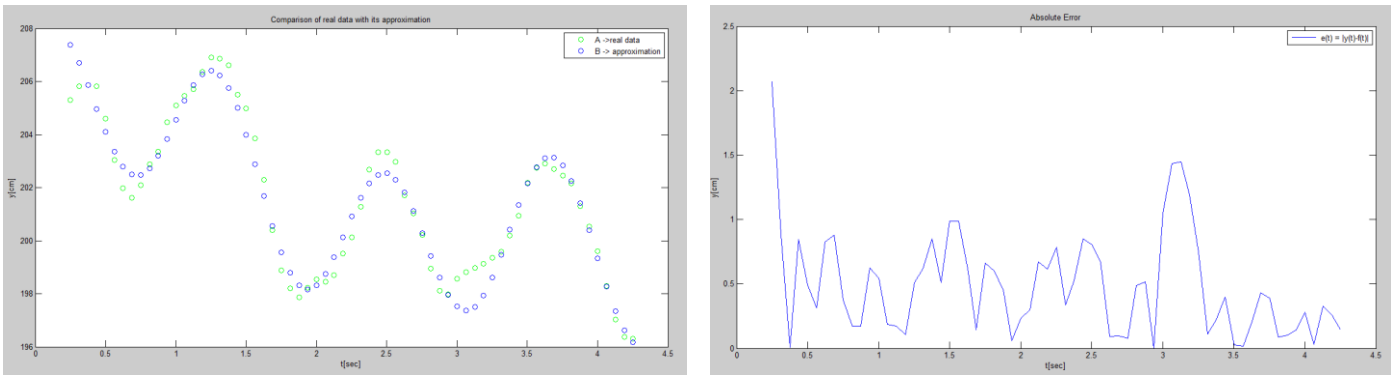

(a) (b)

Figure 5.11 Comparison of the equation and the real data in the time domain for the upper pedestrian
(a) Representation of the trajectories of the equation and the real data
(b) The absolute error between the two trajectories

c) The equation for the lower pedestrian with the best score is:

$$f(\ldots) = 128. + 5.20\sin(t - 0.415) + 1.66\cos(2.93t) - 3.52\cos(5.44t - 0.300) - 3.53t$$

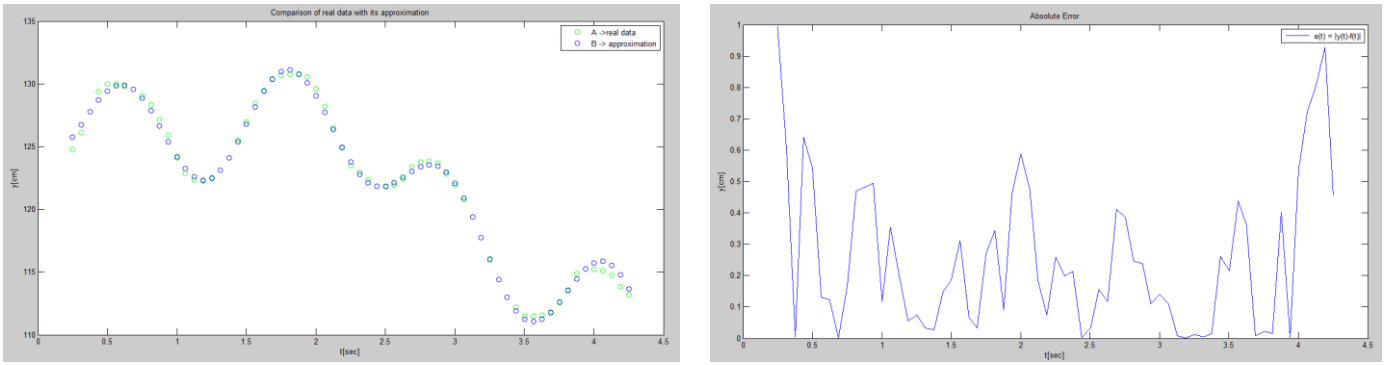

(a) (b)

Figure 5.12 Comparison of the equation and the real data in the time domain for the lower pedestrian
(a) Representation of the trajectories of the equation and the real data
(b) The absolute error between the two trajectories

5.3.3. Third video recording

a) The equation for the middle pedestrian with the best score is:

$$f(\ldots) = 97.8 + 0.375y_3 + 9.04\sin(t) + \cos(0.280 + 4.41t) + 2.14\sin(21.5 + 2.23t)$$

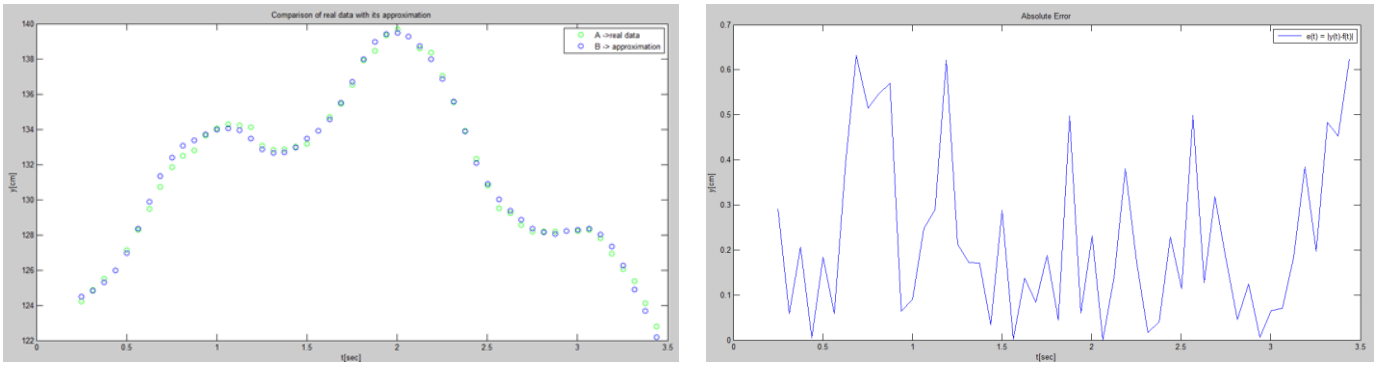

(a) (b)

Figure 5.13 Comparison of the equation and the real data in the time domain for the middle pedestrian
(a) Representation of the trajectories of the equation and the real data
(b) The absolute error between the two trajectories

b) The equation for the upper pedestrian with the best score is:

$$f(...) = 175. + 6.30\sin(5.23\,t) + 2.95\sin(t) - 3.87\cos(32.7 - 2.41\,t) - 3.52\,t$$

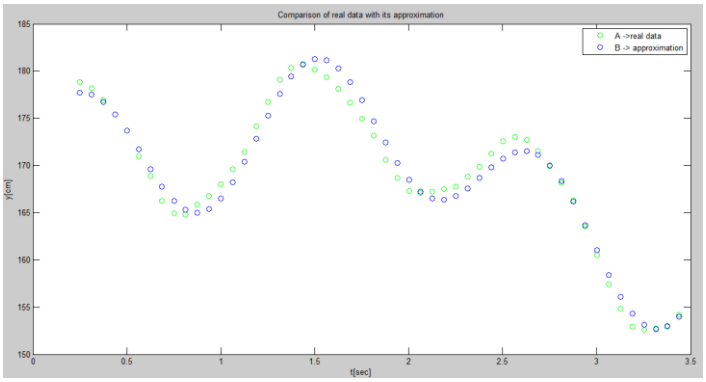

(a)

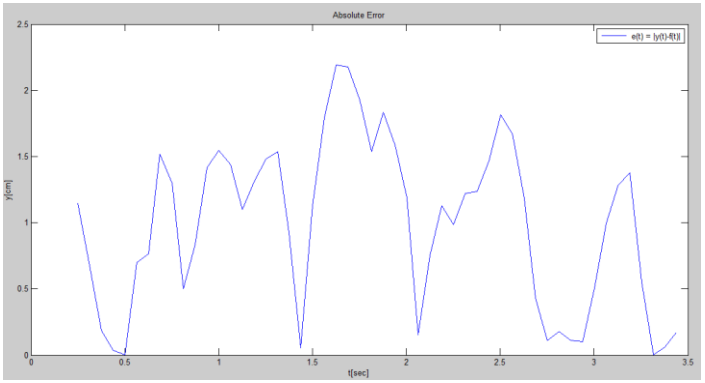

(b)

Figure 5.14 Comparison of the equation and the real data in the time domain for the upper pedestrian
(a) Representation of the trajectories of the equation and the real data
(b) The absolute error between the two trajectories

c) The equation for the lower pedestrian with the best score is:

$$f(...) = y + 4.67\sin(-5.32\,t) + \sin(3.95\,t) - 2.55\,t\sin(1.21\,t) - 54.4$$

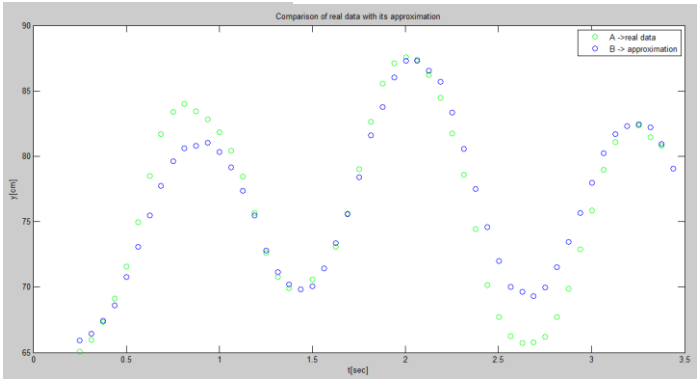

(a)

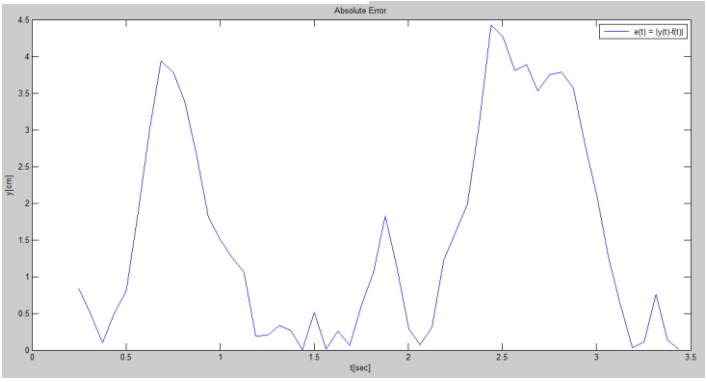

(b)

Figure 5.15 Comparison of the equation and the real data in the time domain for the lower pedestrian
(a) Representation of the trajectories of the equation and the real data
(b) The absolute error between the two trajectories

5.3.4. Fourth video recording

a) The equation for the middle pedestrian with the best score is:

$$f(...) = 113. + t^2 + 1.50\sin(113. + 1.37t + 1.12t^2) - 4.50\sin(0.436 + 6.39\,t)$$

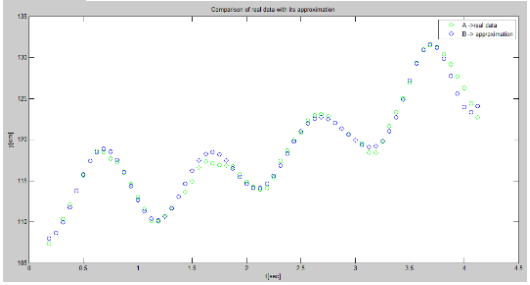

(a)

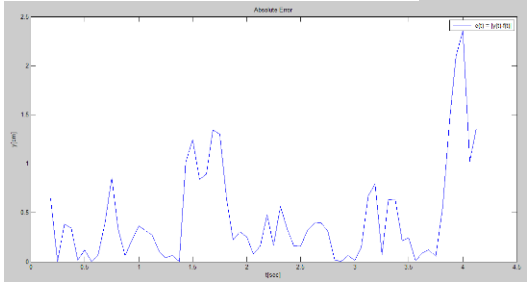

(b)

Figure 5.16 Comparison of the equation and the real data in the time domain for the middle pedestrian
(a) Representation of the trajectories of the equation and the real data
(b) The absolute error between the two trajectories

b) The equation for the upper pedestrian with the best score is:

$$f(\ldots) = 160. + t + 6.31\cos(-5.35\,t - 76.3) - 0.687\,t\cos(2.65\,t) - 7.36\cos(t)$$

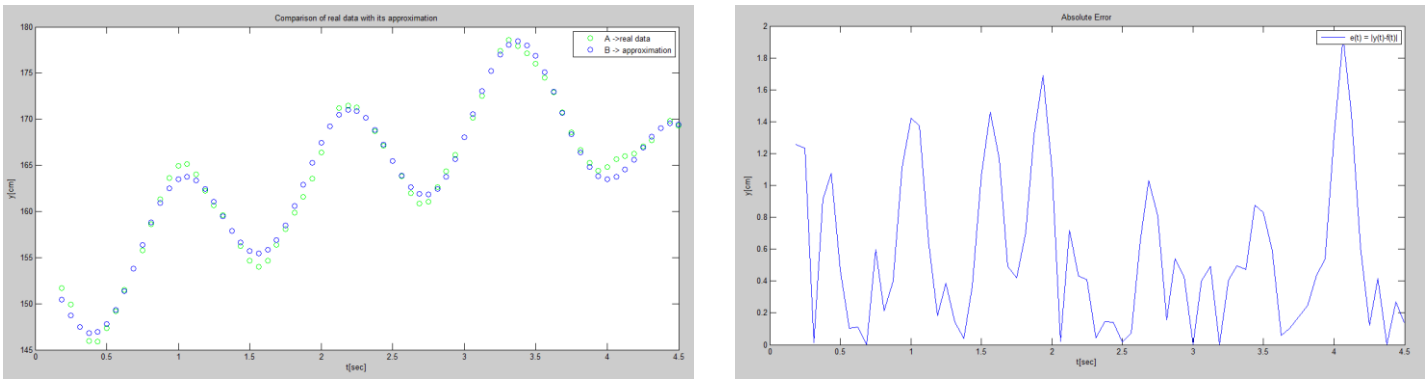

(a) (b)

Figure 5.17 Comparison of the equation and the real data in the time domain for the upper pedestrian
(a) Representation of the trajectories of the equation and the real data
(b) The absolute error between the two trajectories

c) The equation for the lower pedestrian with the best score is:

$$f(\ldots) = 81.5 - 0.120\exp(t) - 1.66\sin(-0.0223\,x) - 8.49\sin(t)\cos(0.177 - t) - 0.0293\,a3\_\{y\}$$

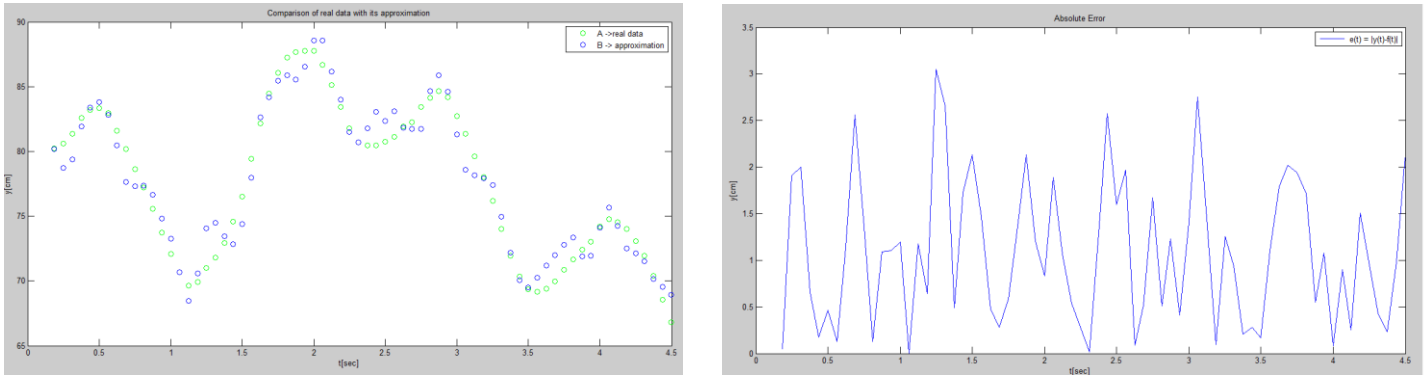

(a) (b)

Figure 5.18 Comparison of the equation and the real data in the time domain for the lower pedestrian
(a) Representation of the trajectories of the equation and the real data
(b) The absolute error between the two trajectories

5.3.5. Fifth video recording

a) The equation for the middle pedestrian with the best score is:

$$f(...) = 135. + 2.96\cos(-4.75\,t) - 5.98\sin(-1.57\,t) - 5.10\cos(0.662 - 5.33\,t) - 0.00702\,a\_\{y\}$$

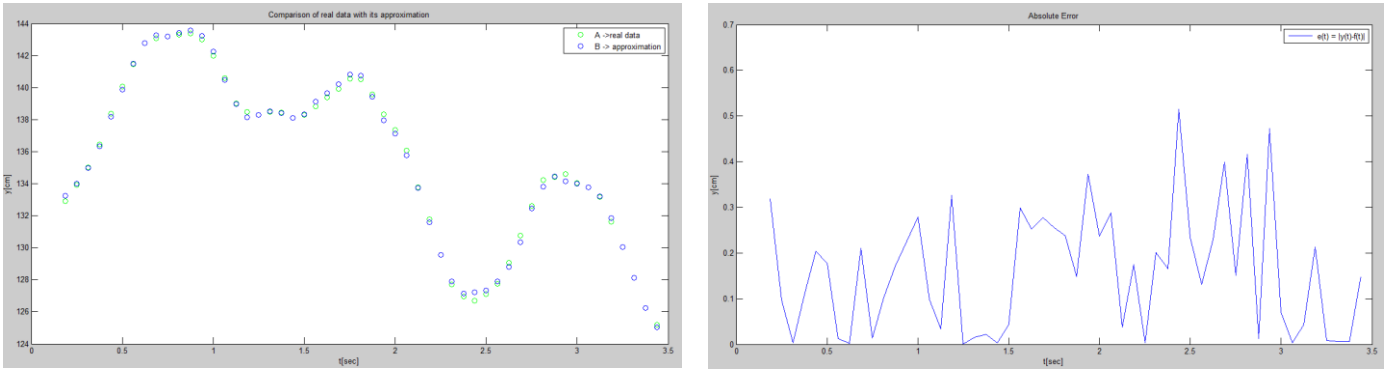

(a) (b)

Figure 5.19 Comparison of the equation and the real data in the time domain for the middle pedestrian
(a) Representation of the trajectories of the equation and the real data
(b) The absolute error between the two trajectories

b) The equation for the upper pedestrian with the best score is:

$$f(...) = 215. + 3.26\sin(5.84 + 5.84\,t) - 7.46\sin(1.90\,t - 0.183) - 0.00556\,a2\_\{y\}$$

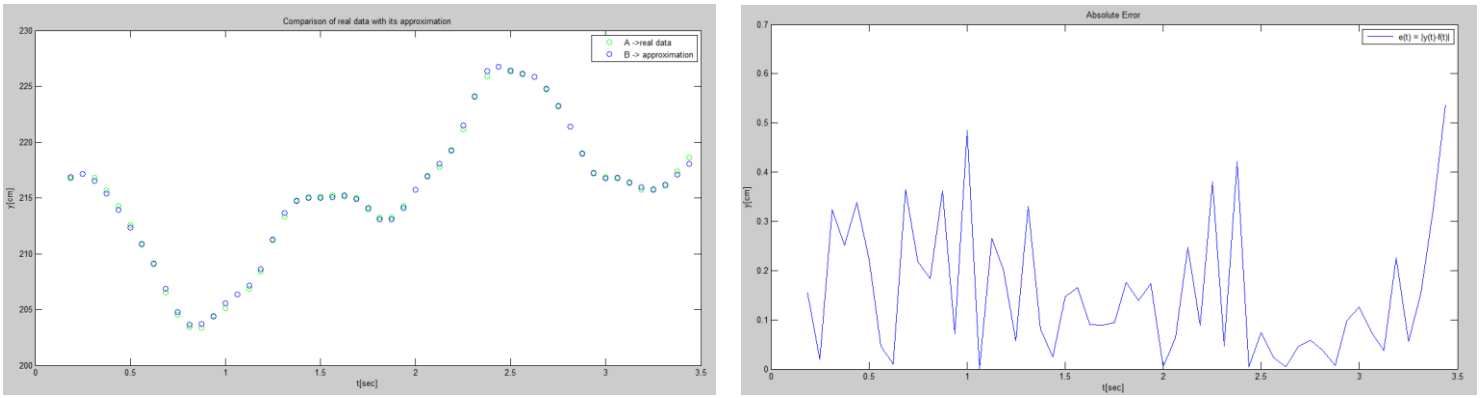

(a) (b)

Figure 5.20 Comparison of the equation and the real data in the time domain for the upper pedestrian
(a) Representation of the trajectories of the equation and the real data
(b) The absolute error between the two trajectories

c) The equation for the lower pedestrian with the best score is:

$$f(\ldots) = 62.3 + 2.41\,t + 3.84\cos(6.52\,t) - \sin(3.47\,t)$$

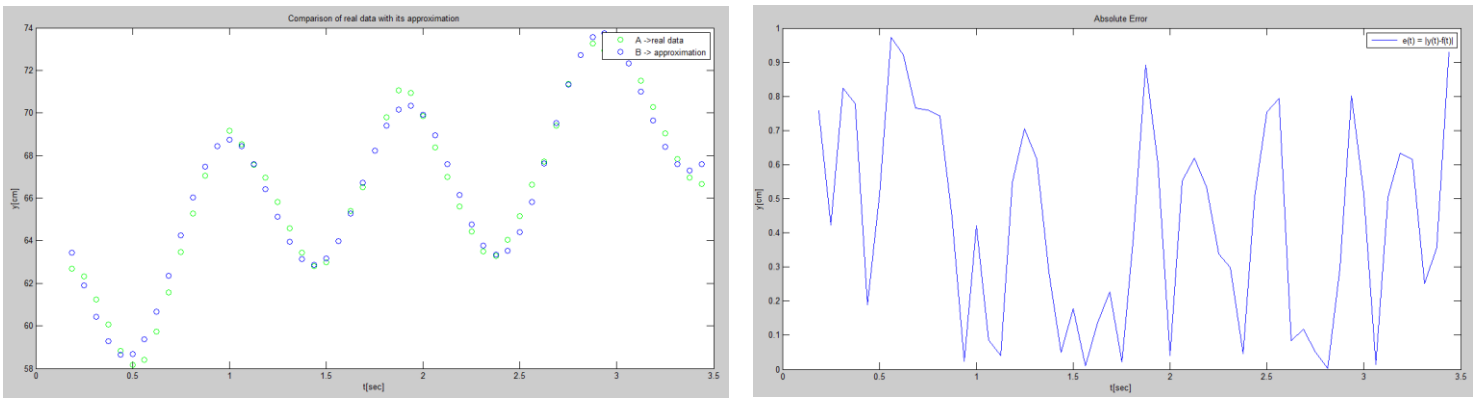

(a) (b)

Figure 5.21 Comparison of the equation and the real data in the time domain for the lower pedestrian
(a) Representation of the trajectories of the equation and the real data
(b) The absolute error between the two trajectories

5.3.6. Sixth video recording

a) The equation for the middle pedestrian with the best score is:

$$f(\ldots) = 133 + 4.02\cos(5.43 + 5.31\,t) + 0.781\,t\cos(3.17\,t) + 5.46\cos(1.67\,t) - 0.00657\,a\_\{y\} - 3.22\,t$$

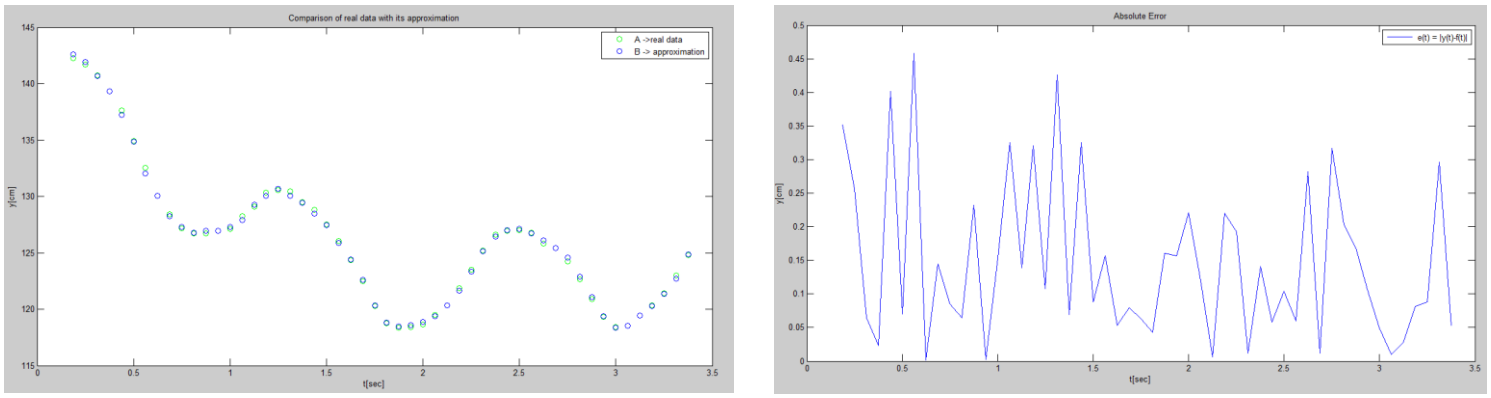

(a) (b)

Figure 5.22 Comparison of the equation and the real data in the time domain for the middle pedestrian
(a) Representation of the trajectories of the equation and the real data
(b) The absolute error between the two trajectories

b) The equation for the upper pedestrian with the best score is:

$$f(\ldots) = 179 + 5.3\sin(-5.06\,t) - 1.57\sin(1.45\,t) - 0.00575\,a2\_\{y\} - 1.39\log(t)\sin(0.464 - 5.01\,t) - 2.96\,t$$

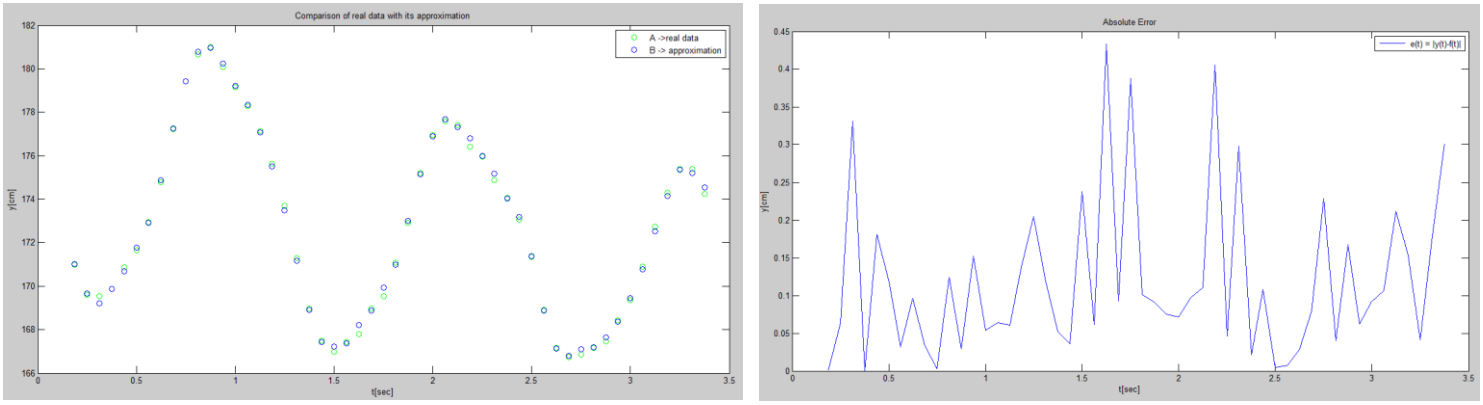

(a) (b)

Figure 5.23 Comparison of the equation and the real data in the time domain for the upper pedestrian
(a) Representation of the trajectories of the equation and the real data
(b) The absolute error between the two trajectories

c) The equation for the lower pedestrian with the best score is:

$$f(\ldots) = 63.1 + 2.15\,t + 4.10\sin(-1.63\,t) - 0.0219\,a3\_\{y\}$$

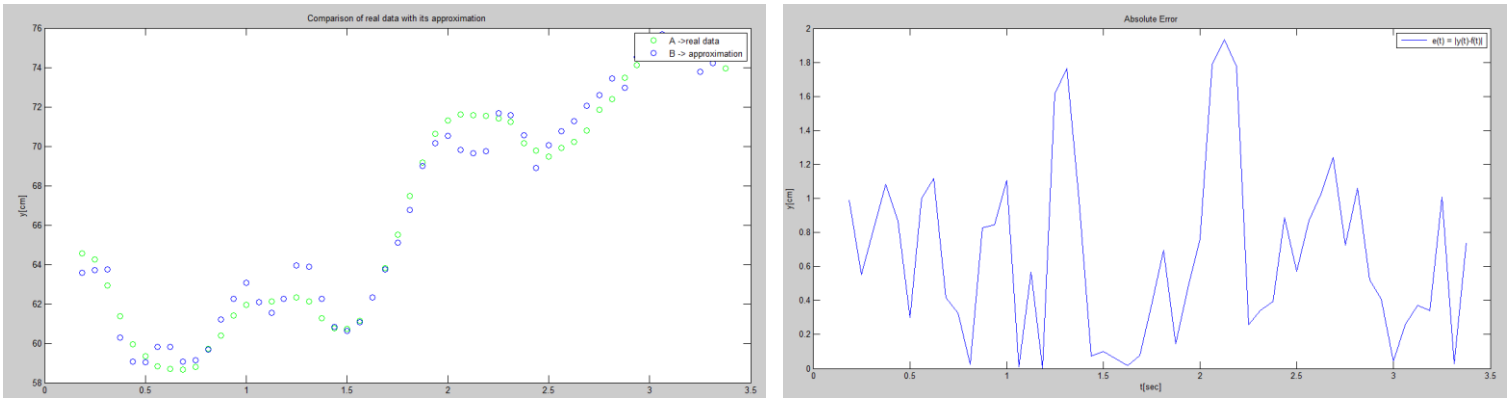

(a) (b)

Figure 5.24 Comparison of the equation and the real data in the time domain for the lower pedestrian
(a) Representation of the trajectories of the equation and the real data
(b) The absolute error between the two trajectories

5.4 Third macroscopic search case

In this section we will present the equations found for the third macroscopic search case, which is an examination of the crowd behavior. We search for the equations that describe the vertical coordinate of each flow as a function of time, velocity, and acceleration. Each of the three crowd flows is the trajectory calculated by the average value of six different pedestrian trajectories.

5.4.1. Results for the movement of the crowd flow at the middle zone of the corridor

The equation with the best score is:

$$f(...) = 1.29\sin(0.135 + 5.45\,t) + 1.37\sin(t)\sin(1.73\,t) + 3.89\sin(t) - 0.00530\,a\_\{y\} - 0.0845$$

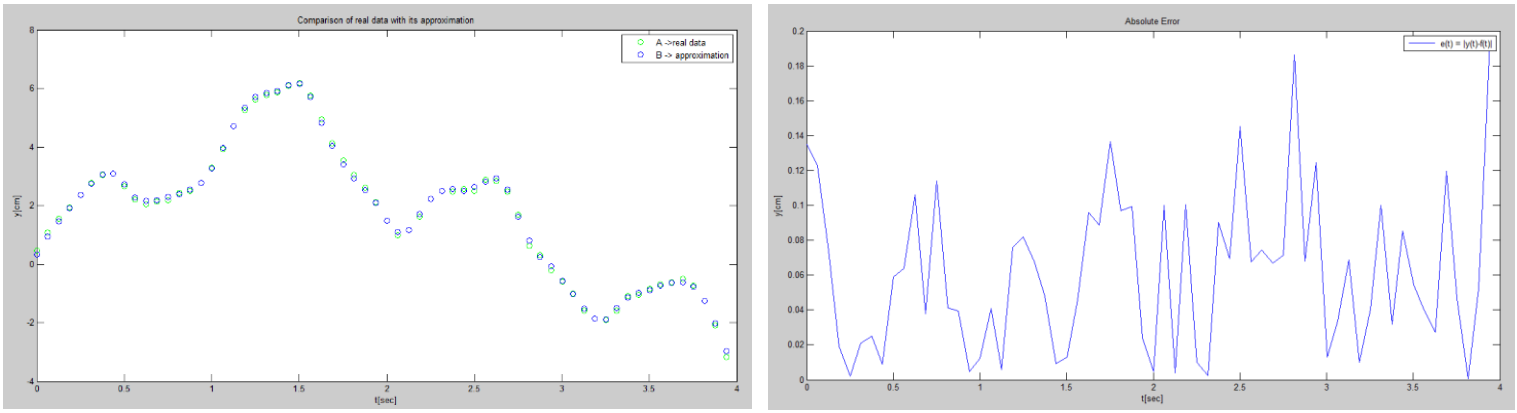

(a) (b)

Figure 5.25 Comparison of the equation and the real data in the time domain for the middle crowd flow
(a) Representation of the trajectories of the equation and the real data
(b) The absolute error between the two trajectories

5.4.2. Results for the movement of the crowd flow at the upper zone of the corridor

The equation with the best score is:

$$f(...) = 2.05 + 1.85\sin(5.30\,t - 0.994) - 0.0932\exp(t) - 0.200\,y - 0.00773\,a2\_\{y\}$$

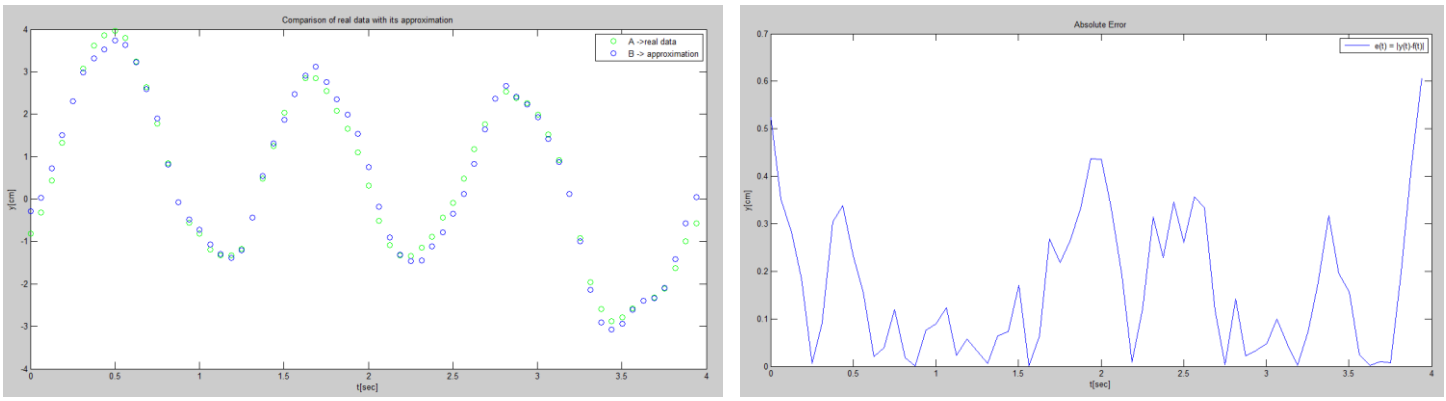

(a) (b)

Figure 5.26 Comparison of the equation and the real data in the time domain for the upper crowd flow
(a) Representation of the trajectories of the equation and the real data
(b) The absolute error between the two trajectories

5.4.3. Results for the movement of the crowd flow at the l zone of the corridor

The equation with the best score is:

$$f(\ldots) = 2.30 + 0.802\,t + \cos\left(0.940\,t^2 - 0.225\right) - \sin(t)\cos\left(1.53\,t + 0.837\,t^2\right) - 0.00595\,a3\_\{y\}$$

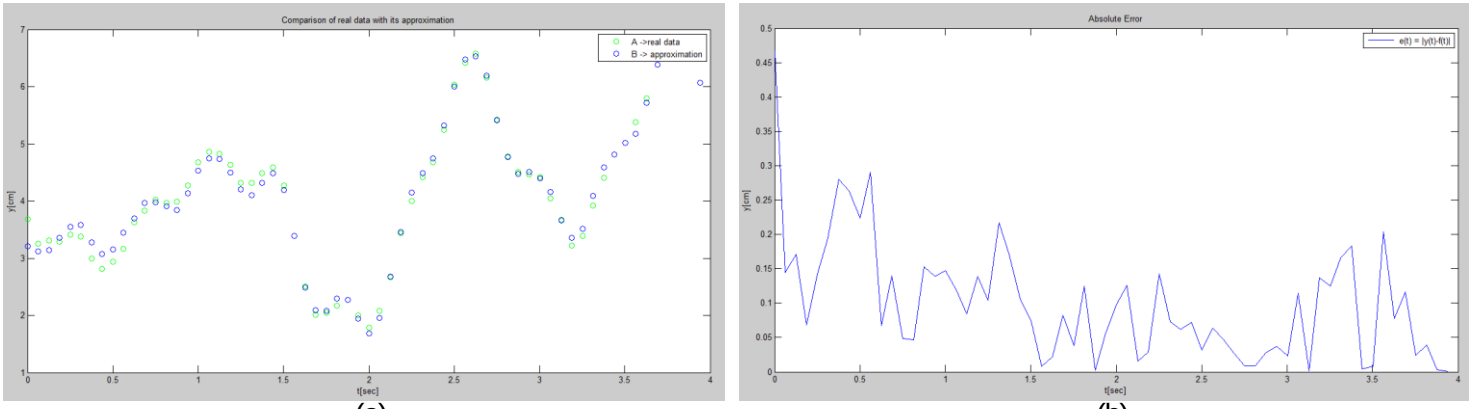

(a) (b)

Figure 5.27 Comparison of the equation and the real data in the time domain for the lower crowd
(a) Representation of the trajectories of the equation and the real data
(b) The absolute error between the two trajectories

6. Overall Results

In this chapter there is a centralized and comparative presentation of the results produced in chapters 4 and 5. In the previous chapter we made a comparison of the equations found with the data from real pedestrian movement in the time domain. We noticed that the equations accurately describe the real data. In this chapter we want to compare the results of chapter 4 with the equations found in chapter 5 in the frequency domain. The aim of the chapter is to draw some conclusions after the comparison. From the theory of oscillations for a simple harmonic oscillation, the removal from the equilibrium position is given by the equation: $x = A\sin(\omega t + \alpha)$, where A is the maximum displacement from the equilibrium position , ω is the circular frequency and α is the initial phase. Additionally, the following equation is valid $\omega_1 = 2\pi f_1$ which connects the circular frequency and frequency. Thus, we can extract from the equations we have found the fundamental frequencies. For example for the first equation of Table 2 we have: ω_1=6.06[rad/sec] , ω_2=1[rad/sec] thus $f_1 = \omega_1 / 2\pi = 0.96[Hz]$ and $f_2 = \omega_2 / 2\pi = 0.16[Hz]$

6.1 Overall results and conclusion for the first microscopic search case

Table 2 The set of equations for the first microscopic case and the comparison of the frequency spectrum with the real data

EQUATIONS FOUND FROM THE FIRST MICROSCOPIC CASE	FREQUENCIES FROM THE EQUATIONS	FREQUENCIES FROM THE REAL DATA
$137. + 0.320\,y1\text{-}y_3 + 0.320\exp(0.160\,t^2) + 1.32\cos(6.06\,t) - 0.565\,t\sin(t) - 0.320\,y1\text{-}y_2$	$f_1 = 0.96[Hz]$ $f_2 = 0.16[Hz]$	$f_1 = 0.84[Hz]$ $f_2 = 0.42[Hz]$ $f_3 = 0.28[Hz]$
$133. + 13.9\log(y1\text{-}y_3) - \exp(0.453\,t) - 0.430\,y1\text{-}y_2$		$f_1 = 1.06[Hz]$ $f_2 = 0.48[Hz]$ $f_3 = 0.3[Hz]$
$140. + 1.49\,t\cos(3.69 + 1.84\,t) + 3.50\,t\sin(t) - 0.286\,y1\text{-}y_2$	$f_1 = 0.3[Hz]$ $f_2 = 0.16[Hz]$	$f_1 = 0.25[Hz]$
$133. + 0.263\,y1\text{-}y_3 - 6.21\cos(t) - 3.05\sin(5.18\,t) - 0.584\,y1\text{-}y_2$	$f_1 = 0.82[Hz]$ $f_2 = 0.16[Hz]$	$f_1 = 1.14[Hz]$ $f_2 = 0.55[Hz]$

		$f_3 = 0.34[Hz]$ $f_4 = 0.25[Hz]$
$169. + 1.39\sin(5.40t - 0.939) + t\sin(1.11t) - 0.427 y1\text{-}y_2 - 0.00365 a\_\{y\}$	$f_1 = 0.86[Hz]$ $f_2 = 0.18[Hz]$	$f_1 = 1.14[Hz]$ $f_2 = 0.44[Hz]$ $f_3 = 0.32[Hz]$
$80.0 + 0.740 y1\text{-}y_3 + 1.34\sin(6.73t) - \cos(t)\log(y1\text{-}y_3)\log(2.25t)$	$f_1 = 1.07[Hz]$ $f_2 = 0.18[Hz]$	$f_1 = 0.90[Hz]$ $f_2 = 0.41[Hz]$ $f_3 = 0.28[Hz]$

In the first microscopic case, we observe that the frequency spectrum of the equations found has some similarity but has less frequencies than the frequency spectrum of the real data. In real data, three basic frequencies are shown, while in the equations of the first search case there is a maximum of two. However, from the time-domain comparison in the previous chapter we have found that the equations accurately describe the real data with an error less than two and a half centimeters (<2.5[cm]). If we observe the form of the equations, we can notice that exists a constant term due to the process of the recording data. Moreover, there are cosines and sines functions that provide us with the abovementioned frequencies. Additionally, in all equations both or only one of the terms $y_1 - y_2$ and $y_1 - y_3$ are depicted which describe the Cartesian difference in the vertical axis to the pedestrian movement direction. The regular presence of the terms $y_1 - y_2$ and $y_1 - y_3$ in the equations that describe the movement of the middle pedestrian and essentially express the changes in the vertical distance between the pedestrians, can confirm our initial reasoning that socio-psychological interactions exist, depending on the distance between the perdestrians. We make this conclusion because these terms are capable to describe the pedestrian movenent, which means that the distances between them and the individual positions are related.

6.2 Overall results and conclusion for the second microscopic search case

6.2.1. First video recording

Table 3 The set of equations for the first video recording of the second microscopic case and the comparison of the frequency spectrum with the real data

EQUATIONS FOUND FROM THE SECOND MICROSCOPIC CASE	FREQUENCIES FROM THE EQUATIONS	FREQUENCIES FROM THE REAL DATA
$134. + 0.658t + 5.61\cos(5.03 - 5.20t) + \cos(3.40t - 101.) - 8.84\cos(t)^2 - 0.00753\,a\_\{y\}$	$f_1 = 0.83[Hz]$ $f_2 = 0.54[Hz]$ $f_3 = 0.16[Hz]$	$f_1 = 0.84[Hz]$ $f_2 = 0.42[Hz]$ $f_3 = 0.28[Hz]$
$220. + 4.92\cos(1.20 - 4.93t) - 3.04t\sin(t - 0.320) - 0.685\cos(3.45t) - 2.57t$	$f_1 = 0.78[Hz]$ $f_2 = 0.55[Hz]$ $f_3 = 0.16[Hz]$	$f_1 = 0.84[Hz]$ $f_2 = 0.38[Hz]$ $f_3 = 0.26[Hz]$
$72.2 + 2.21\cos(3.00t - 2.20) - 1.82t\sin(1.28 + t) - 5.87\sin(0.291 + t) - 0.0265\,a3\_\{y\}$	$f_1 = 0.47[Hz]$ $f_2 = 0.16[Hz]$	$f_1 = 0.46[Hz]$

6.2.2. Second video recording

Table 4 The set of equations for the second video recording of the second microscopic case and the comparison of the frequency spectrum with the real data

EQUATIONS FOUND FROM THE SECOND MICROSCOPIC CASE	FREQUENCIES FROM THE EQUATIONS	FREQUENCIES FROM THE REAL DATA
$159. + 3.15t + 1.84\cos(5.86 - 5.76t) - 2.59\cos(1.08 + 2.79t)$	$f_1 = 0.91[Hz]$ $f_2 = 0.44[Hz]$	$f_1 = 1.06[Hz]$ $f_2 = 0.48[Hz]$ $f_3 = 0.3[Hz]$
$205. + 2.77\sin(0.975 + 5.29t) + 1.35\sin(2.07t) - 1.62t$	$f_1 = 0.84[Hz]$ $f_2 = 0.33[Hz]$	$f_1 = 0.9[Hz]$ $f_2 = 0.44[Hz]$ $f_3 = 0.28[Hz]$
$128. + 5.20\sin(t - 0.415) + 1.66\cos(2.93t) - 3.52\cos(5.44t - 0.300) - 3.53t$	$f_1 = 0.86[Hz]$ $f_2 = 0.16[Hz]$ $f_3 = 0.46[Hz]$	$f_1 = 0.47[Hz]$

6.2.3. Third video recording

Table 5 The set of equations for the third video recording of the second microscopic case and the comparison of the frequency spectrum with the real data.

EQUATIONS FOUND FROM THE SECOND MICROSCOPIC CASE	FREQUENCIES FROM THE EQUATIONS	FREQUENCIES FROM THE REAL DATA
$97.8 + 0.375y_3 + 9.04\sin(t) + \cos(0.280 + 4.41t) + 2.14\sin(21.5 + 2.23t)$	$f_1 = 0.16[Hz]$ $f_2 = 0.7[Hz]$ $f_3 = 0.35[Hz]$	$f_1 = 0.25[Hz]$
$175. + 6.30\sin(5.23t) + 2.95\sin(t) - 3.87\cos(32.7 - 2.41t) - 3.52t$	$f_1 = 0.83[Hz]$ $f_2 = 0.16[Hz]$ $f_3 = 0.38[Hz]$	$f_1 = 0.88[Hz]$ $f_2 = 0.42[Hz]$ $f_3 = 0.26[Hz]$
$y + 4.67\sin(-5.32t) + \sin(3.95t) - 2.55t\sin(1.21t) - 54.4$	$f_1 = 0.84[Hz]$ $f_1 = 0.63[Hz]$ $f_1 = 0.19[Hz]$	$f_1 = 0.84[Hz]$ $f_2 = 0.42[Hz]$ $f_3 = 0.26[Hz]$

6.2.4. Fourth video recording

Table 6 The set of equations for the fourth video recording of the second microscopic case and the comparison of the frequency spectrum with the real data.

EQUATIONS FOUND FROM THE SECOND MICROSCOPIC CASE	FREQUENCIES FROM THE EQUATIONS	FREQUENCIES FROM THE REAL DATA
$113. + t^2 + 1.50\sin(113. + 1.37t + 1.12t^2) - 4.50\sin(0.436 + 6.39t)$	$f_1 = 1.01[Hz]$	$f_1 = 1.14[Hz]$ $f_2 = 0.55[Hz]$ $f_3 = 0.34[Hz]$ $f_4 = 0.25[Hz]$
$160. + t + 6.31\cos(-5.35t - 76.3) - 0.687t\cos(2.65t) - 7.36\cos(t)$	$f_1 = 0.85[Hz]$ $f_2 = 0.42[Hz]$ $f_3 = 0.16[Hz]$	$f_1 = 0.88[Hz]$ $f_2 = 0.43[Hz]$ $f_3 = 0.28[Hz]$
$81.5 - 0.120\exp(t) - 1.66\sin(-0.0223x) - 8.49\sin(t)\cos(0.177 - t) - 0.0293\,a3\_\{y\}$		$f_1 = 0.94[Hz]$ $f_2 = 0.59[Hz]$ $f_3 = 0.41[Hz]$

6.2.5. Fifth video recording

Table 7 The set of equations for the fifth video recording of the second microscopic case and the comparison of the frequency spectrum with the real data.

EQUATIONS FOUND FROM THE SECOND MICROSCOPIC CASE	FREQUENCIES FROM THE EQUATIONS	FREQUENCIES FROM THE REAL DATA
$135. + 2.96\cos(-4.75t) - 5.98\sin(-1.57t) - 5.10\cos(0.662 - 5.33t) - 0.00702 a\_\{y\}$	$f_1 = 0.75[Hz]$ $f_2 = 0.25[Hz]$ $f_3 = 0.84[Hz]$	$f_1 = 1.14[Hz]$ $f_2 = 0.44[Hz]$ $f_3 = 0.32[Hz]$
$215. + 3.26\sin(5.84 + 5.84t) - 7.46\sin(1.90t - 0.183) - 0.00556 a2\_\{y\}$	$f_1 = 0.93[Hz]$ $f_2 = 0.30[Hz]$	$f_1 = 0.33[Hz]$
$62.3 + 2.41t + 3.84\cos(6.52t) - \sin(3.47t)$	$f_1 = 1.03[Hz]$ $f_2 = 0.55[Hz]$	$f_1 = 1.06[Hz]$ $f_2 = 0.53[Hz]$

6.2.6. Sixth video recording

Table 8 The set of equations for the sixth video recording of the second microscopic case and the comparison of the frequency spectrum with the real data

EQUATIONS FOUND FROM THE SECOND MICROSCOPIC CASE	FREQUENCIES FROM THE EQUATIONS	FREQUENCIES FROM THE REAL DATA
$133 + 4.02\cos(5.43 + 5.31t) + 0.781t\cos(3.17t) + 5.46\cos(1.67t) - 0.00657 a\_\{y\} - 3.22t$	$f_1 = 0.84[Hz]$ $f_2 = 0.50[Hz]$ $f_3 = 0.26[Hz]$	$f_1 = 0.9[Hz]$ $f_2 = 0.41[Hz]$ $f_3 = 0.28[Hz]$
$179 + 5.3\sin(-5.06t) - 1.57\sin(1.45t) - 0.00575 a2\_\{y\} - 1.39\log(t)\sin(0.464 - 5.01t) - 2.96t$	$f_1 = 0.80[Hz]$ $f_2 = 0.23[Hz]$ $f_3 = 0.79[Hz]$	$f_1 = 0.83[Hz]$ $f_2 = 0.4[Hz]$ $f_3 = 0.27[Hz]$
$63.1 + 2.15t + 4.10\sin(-1.63t) - 0.0219 a3\_\{y\}$	$f_1 = 0.26[Hz]$	

About the second microscopic approach we observe that the equations found consist of a fixed term, sine and cosine functions and the acceleration term. In this case, the spectrum of the equations is similar to the spectrum of real data. Furthermore, according to the previous chapter

comparison in time domain, we conclude that the equations accurately describe the real data with an error less than two and a half centimeters (<2.5[cm]), except for two cases with error less than <4.5 [cm]). We can notice that the different frequencies are not random but obey to a specific role. To clarify this role, we use the case of the lower person from the second video clip as shown in the Figure 6.1. Figure 6.1 (a) depicts the waveform of the equation found(purple) and we can notice how accurately corresponds to the real data(green). The equation is set below Figure 6.1 (a). Figure 6.1 (b) depicts the waveform of the equation which includes the fixed term and one of the three sines, meaning one of the three frequencies. We can notice from the waveform that this oscillation has the same width and its peaks are in parallel to the peaks of the total movement of the individual. Therefore, it could be due to the periodic motion caused by the person's walk. Then, we notice in Figure 6.1 (c) the waveform that consists of the same constant term and the other two frequencies which make up the overall equation of the pedestrian movement. We can understand that the waveform could be the movement that carries the center of gravity of the human body, as it appears that around this graphical representation the total movement-oscillation of the person is performed. In other words, Figure 6.1 (b) contains the terms and depiction that is caused due to the physiology of human walking and Figure 6.1 (c) contains the terms and depiction that is caused due to the

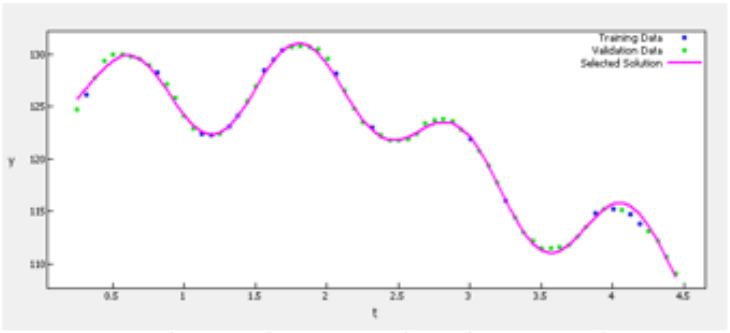

$$f(\ldots) = 128. + 5.20\sin(t - 0.415) + 1.66\cos(2.93t) - 3.52\cos(5.44t - 0.300) - 3.53t$$

(α)

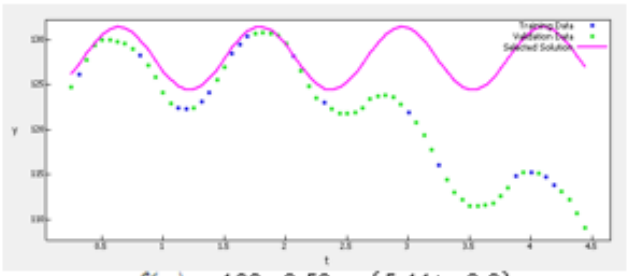

$$f(\ldots) = 128 - 3.52\cos(5.44t - 0.3)$$

(β)

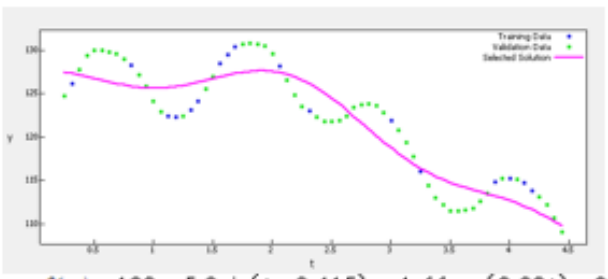

$$f(\ldots) = 128 + 5.2\sin(t - 0.415) + 1.66\cos(2.93t) - 3.53t$$

(γ)

Figure 6.1 Comparative presentation of the real trajectory and the plot of parts as well as of the overall equation that describes the movement of the lower individual from the second video clip.
(A) The waveform of the total equation in comparison with the real trajectory
(B) The waveform of a part of the total equation in comparison with the real trajectory
(C) The waveform of the complementary part of the total equation in comparison with the real trajectory

external interactions which are developed between the pedestrians and therefore change the position of center gravity and hence of the person. Thus, the overall equation is created by the combination of the two partial equations.

6.3 Overall results and conclusion for the second macroscopic search case

Movement of the crowd flow in the middle part of the corridor

Table 9 The crowd movement equation in the middle part of the corridor from the third macroscopic case and its frequency spectrum

EQUATIONS FOUND FROM THE THIRD MACROSCOPIC CASE	FREQUENCIES FROM THE EQUATIONS	FREQUENCIES FROM THE REAL DATA
$1.29\sin(0.135 + 5.45t) + 1.37\sin(t)\sin(1.73t) + 3.89\sin(t) - 0.00530\,a\_\{y\} - 0.0845$	$f_1 = 0.86[Hz]$ $f_2 = 0.43[Hz]$ $f_3 = 0.12[Hz]$	$f_1 = 0.3[Hz]$ $f_2 = 0.25[Hz]$

The following equation is valid: $\sin(x)\sin(y)=1/2[\cos(x-y)-\cos(x+y)]$

Movement of the crowd flow in the upper part of the corridor

Table 10 The crowd movement equation in the upper part of the corridor from the third macroscopic case and its frequency spectrum

EQUATIONS FOUND FROM THE THIRD MACROSCOPIC CASE	FREQUENCIES FROM THE EQUATIONS	FREQUENCIES FROM THE REAL DATA
$2.05 + 1.85\sin(5.30t - 0.994) - 0.0932\exp(t) - 0.200y - 0.00773\,a2\_\{y\}$	$f_1 = 0.84[Hz]$	$f_1 = 0.84[Hz]$ $f_2 = 0.41[Hz]$ $f_3 = 0.26[Hz]$

Movement of the crowd flow in the lower part of the corridor

Table 11 The crowd movement equation in the lower part of the corridor from the third macroscopic case and its frequency spectrum

EQUATIONS FOUND FROM THE THIRD MACROSCOPIC CASE	FREQUENCIES FROM THE EQUATIONS	FREQUENCIES FROM THE REAL DATA
$2.30 + 0.802t + \cos(0.940t^2 - 0.225) - \sin(t)\cos(1.53t + 0.837t^2) - 0.00595\,a3\_\{y\}$		$f_1 = 0.80[Hz]$ $f_2 = 0.36[Hz]$

For the third macroscopic approach, we observe that the equations found consist of a fixed term, sine and cosine functions and the acceleration term. They have several similarities to the equations of the second microscopic approach. In this case, the frequency spectrum of the equations is similar to that of the real data, but it is clearly poorer. From the previous chapter, the comparison in the time domain showed that the equations describe the average of real data with great accuracy with an error less than one centimeters (<1 [cm]). Frequency spectrum values for the movement of crowd flows are very close to the frequency values that describe the pedestrian movement. Thus, we have a direct correlation of the total movement of the crowd with that of the individual, which indicates that the pedestrians are synchronized. This could be expected because of the similar anatomy of the people who constitute the crowd. However, in several cases where pedestrians have empty space in front of them and have the ability to accelerate by changing the frequency spectrum of their movement, they seem to choose not to differentiate themselves from the overall movement and the frequency spectrum of the rest of the crowd.

7. Conclusions and Future Work

In the final chapter of this diploma thesis we will analyze the perspectives and possible future research directions related to the problem we have encountered.

Initially, it could be examined a larger number of different video clips covering a larger range of cases and behaviors. As we have seen in a previous chapter, the parameters of the video scenes examined cover only a small range of possible scenarios. For example, videos of people of different age, background, educational background and different walking habits could be examined to investigate their behavior and similarities to the results already exported. Different layout arrangements could also be used, such as corridors with angles, T-shaped crossings and also movement in two or more directions. In addition, different flow densities could be used where it is possible that more or less collisions will occur between individuals and different recording time in order to ensure more extensive examination.

Moreover, in our study we analyze only the vertical coordinate in the direction of movement. A future study could investigate the parallel coordinate in the direction of pedestrian movement, which may display equally interesting behaviors as well as the investigation of the coordinates of speed and acceleration.

On another level, it could be designed a model of the crowd movement through the results and conclusions of our study. Such a research should complement a number of gaps and deal with modeling factors that did not concern our study, such as details of the representation of individuals or the way of measuring the quality of the interactions. However, it would be a very interesting future research because our study deals both at microscopic and macroscopic level with the interactions and movement of the crowd.

Bibliography

[1] Helbing D and Molnar P 1995 Social force model for pedestrian dynamics *Phys. Rev. E*

[2] Helbing D, Molnár P, Farkas I J and Bolay K 2001 Self-organizing pedestrian movement *Environ. Plan. B Plan. Des.*

[3] Fruin J J, Port T and Authority Y 1971 Designing for Pedestrians : a Level-of-Service Concept *50th Annu. Meet. Highw. Res. Board*

[4] Henderson L F 1971 The Statistics of Crowd Fluids *Nature*

[5] Pauls J 1984 The movement of people in buildings and design solutions for means of egress *Fire Technol.*

[6] Helbing D, Buzna L, Johansson A and Werner T 2005 Self-Organized Pedestrian Crowd Dynamics: Experiments, Simulations, and Design Solutions *Transp. Sci.*

[7] Tolujew J and Alcalá F 2004 A mesoscopic approach to modeling and simulation of pedestrian traffic flows *Proc. 18th Eur. Simul. Multiconferece, 2004*

[8] Milazzo J, Rouphail N, Hummer J and Allen D 1998 Effect of Pedestrians on Capacity of Signalized Intersections *Transp. Res. Rec.*

[9] Hoogendoorn S P and Bovy P H L 2005 Pedestrian travel behavior modeling *Networks Spat. Econ.*

[10] Lovas G 1994 Modeling and simulation of pedestrian traffic flow *Transp. Res. Part B Methodol.*

[11] Reynolds C W 1987 Flocks, herds and schools: A distributed behavioral model *ACM SIGGRAPH Comput. Graph.*

[12] Helbing D, Farkas I and Vicsek T 2000 Simulating Dynamical Features of Escape Panic **794** 487–90

[13] Wąs J, Gudowski B and Matuszyk P J 2006 Social Distances Model of Pedestrian Dynamics *7th Int. Conf. Cell. Autom.* **4173 LNCS** 492–501

[14] Moussaid M, Helbing D and Theraulaz G 2011 How simple rules determine pedestrian behavior and crowd disasters *Proc. Natl. Acad. Sci.* **108** 6884–8

[15] Czerlinski J, Gigerenzer G and Goldstein D G 1999 Simple Heuristics That Make Us Smart *Simple Heuristics that make us smart*

[16] Koza J R 1992 *Genetic programming: on the programming of computers by means of natural selection (Vol. 1)*

[17] Mitchell M 1995 *An Introduction to Genetic Algorithms*

[18] Georgoudas I G, Kyriakos P, Sirakoulis G C and Andreadis I T 2010 An FPGA implemented cellular automaton crowd evacuation model inspired by the electrostatic-induced potential fields *Microprocess. Microsyst.*

[19] Schmidt M and Lipson H 2009 Distilling Free-Form Natural Laws from Experimental Data *Science (80-.).* **324** 81–5